공학박사 학위논문

공기열원 히트펌프 내 최적 및 현재 충전량 실시간 예측 방법에 관한 연구

A Real Time Prediction Method of Current and Optimal Refrigerant Charge in Air Source Heat Pump System

2020년 2월

서울대학교 대학원

기계항공공학부

홍 성 빈

Abstract

A Real Time Prediction Method of Current and Optimal Refrigerant Charge in Air Source Heat Pump Systems

Sung Bin Hong
Department of Mechanical and Aerospace Engineering
The Graduate School
Seoul National University

Heat pump system has an optimal refrigerant charge. In order to improve the performance of the heat pump and to prevent off-design operation, it is desirable that the amount of refrigerant in the heat pump system is always maintained optimally. In order to maintain the optimal charge level, it is necessary to accurately predict the current charge amount in the system. There are various studies for predicting the refrigerant charge, but most of the methods are data-based, which is difficult to be applied to various systems. In this study, physic-based charge prediction method is proposed to reduce the

cost and increase the accuracy of charge amount prediction.

First, a simulation-based charge prediction method is presented. The configuration and geometry of the heat pump system is very complex, and this system characteristic affects the refrigerant charge. Therefore, the geometry and characteristics of the heat pump system are considered in detail in this study. In addition, the lubricating oil charged in the compressor has a significant effect on the refrigerant charge amount. Therefore, the effect of lubricant in the compressor is considered in the modeling. Through the simulation of the heat pump system, the amount of refrigerant was predicted, and the error of prediction was 6.3%, indicating that the simulation-based charge prediction method was very accurate. However, since the heat pump system is considered in detail, the simulation-based method has a disadvantage in its applicability.

In order to develop charge prediction method that can be universally applied, a heat pump system was simplified and analyzed. Through some assumptions and basic heat transfer analysis, a generalized charge prediction equation was presented. A commercial heat pump experiment was conducted to verify the accuracy of the proposed charge prediction equation. The prediction error of the charge prediction equation was 3.7% for cooling mode and 8.2% for heating mode. Since the charge prediction equation is presented

based on the phenomenon occurring in the overall air source heat pump, it can be used universally. Nevertheless, some limitations exist. In this study, to overcome these limitations, extended methods of charge prediction equation were suggested.

First, in case of continuous operation, there always exist the points where the assumptions are not satisfied so that the accuracy of the charge prediction equation becomes low. For example, the accuracy of charge prediction equation is drastically reduced during transient operation or if compressor is not operating. Therefore, in order to increase the accuracy of charge prediction equation in continuous driving, a criterion was presented for selecting the points in which the assumptions are valid. Using the criterion, the points of high accuracy of charge prediction equation were selected. Through this process, the error of charge prediction equation was reduced to 6.11% even during continuous operation.

Next, the accuracy of charge prediction equation was verified in small systems such as residential heat pump systems. In small heat pump systems, it is impossible to ensure the presence of degree of subcool (DSC). In severely undercharge case, where no DSC exists, the accuracy of the charge prediction equation is greatly reduced, so this severe undercharged case was eliminated by the leakage detection method. When the leakage is detected, it is obvious

that the system needs to be recharged. Therefore, the charge prediction equation is attempted only when the leakage is not detected. In this case, the error of charge prediction decreased greatly from 18.6% to 5.16%.

For optimal control of the refrigerant charge, it is necessary to know the optimal charge. The optimal charge of the system varies depending on the configuration, controls, and operating conditions of the system. Therefore, in this study, a real-time optimal charge prediction method was presented. To predict the optimal charge, it is necessary to predict the performance change of the system according to the charge amount. However, it is very difficult to predict the performance of the system directly from the charge amount. Therefore, in this study, the system performance was first predicted according to the operating information, and the operating information was converted into the charge amount using the charge prediction equation. Through this process, it was possible to predict the system performance and the optimal charge amount. The optimal charge prediction method was verified by experimental data. The prediction error of the optimal refrigerant charge was 6.97%.

In conclusion, the optimal control of charge amount is available by combining the current charge prediction method and the optimal charge prediction method. In this study, the effect of the optimal control of charge

amount was evaluated. COP improvement of 6.04% is expected by optimal control of charge amount.

Keywords: Air Source Heat Pump, Refrigerant Charge, Optimal Charge, Optimal Control, Heat Pump Modeling

***Identification Number*: 2014-21573**

Contents

List of Figures

List of Tables

Nomenclature

A	area (m^2)
Bo	Boiling number
C_p	specific heat (kJ/kg·K)
COP	coefficient of performance
D	diameter (m)
DSC	degree of subcool (K)
DSH	degree of superheat (K)
EEV	electronic expansion valve
f	friction factor
G	mass flux ($kg/s \cdot m^2$)
g	gravitational accerleration (= 9.81 m/s^2)
h	heat transfer coefficient ($kW/m^2 \cdot K$)
h_{fg}	speicif latent heat (kJ/kg)
i	enthalpy (kJ/kg)
j	Couburn j factor
k	thermal conductivity (kW/m·K)
L	length (m)
m	mass (kg)
$\dot{m}$	mass flow rate (kg/s)
Nu	Nusselt number
n	polytropic coefficient

P	pressure (kPa)
Pr	Prandtl number
Q	capacity (kW)
Q’	heat flux (kW/m)
Re	Reynolds number
s	gradient
T	temperature (K)
U	overall heat transfer coefficient ($kW/m^2 \cdot K$)
V	velocity (m/s)
v	specific volume (m^3/kg)
W	work (kW)
x	vapor quality

Greek

η	efficiency
ε	void fraction
μ	dynamic viscisity (Pa·s)
ρ	density (kg/m^3)
σ	surface tension (N/m)
ω	frequency (Hz)

Subscript

air	air side
amb	ambient
C	cooling
comp	compressor
cond	condenser
dis	dischrage
disp	displacement
eev	electronic expansion valve
g	gas
H	heating
hps	high pressure side
i	inside
in	inlet
l	liquid
ll	liquid line
lps	low pressure side
max	maximum
o	outside
oil	lubricant
out	outlet
s	surface
sat	saturate

sc	subcooled
sh	superheated
sol	solubility
tp	two phase
v	vapor
V	volumetric
w	wall

Chapter 1. Introduction

1.1 Background of the study

Rapid industrialization and population growth have created tremendous energy demand. Considered as one of the most commonly used energy sources, fossil fuels expected to face its depletion in near future, and hence it is inevitable to develop the renewable energy and to adjust the demand for the energy. According to the U.S. Energy Information Administration (2019), more than 70% of the total electricity consumption is for the home and the commercial usage, of which nearly 40% is used for the space cooling and heating. Therefore, adjusting the energy demand of space cooling and heating will have a great impact on reducing the overall energy demand.

Air source heat pump system provides cooling and heating, is known as one of the most widely used and reliable systems. In case of cooling, the heat pump is most commonly used device for satisfying the cooling demand, and even in case of heating, the heat pump replaces the conventional systems such as boilers or electric heaters due to its high efficiency. The rapid increase of the heat pump penetration rate is a natural consequence. Nowak et al., (2014) shown in Fig. 1.1, reported that the heat pumps are rapidly popularized among

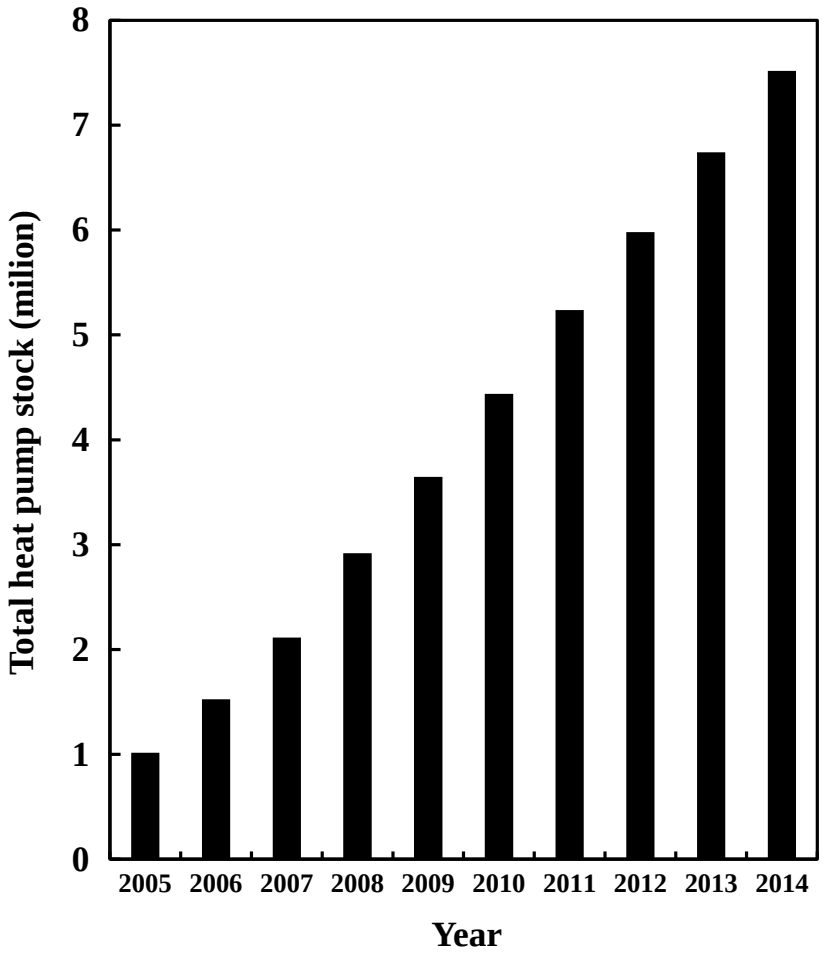

Fig. 1.1 Total stock of heat pumps in Europe

Europe. They estimated that the number of heat pumps in Europe would have increased more than seven times over the last decade. In addition, Biddle (2008) reported that the rate of residential heat pump penetration in the United States in 1980s increased about five times compared to that of the 1950s. Since the heat pump system has a high penetration rate and demand, the failure or malfunction of the heat pump system could cause a great inconvenience and waste of energy. Therefore, the research on maintenance and optimal control for improving the efficiency of the heat pump system is very important.

The most common fault in an air heat source heat pump system is related to refrigerant charge. There is an optimal amount of refrigerant charge in the heat pump system, and the adequate amount of refrigerant must be charged in the system. In real situation, however, there are cases that the refrigerant is often overcharged or leaked during the installation or operation of the heat pump system, and thus the amount of charge often varies significantly from its optimal amount. As can be seen in Fig. 1.2, Rossi (2004) found that refrigerant leakage accounts for 63% of all tune-up faults. Moreover, according to Madani and Roccatello (2014), 17% of the maintenance costs of an air source heat pump are due to refrigerant leakage. According to Kim et al., (2007), if the system is undercharged or overcharged, the coefficient of

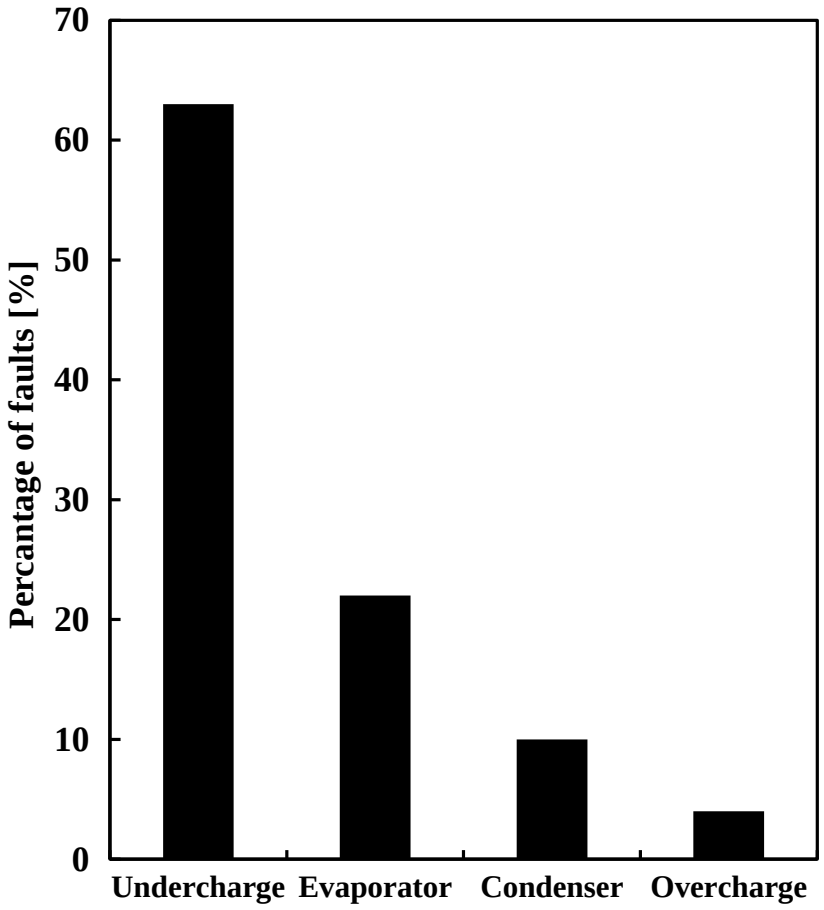

Fig. 1.2 Frequency of tune-up faults in air source heat pump system (Rossi, 2004)

performance (COP) and cooling (or heating capacity) of the system are reduced as shown in Fig. 1.3. Many researchers have reported this result. (Kim et al., 2007; Corberán et al., 2008; Heo et al., 2008; Kim et al., 2009; Corberán et al., 2011; Kim et al., 2014; Yoo et al., 2017)

To avoid this off-design operation, the refrigerant charge in the heat pump system must be checked in real time. However, checking the charge amount in real time is extremely difficult since the method for directly measuring the charge amount does not exist. Fortunately, the heat pump system is usually equipped with a variety of sensors for control and fault detection. Therefore, the amount of refrigerant charge can be indirectly predicted in real time using this sensor information. However, since the heat pump system has very complicated operating conditions and components, it is not easy to predict the amount of the refrigerant charge through the sensor information. Therefore, it is necessary to develop a method to predict the amount of refrigerant charge in various heat pump systems with high accuracy.

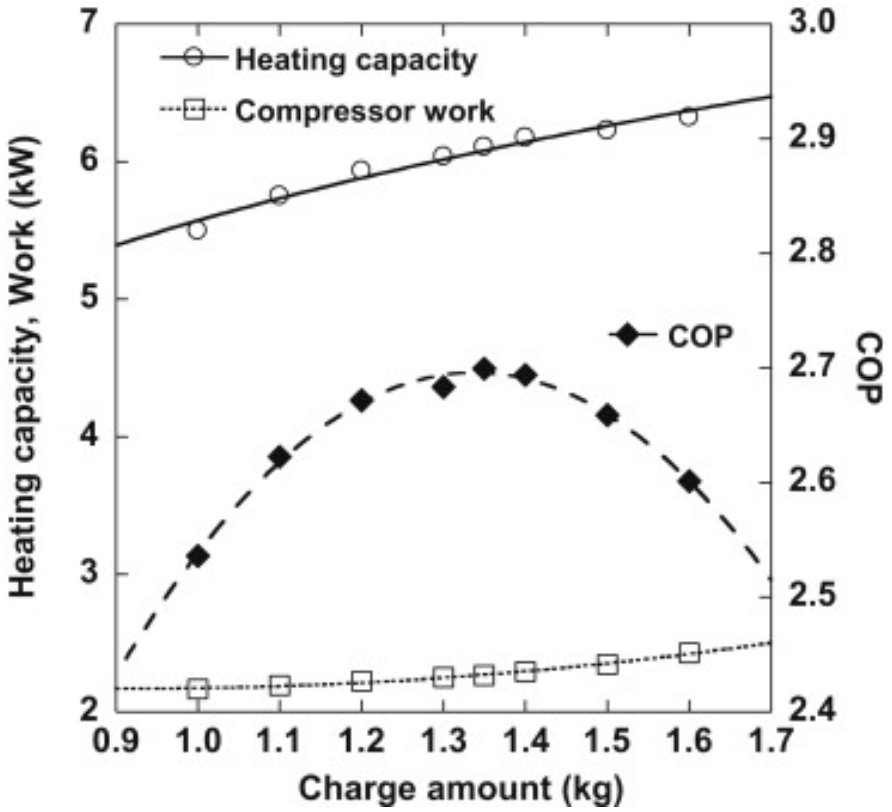

Fig. 1.3 COP and capacity variation with respect to charge amount (Kim et al., 2014)

1.2 Literature survey

1.2.1 Refrigerant charge prediction method

Various sensors exist in the heat pump system. There are also a various ways to estimate the refrigerant charge. The studies on the refrigerant charge prediction are classified into two main categories; leakage detection and charge prediction. The two methods differ in the scope of the target refrigerant charge detection. Leakage detection determines whether significant amount of refrigerant is leaked from the system, and charge prediction quantitatively predicts refrigerant charge, including normal and overcharge region.

First of all, leakage detection methods are often studied as part of heat pump fault detection and diagnosis (FDD). Rossi and Braun (1997) classified various faults of heat pumps and used them to detect refrigerant leakage. In the study, they classified the faults by the temperature, such as condensation, evaporation temperature, degree of superheat (DSH), and degree of subcool (DSC), and reported that among the temperatures, the DSC at the condenser outlet was the most sensitive to refrigerant leakage. Kim and Kim (2005) also found that DSC decreased with leakage of refrigerant. Tassou and Grace (2005) developed a fault diagnosis and leakage detection system through

artificial intelligence and real-time performance monitoring. Through this system, it was possible to distinguish the charge range from undercharged (under 67%), normal (67 to 133%), to overcharged (over 133%). Kocyigit et al. (2014) developed a fault diagnosis method based on P-h diagram. The researchers distinguished various faults and detected low and overcharge by using a P-h diagram of a heat pump that different for various faults. Yoo et al. (2017) presented a method for determining refrigerant leakage using only two sensors. Various refrigerant leakage detection methods have been proposed by using machine learning. Shi et al. (2017) presented a refrigerant charge fault detection method using Bayesian artificial neural network connected with Relief filter. Guo et al. (2017) used four back-propagation neural networks to detect four different faults in a heat pump system. While there are various methods of detecting the refrigerants leakage, most of the methods can only detect the faults under severe under or overcharged state. (under 60% or over 130%) Furthermore, since the amount of refrigerant is not quantitatively predicted and only the leakage is determined, it is inevitable that the system experiences a deterioration of the performance in the region which is considered to be the normal region (60 to 130%).

In addition to the leakage detection methods, the charge prediction method quantitatively predicts the amount of refrigerant using various sensors.

This also can be classified in two ways. One is black box model which is data-based method, and the other is physics based method. First, the data-based model which is based on advanced data analysis technology and big data, can accurately predict the amount of charge using actual sensor information regardless of physical phenomenon. The artificial neural networks (ANN) are a representative black box model. Eom et al. (2019) quantitatively predicted the amount of charge in the heat pump system using ANN. The black box model can be used without a detailed understanding of the system, so it can be applied to extremely complex systems and situations. However, this method is can only be applied to the specific system from which the data was collected. This method is mostly not useful when the system is different because it requires a lot of data to apply to the new system.

In order to apply the prediction method to various systems, the method must be developed based on the physical analysis. In the refrigerant charge prediction, there are no complete physics based model, but the most similar one is the virtual refrigerant charge sensor (VRC) developed by Li and Braun (2009). The virtual refrigerant charge sensor predicts the refrigerant charge using the assumption that the DSC and DSH have a linear relationship with the charge. VRC is a very useful method, but it has a disadvantage of low accuracy depending on the system. In order to overcome these drawbacks, a

number of extended versions of VRC have been proposed. Kim and Braun (2015) added the refrigerant quality at evaporator inlet and DSH at compressor discharge to the VRC, and improved the accuracy of charge prediction. Li et al. (2016) reduced the errors of the VRC by using the support vector regression. VRC is a simple and useful method, but it is still more an empirical method than a physical method. Therefore, a large number of experimental data are required, and reliability varies greatly depending on the system.

Although there have been multiple studies of various refrigerant charges, studies on charge prediction methods based on physical phenomena and characteristics are still insufficient. In order to increase the accuracy of charge prediction and reduce the cost, it is necessary to develop a physics based charge prediction method. In particular, it is important to develop a prediction method of the charge amount which has the high accuracy in various systems.

1.2.2 Optimal control of air source heat pump

Although there are various studies on optimal control of heat pump, not many degree of freedom of heat pump control is manipulated. Fig. 1.4 shows the P-h diagram of a typical heat pump system. As shown in the figure, the P-h diagram of the heat pump system is determined when the status at compressor inlet and condenser outlet is given. Thus, it has four degrees of freedom. In addition, the mass flow rate of refrigerant is separately adjustable from the P-h diagram. Thus, conventional heat pump systems have a maximum five degree of freedom. Ideally, all five of these variables should be independently adjusted properly to achieve the best performance. However, according to Goyal et al.(2019), most heat pump systems only control compressor inverter speed and expansion valve opening. The compressor and expansion valve control the mass flow rate of refrigerant and evaporating pressure respectively. The remaining variables are determined depend on the characteristics of the systems and operating conditions. Consequently, practically only two degree of freedom is used to control the heat pump system. Most studies on controlling air source heat pump suggest the method of maximizing COP or demanding response using this two degree of freedom. (Marcinichen et al., 2008; He et al., 1997;)

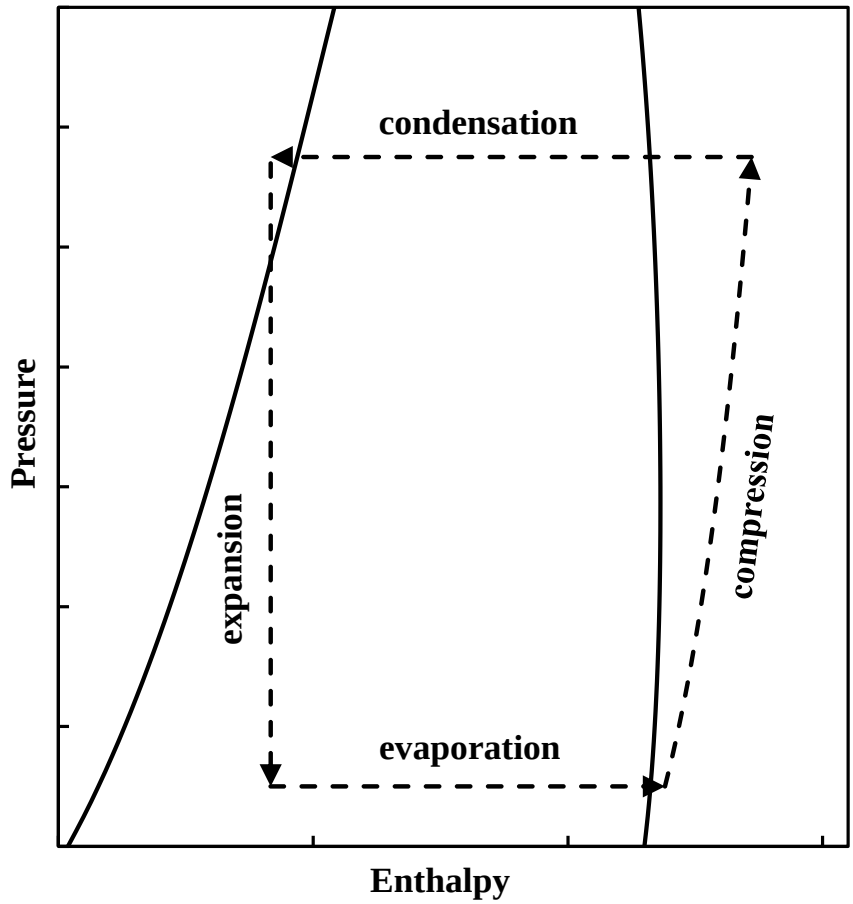

Fig. 1.4 P-h diagram of vapor compression heat pump system

First of all, many researchers including Qureshi and Tassou (1996) suggested feedback control model using variable speed compressor and expansion valve. (Vargas and Parise, 1995; Outtagarts et al., 1997; Finn and Doyle, 2000) For further improvement of heat pump performance, diverse versions of multi-input multi output (MIMO) feedback control strategy of heat pump system were also presented. Shah et al. (2004) suggested a multivariable control method for automotive heat pump system through simulation analysis. Also, an optimal controller for heat pump system was developed by Larsen. (2006) According to Larsen, the controller is able to deal with the various driving status change by a cascade feedback loop.

Advanced to conventional control model, a predictive control model is actively researched. The predictive control model has the disadvantage that the modeling process is complicated, but it is advantageous to deal with the driving condition or load changes of the system because it predicts and copes with the movements in advance. (Garcia et al., 1989). Also, thanks to advanced data analysis technology and big data, many data-based control models have been developed. Artificial neural network is a representative data-based control method. Nanayakkara et al. (2002) presented an expansion valve opening control model based on artificial neural network. Ekren et al. (2010) suggested simultaneous control method of expansion

valve and compressor inverter frequency by artificial neural network.

While various heat pump optimization studies exist as described above, few research has been made on refrigerant charge optimization. However, refrigerant charge control allows an additional degree of freedom to heat pump. Therefore, if the condensing pressure is controlled independently through charge adjustment, increase in the performance of the heat pump is expected. However, optimal adjustment of refrigerant charge is currently difficult in most heat pump systems. Currently, information on the optimal charge is provided by the heat pump manufacturer through the experiment. However, this pre-obtained charge amount is highly likable to be different from the actual optimal amount of the refrigerant charge. There are two reasons for this. Firstly, the condenser and evaporator of the heat pump are connected via liquid line and vapor line, and the length of the two tubes have a great influence on the refrigerant charge in the heat pump. Although additional refrigerant is injected depending on the length of the liquid and vapor lines, it is very difficult to accurately measure the length of this tube, and the optimal additional charge also depends on the conditions. Moreover, the optimal charge amount of the heat pump depends on the operating conditions. Since heat pumps are used in a variety of climatic conditions, the operating condition varies; heating/cooling mode operation,

part/nominal/full load conditions. Although the optimal charge amount changes according to the operating conditions, it is excessively expensive to obtain the optimal charge through experiments in all conditions.

If accurate prediction of the optimal charge is possible, the charge can be optimally adjusted yearly, seasonally, or ideally in real time, and it can consequence an improvement in the performance of the heat pump. Therefore, it is necessary to develop a predicting method of optimal charge amount in real time operation using the driving information of the heat pump.

.

1.3 Objectives and scopes

In order to increase the accuracy of charge prediction in the heat pump and reduce the cost, it is necessary to develop a method of predicting the charge amount based on the physics. In this study, a method of estimating the refrigerant charge of the air heat source heat pump system is proposed using the sensor information and is verified the accuracy through experimental data. In particular, through theoretical analysis, method was developed which is applicable to the various systems. Also, both charge prediction method using detailed physical modeling of heat pump system and charge prediction equation from theoretical analysis of refrigerant charge with simplified system were proposed and verified. In order to verify the applicability in various systems, experiments were conducted on both residential and commercial air source heat pump systems.

In addition, extended versions of the proposed charge prediction method were suggested for estimating refrigerant charge amount in various situations, such as a charge prediction method while transient driving and a charge prediction for a system with extremely limited number of sensors. Finally, a method of predicting the optimal charge amount through theoretical analysis was developed and the effect of real-time refrigerant amount control was evaluated. The detailed objectives and scopes for each

chapter are as follows.

The chapter 2 shows how to predict the charge amount in a heat pump system by detailed modeling of heat pump component. In this chapter, modeling of the heat pump system was performed in detail by simulating the commercial heat pump used in the experiment. In this modeling, however, unlike general heat pump modeling, the amount of refrigerant charge is an output value rather than an input value, and the sensor information (or state of refrigerant) is an input value, rather than an output value. Through the simulation of this model, the amount of refrigerant in the system is estimated using the sensor information and the result is compared with the experimental results. In addition, the distribution of the charge amount in each component was investigated.

The chapter 3 presents the generalized theoretical charge prediction equation. In order to apply a single refrigerant charge prediction method to a general heat pump, it is necessary to estimate the amount of refrigerant using a common phenomenon which appears in all heat pump systems. Thus in this chapter, the heat pump system is very simplified to derive the charge prediction equation. Through the theoretical analysis of this simplified system the generalized charge prediction equation was proposed, and the accuracy of the equation was verified through the experiments. Also, in order

to overcome the limitations of the proposed equation, the extended versions of charge prediction equation are presented for each situation and verified through the experiments.

Finally, the chapter 4 presents a method for predicting the optimal refrigerant charge of the system based on the current charge prediction. Since the optimal refrigerant charge differs in both the system and operating condition, it is possible to control the refrigerant in real time if the optimal charge amount is predicted in real time. Therefore, in this chapter, a real-time optimal charge prediction method is suggested through theoretical analysis and is verified through experiments. Finally, the optimal control of the refrigerant charge is evaluated.

Chapter 2. Charge amount prediction of air source heat pump using cycle modeling

2.1 Introduction

Major components of the vapor compression system are the compressor, condenser, expansion device and evaporator. Since the state change of the refrigerant occurs only in these major components, general heat pump modeling models these four components. However, there are additional components to consider in heat pump modeling for charge prediction. The condenser and evaporator are connected by vapor line and liquid line, and there is a considerable amount of refrigerant in both lines. In addition, refrigerant also exists in the accumulator. These components do not change the state of the refrigerant but have a great influence on the amount of refrigerant, and therefore must be considered in the charge amount prediction model. Likewise, the effects of lubricant in the compressor should also be considered. The compressor of heat pump system is filled with lubricant. Since the lubricant is very well mixed with the refrigerant, a considerable amount of refrigerant may be dissolved in the lubricant depending on the operating conditions. In this model the refrigerant charge

amount is calculated in consideration of the effect of this lubricant. The geometry of a typical air source heat pump is very complex. This system specification also affects the refrigerant charge. Therefore, in order to accurately estimate refrigerant charge through modeling, the geometry of specific heat pump should be considered.

The modeling target system in this chapter is the commercial heat pump system with nominal capacity of 30 kW used in the experiments in chapter 3. The modeling process is similar to a general heat pump system, but in this modeling, the refrigerant charge amount is an output value instead of an input value, and the state value of the refrigerant is an input value, not an output value. Therefore, using this modeling, it is possible to predict the amount of refrigerant by using the sensor information. The simulation is performed under various cooling/heating conditions, and the accuracy of charge prediction through modeling is verified. In addition, the distribution of refrigerant for each system component is determined according to the amount of charge.

2.2 Heat pump modeling

2.2.1 Heat exchangers

In this modeling, the operation information is the input value. In the case of a commercial heat pump, the sensor information is very diverse, and when all of them are input to modeling, modeling is over-defined. Therefore, it is preferable to input only the operation information having a small measurement error and having a large influence on the system. Therefore, inlet and outlet pressure of the compressor were given to the modeling, in addition to operating information such as rotational speed of compressor, air flow rate at condenser and evaporator, and indoor/outdoor air temperature.

Inputs to heat exchanger modeling are air flow rate, air inlet temperature, mass flow rate of refrigerant, inlet pressure of refrigerant (condenser), outlet pressure of refrigerant (evaporator) and inlet enthalpy of refrigerant. The outputs are outlet pressure of refrigerant (condenser), inlet pressure of refrigerant (evaporator), outlet enthalpy of refrigerant, and the charge amount in the heat exchanger.

Fig. 2.1 and Fig. 2.2 illustrate the schematic diagram of flow path of outdoor heat exchanger and indoor heat exchanger, respectively. As can be

seen, the heat exchanger geometry of the commercial heat pump is very complex. Nevertheless, this geometry has been considered in detail because it affects the heat pump performance and charge amount. The figures show the refrigerant flow in the cooling mode, and in the heating mode the refrigerant flow is reversed. Therefore, air and refrigerant flow counter-cross in the outdoor unit and parallel-cross in the indoor unit when operating in cooling mode. On the contrary, in heating mode operation, air and refrigerant flow parallel-cross in outdoor unit and counter-cross in indoor unit. In addition, as shown in the figure, the refrigerant is split into nine paths on the upper side of the outdoor unit, then merged and split again to twelve paths on the lower side. In the indoor unit, the refrigerant is branched into ten paths and merged. In this process, the flow rate of the refrigerant may be divided differently for each path. However, this divided ratio is very difficult to predict, so this study assumes that it is split with the same weight. In addition, in the case of the air flow rate, it is assumed that the flow rate is evenly distributed throughout the heat exchanger. For heat exchanger modeling, the heat exchanger was subdivided following the flow direction of the refrigerant. Single part of the upper and lower side of the outdoor unit was divided into 60 elements, and also the single flow path of the indoor unit was divided into 60 elements each.

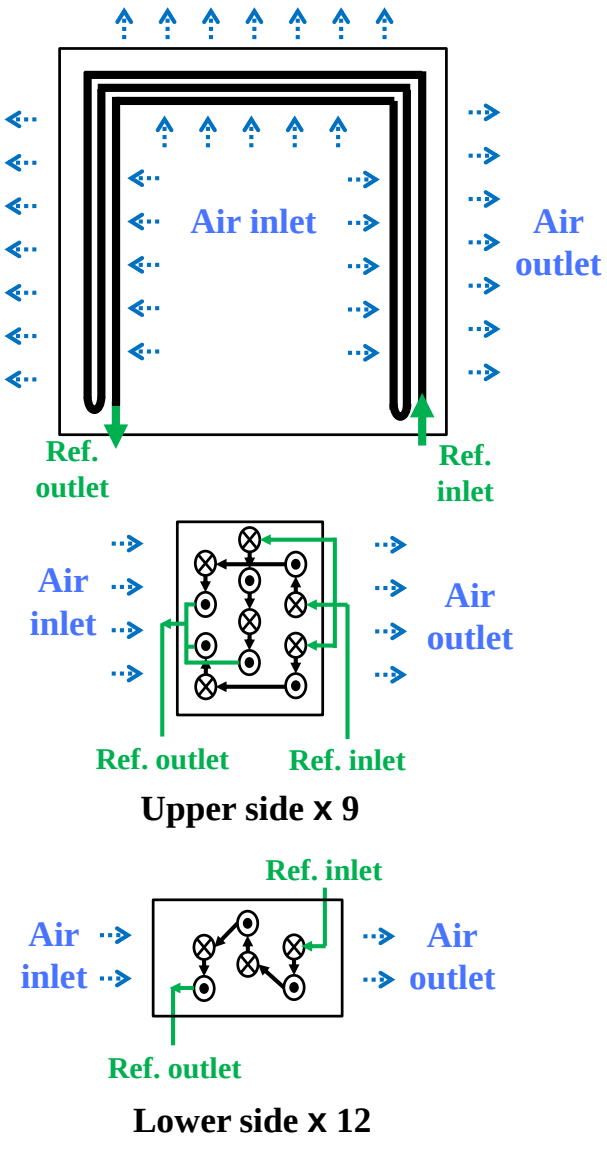

Fig. 2.1 Flow path of outdoor heat exchanger

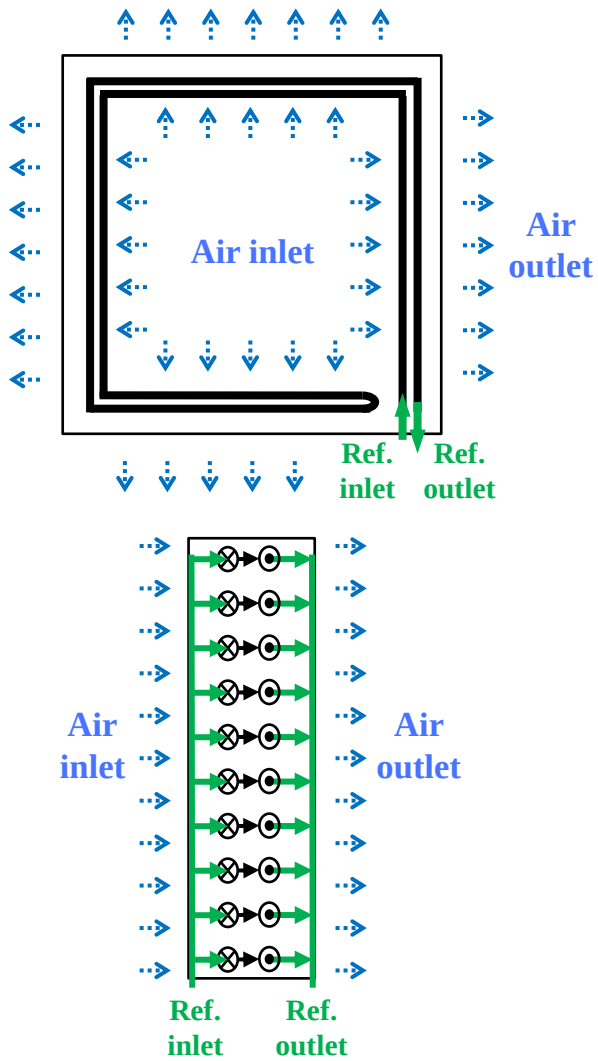

Fig. 2.2 Flow path of indoor heat exchanger

In order to perform heat exchanger modeling, the overall heat transfer coefficient must first be obtained. The overall heat transfer coefficient can be obtained from overall heat transfer resistance as in Eq. (2.1).

$$\frac{1}{UA} = \frac{1}{\eta_o U_o A_o} + \frac{1}{2}\ln\left(\frac{D_o}{D_i}\right)\frac{D_o}{k_w A_w} + \frac{1}{h_i A_i} \tag{2.1}$$

Here, since the term relating to conduction can be easily obtained, the refrigerant side heat transfer coefficient and the air side heat transfer coefficient should be obtained, individually.

The heat transfer coefficient of refrigerant side depends on the state of the refrigerant. First, if the refrigerant is in single phase, the Nusselt number can be predicted by Eqns. (2.2), (2.3). (Colburn, 1964)

$$\mathrm{Nu} = 4.36 \quad \text{(for laminar)} \tag{2.2}$$

$$\mathrm{Nu} = 0.023\mathrm{Re}^{4/5}\mathrm{Pr}^{1/3} \quad \text{(for turbulent)} \tag{2.3}$$

When estimating the Nusselt number, the assumptions may not be fully acceptable to the actual heat pump. However, considering that the air side heat exchange coefficient has a dominant influence on the overall heat exchange coefficient, the error of the refrigerant side heat transfer coefficient

is acceptable.

As Eqns. (2.4) and (2.5), the correlation of Chato (1960) was used for the condensation process. Here, the surface temperature in the tube, T_{sat}, should be predicted by trial and error in each element.

$$h = 0.555\left[\frac{g\rho_l(\rho_l - \rho_v)k_l^3 h'_{fg}}{\mu_l(T_{sat} - T_s)}\right]^{1/4} \tag{2.4}$$

$$h'_{fg} = h_{fg} + \frac{3}{8}c_{p,l}(T_{sat} - T_s) \tag{2.5}$$

Boiling coefficient was calculated using the correlation for horizontal tube of Gungor and Winterton (1986) shown in Eqns. (2.6) and (2.7). Boiling number, Bo, was calculated by trial and error in each element.

$$\frac{h_{TP}}{h_l} = 1 + 3000\mathrm{Bo}^{0.86} + \left[\frac{x}{1-x}\right]^{0.75}\left(\frac{\rho_l}{\rho_g}\right)^{0.41} \tag{2.6}$$

$$\mathrm{Bo} = \frac{q}{h_{fg}G} \tag{2.7}$$

Now, the air side heat transfer resistance should be obtained. Surface efficiency, η_o is determined by the heat exchanger geometry. Therefore, in order to obtain air side heat transfer resistance, the air side heat transfer coefficient should be obtained. The air side heat transfer coefficient can be

obtained by using Colburn j factor as Eq. (2.8). (Wang et al., 2000)

$$j = \frac{h_o}{\rho_{air} V_{max} C_{P_a}} Pr^{2/3} \tag{2.8}$$

According to Wang et al. (2000), there are various correlations for this Colburn j factor. However, this value is highly dependent on the geometry of the heat exchanger and has a great impact on the results. Therefore, using the Colburn j factor derived through actual system experiments can contribute to the improvement of modeling accuracy. The basic form of the Colburn j factor is shown in Eq. (2.9).

$$j = C_1 \mathrm{Re}_{\mathrm{d_c}}^{\mathrm{C_2}} \tag{2.9}$$

In this study, C_1 and C_2 values were derived experimentally for the condenser and evaporator.

Next, the pressure drop in the heat exchanger should be calculated. For single phase pressure drop, the friction factor for laminar and turbulent flow can be applied as shown in Eqns. (2.10), (2.11), and (2.12). (Petukhov, 1970)

$$\frac{\Delta P}{L} = f \frac{\rho}{2} \frac{v^2}{D} \tag{2.10}$$

$$f = \frac{64}{\mathrm{Re}} \quad \text{(for laminar)} \qquad (2.11)$$

$$f = (0.790 \ln \mathrm{Re_D} - 1.64)^{-2} \quad \text{(for turbulent)} \qquad (2.12)$$

For 2-phase region pressure drop, Muller-steinhagen and Heck correlation (1986) was used as Eq. (2.13).

$$\left(\frac{dP}{dL}\right)_{tp} = \left(\left(\frac{dP}{dL}\right)_l + 2\left(\left(\frac{dP}{dL}\right)_g - \left(\frac{dP}{dL}\right)_l\right)x\right)(1-x)^{1/3} + \left(\frac{dP}{dL}\right)_g x^3 \qquad (2.13)$$

Through previous heat exchanger modeling, it is possible to predict the state change of the refrigerant in the heat exchanger. Then, the refrigerant charge in the heat exchanger can be calculated. In case of single phase region, charge amount is a product of inner volume of heat exchanger and the density of the refrigerant. For 2-phase region, the void fraction should be predicted. A void fraction correlation for horizontal tube suggested Rouhani (1969), which is shown in Eq. (2.14), was used to predict the void fraction in condenser and evaporator.

$$\varepsilon = \frac{x}{\rho_G}\left[\left(1 + c_0(1-x)\right)\left(\frac{x}{\rho_G} + \frac{1-x}{\rho_L}\right) + \frac{C_U(1-x)\left[\frac{g\sigma(\rho_L - \rho_G)}{{\rho_L}^2}\right]^{\frac{1}{4}}}{\dot{m}}\right]^{-1} \quad (2.14)$$

The c_o and C_u values are empirical values that vary with operating conditions and geometry of the heat exchanger. Therefore, the two coefficients were determined using the experimental results to minimize the prediction error of the charge amount. Once the void fraction is obtained, the refrigerant charge of the 2-phase region can be calculated.

Through the modeling process, it is possible to calculate the state change of the refrigerant in the condenser and evaporator. Also, the refrigerant charge in the heat exchanger can be predicted.

2.2.2 Compressor and expansion device

The commercial heat pump system, which is the modeling target, is equipped with a 62 cc scroll compressor. In compressor modeling, the input properties are suction pressure, discharge pressure, and suction temperature. This results in mass flow rate of refrigerant, and discharge temperature. Compression process of scroll compressor can be assumed to be a polytropic process. Then, the specific volume of discharged refrigerant can be calculated as Eqns. (2.15), (2.16)

$$n = \frac{\ln P_s/P_d}{\ln v_d/v_s} \tag{2.15}$$

$$v_d = \left(\frac{P_s}{P_d}\right)^{\frac{1}{n}} v_s \tag{2.16}$$

Here, the temperature and the enthalpy of the discharged refrigerant also can be easily found. The mass flow rate from the compressor can be obtained from Eq. (2.17).

$$\dot{m}_{comp} = \eta_V \rho_s V_{disp} \omega \tag{2.17}$$

The volumetric efficiency, η_V, is a pre-obtained value from the

experiments.

In this system, an electronic expansion valve is used as the expansion device. The refrigerant isenthalpic expands in the electronic expansion valve, so in steady-state modeling, the expansion valve can be simplified as the following Eq. (2.18).

$$i_{eev,in} = i_{eev,out} \tag{2.18}$$

2.2.3 Lubricant and other components

The compressor of the heat pump system is filled with oil for lubrication. If phase separation of lubricant and refrigerant occurs, lubrication cannot be performed properly and may cause compressor failure. Accordingly, the refrigerant and the lubricant have a high solubility to each other. As a result, there large amount of refrigerant may exist in the lubricant.

Ideally, lubricants present only in the compressor, but some lubricants are inevitably discharged from the compressor with refrigerant. Therefore, the oil separator for the recovery of such lubricant is provided in the compressor. Most of discharged oil is returned to the compressor through oil separator. Therefore, most lubricants are always present in the compressor. According to Kim (2015), the lubricant amount out of compressor is less than 1% of the total system volume. Therefore, most of the lubricant effects occur only in the compressor. In addition, it is difficult to predict the actual amount of lubricant circulating the system because it is very difficult to measure the amount of oil discharged from the compressor. Therefore, only the lubricant in the compressor is considered in this study.

The compressor of the modeling target was filled with 3 kg of lubricant. In order to calculate the refrigerant charge dissolved in the lubricant, it is necessary to predict the lubricant temperature, and pressure and the

solubility of the refrigerant. First, the lubricant pressure is the same as the suction pressure due to the compressor structure. In general, the temperature of oil is not measured, so it must be obtained by calculation. Oil temperature correlation for scroll compressor suggested by Navarro et al. (2012) calculates the temperature of oil from measuring temperature as shown in Eq. (2.19).

$$T_{oil} = 0.388\,T_{discharge} + 0.36\,T_{comp,\,inlet} + 0.22\,T_{amb} \tag{2.19}$$

Then, the solubility of the refrigerant can be found from the empirical correlation proposed by Geller and Lapardin (2016) as Eq. (2.20). Where the coefficients a_{ij} are given value for the combination of refrigerant and lubricant.

$$P = \sum_{i=0}^{3}\sum_{j=0}^{2} a_{ij}\,T^{i}x_{sol}^{j} \tag{2.20}$$

From the solubility and the charged amount of lubricant, the dissolved amount of refrigerant can be obtained.

Finally, charge amount in other components should be calculated, such

as liquid line, vapor line, and accumulator that do not affects the refrigerant state, but contain significant amount of refrigerant. In these components there is no state change of the refrigerant. Thus, the refrigerant in such charge container is given by Eq. (2.21) or Eq. (2.22).

$$m_{ll} = V_{ll}\rho_l \quad \text{(single phase)} \quad (2.21)$$

$$m_{ll} = (1-\varepsilon)V_{ll}\rho_l + \varepsilon V_{ll}\rho_v \quad \text{(2-phase)} \quad (2.22)$$

2.2.4 Cycle modeling and simulating condition

With the component modeling of heat pump system, a detailed cycle modeling and simulation are possible for charge prediction. Unlikely to typical heat pump simulation, the driving information is given and then the charge amount is calculated.

Fig. 2.3 describes the flow chart of the simulation. First, driving conditions, such as in/outdoor temperature, condensing/evaporating pressure, compressor inverter speed, etc. are given to modeling. Then, compressor simulation is possible using the assumed DSH. Through compressor simulation it is able to calculate the mass flow rate of refrigerant and a state of discharged refrigerant. Then, calculate the condenser. As described above, the surface temperature of the condenser tube should be obtained through trial and error. Once the surface temperature is obtained for each element, condenser outlet temperature and pressure can be calculated by condenser simulation. Next, inlet pressure of evaporator is assumed for evaporator simulation. Only the pressure of evaporator outlet is given, the pressure of evaporator inlet should be assumed and adjusted by calculation. Similarly to the condenser, the heat transfer rate of each element in the evaporator must be calculated through trial and error. Once the heat transfer rate is calculated, the boiling number, Bo, can be obtained. Using this, the evaporator can be

simulated and the pressure and temperature of evaporator outlet can be obtained. When the outlet pressure of the evaporator is different from the driving conditions, the pressure of the evaporator inlet is adjusted. If the calculated evaporator outlet pressure and the given outlet pressure of evaporator are the same, an error of DSH at compressor inlet is checked. If the calculated temperature of evaporator outlet differs from the assumed temperature of compressor inlet, the assumed DSH at the compressor inlet is adjusted.

When all the calculated values converge to the given value through the above process, the cycle simulation is completed. The total charge amount in the system can then be estimated.

Simulation conditions were set the same to experimental conditions. Simulation condition for cooling mode is shown in Table 2.1 and Simulation condition for heating mode is shown in Table 2.2.

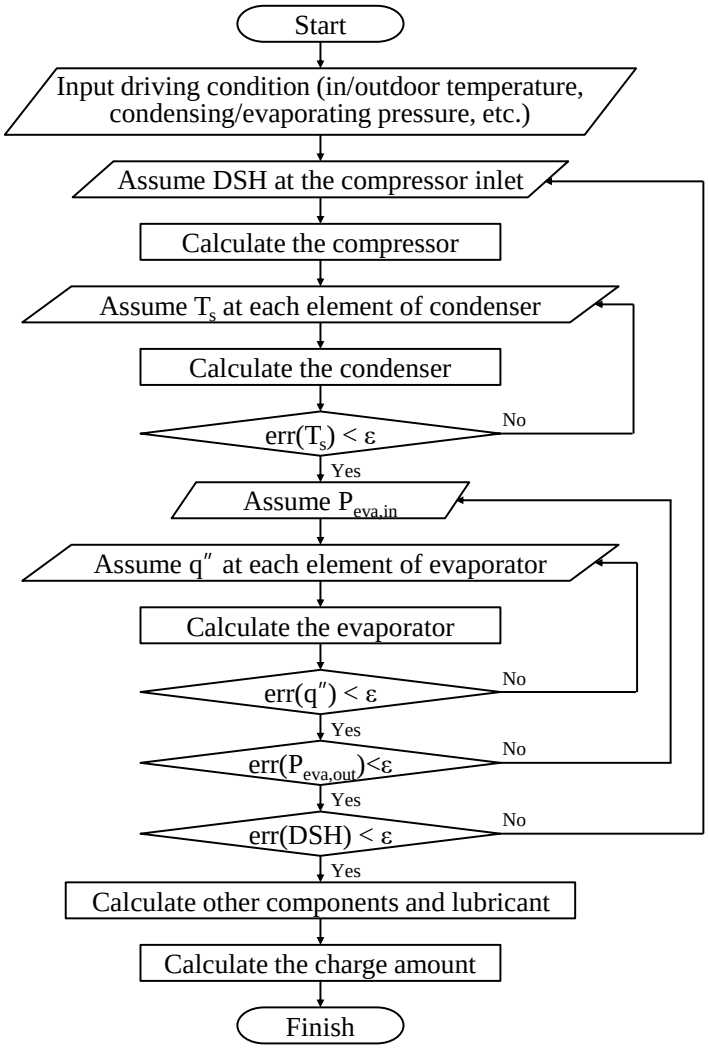

Fig. 2.3 Flow chart of the heat pump simulation

Table 2.1 Driving condition for cooling mode operation

Variables	**Values**			
Refrigerant	R410A			
Number of indoor units	2			
Driving mode	Cooling			
Charge amount (kg)	6~11 (Δ=1 kg)			
Target DSH (K)	5, 10, 15			
Air temperature condition	Rating	Low Temp.	Max load	Condensate
Indoor dry bulb temp. (^{o}C)	26.7	19.4	26.7	26.7
Indoor wet bulb temp. (^{o}C)	19.4	13.9	19.4	23.9
Outdoor dry bulb temp. (^{o}C)	35.0	19.4	46.1	26.7
Outdoor wet bulb temp. (^{o}C)	23.9	13.9	23.9	23.9
Compressor inverter speed (Hz)	60, 100	60	60, 100	60, 100

Table 2.2 Driving condition for heating mode operation

Variables	**Values**		
Refrigerant	R410A		
Number of indoor units	2		
Driving mode	Heating		
Charge amount (kg)	4~8 (Δ=0.5 kg)		
Target DSH (K)	5, 10		
Air temperature condition	High Temp	Low Temp.	Maximum Temp
Indoor dry bulb temp. (^{o}C)	21.1	21.1	26.7
Indoor wet bulb temp. (^{o}C)	15.6	15.6	-
Outdoor dry bulb temp. (^{o}C)	8.3	-8.3	23.9
Outdoor wet bulb temp. (^{o}C)	6.1	-9.4	18.3
Compressor inverter speed (Hz)	60	60	30

2.3 Simulation results

2.3.1 Charge prediction using heat pump simulation

Heat pump model simulation was performed under the same conditions to experiments. Through this, it was possible to predict the amount of refrigerant in the system according to the operating conditions. Fig. 2.4 shows the charge prediction results through simulation during the cooling mode operation. As can be seen, the accuracy of the prediction is very high. The root mean square error (RMS error) is 4.95% and the absolute average deviation (AAD) is 4.32%, which is very low. This proves that the charge amount can be accurately predicted using only sensor information under various operating conditions using heat pump simulation. Fig. 2.5 shows the charge predictions for heating mode operation. Similarly, the accuracy of charge amount prediction is very high, with RMS error 6.26% and AAD 5.62%.

This heat pump simulation takes into account complex system configuration and geometry, and at the same time includes many empirical coefficients. Thus, the simulation method cannot be applied to various heat pump systems universally. Nevertheless, the accuracy of refrigerant charge

prediction is very high and provides much information that the generalized charge prediction equation does not provide. In other words, when a variety of information, such as charge amount, refrigerant amount distribution or heat pump performance prediction in extreme undercharge case, is needed, charge prediction through heat pump simulation has an advantage.

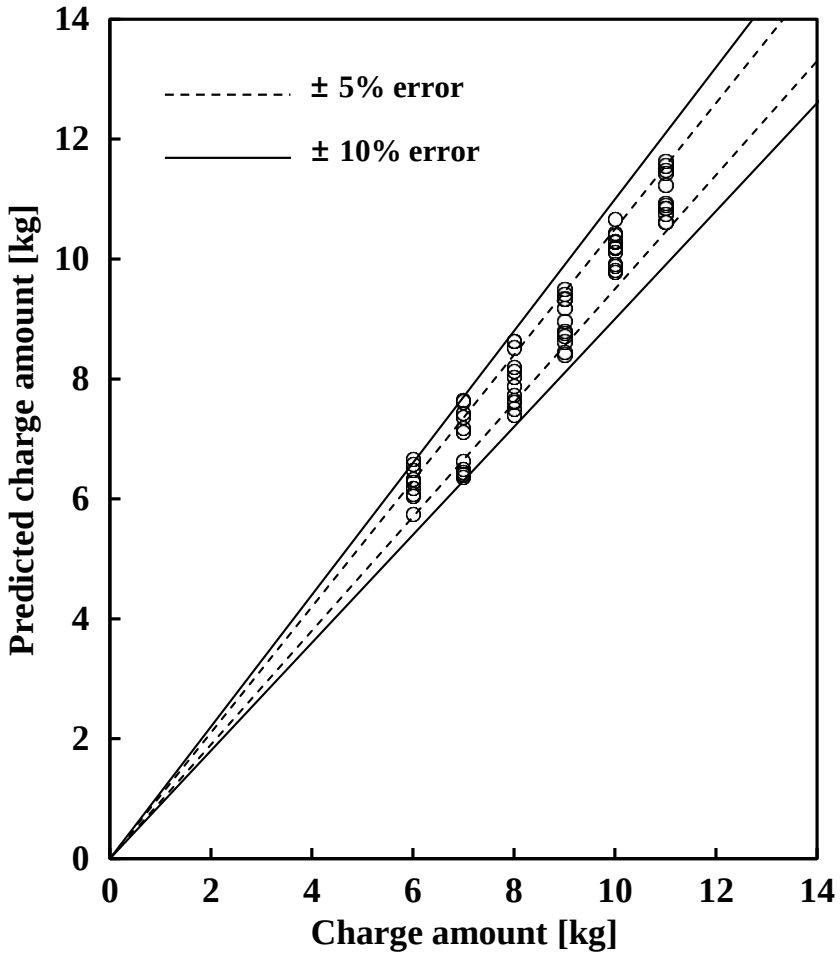

Fig. 2.4 Charge prediction result by heat pump simulation (cooling mode)

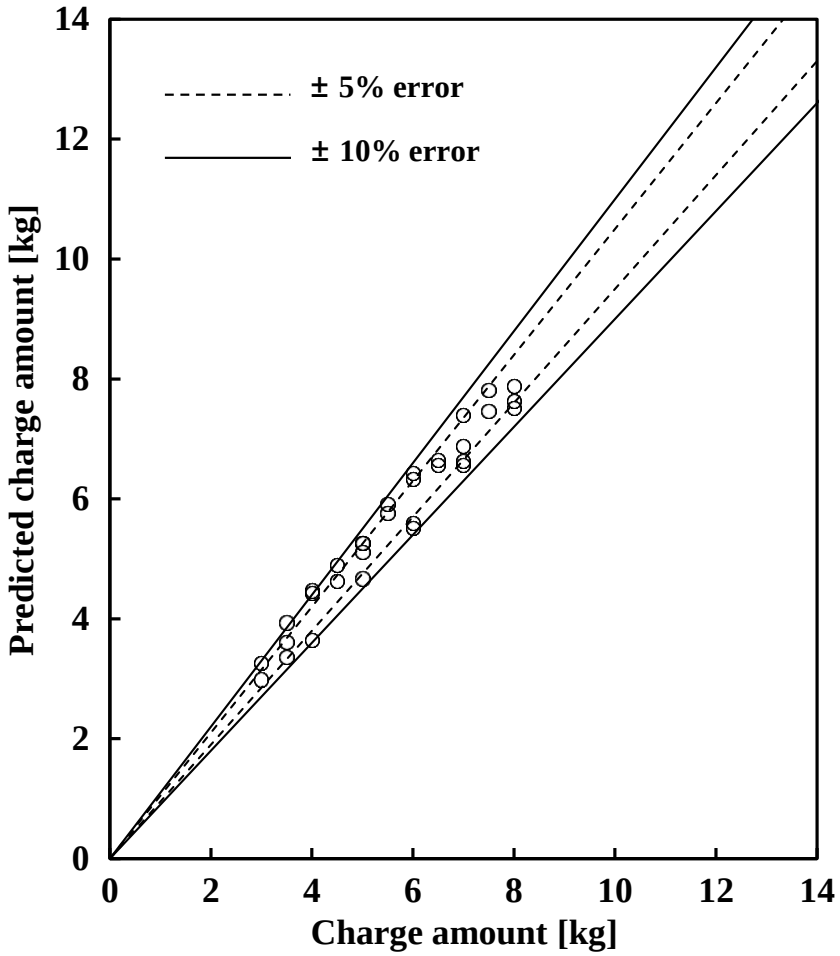

Fig. 2.5 Charge prediction result by heat pump simulation (heating mode)

2.3.2 Refrigerant charge distribution

Heat pump simulation provides a number of other information in addition to quantitative prediction of charge amount. In this part, the distribution of refrigerant in the heat pump system was analyzed for the development of the generalized charge prediction method in the next chapter. Fig. 2.6 is a diagram showing a refrigerant distribution of cooling mode operation under rating condition. As can be seen, the most refrigerant is present in the condenser. In addition, except the severely undercharge case, more than 90% of the charge amount change occurs in the condenser. Considering that the charge prediction error of the detailed simulation is 5.6%, the error of the charge prediction method may allow around 5~10%. Therefore, if the amount of refrigerant in the condenser can be accurately predicted, the accuracy of the charge amount prediction can be guaranteed.

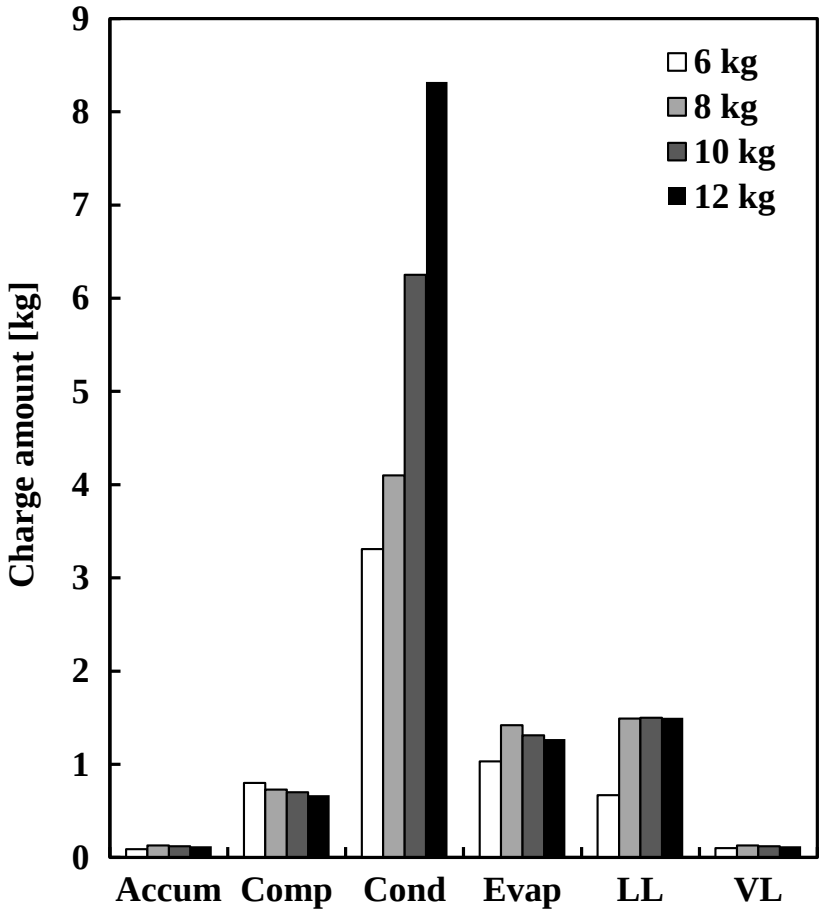

Fig. 2.6 Refrigerant distribution in each component
(cooling mode, rating condition)

2.4 Summary

There are many ways to predict the amount of charge in a heat pump system. However, in order to reduce the cost of charge prediction and improve the accuracy, it is necessary to propose a method based on a physical model. The first physics-based prediction method is charge prediction through heat pump simulation. In this chapter, detailed modeling of the heat pump system was performed. The modeling target was a commercial air source heat pump system used in the experiment. First, component modeling for the compressor, condenser, evaporator, and expansion valve was performed in detail. In particular, the geometry of the condenser and evaporator is considered in detail because the geometry of the heat exchanger can affect the simulation results. In addition, unlike general heat pump system modeling, the effect of lubricant was considered in this modeling to accurately estimate the charge amount. Since several empirical coefficients exist in modeling, these coefficients should be given through experiments. Finally, the heat pump was simulated using the completed model. Here, the charge amount is an output value, not an input value, and through this process, the amount of refrigerant charge according to the operation information could be predicted.

The predicted refrigerant charge through simulation was compared with

experimental results. The RMS error of the simulation-based charge prediction was very high at 4.95% in cooling mode. In the heating mode, the RMS error was 6.26%.

Simulation based charge prediction method has several advantages. First, the refrigerant charge amount can be predicted in all charge level. In addition to the charge amount, various information such as the performance of the heat pump and the refrigerant distribution can be predicted through the simulation. In order to develop the generalized charge prediction method in the next chapter, prediction of the refrigerant distribution was performed. As a result, most of the refrigerant charge in the heat pump is present in the condenser. In addition, more than 90% change in refrigerant charge occurs in the condenser. Therefore, it was found that even if only the charge amount in the condenser is accurately predicted, the total refrigerant charge amount can be accurately predicted.

Chapter 3. Generalized charge prediction method for air source heat pump systems

3.1 Introduction

In the previous chapter, heat pump simulations accurately predicted refrigerant charge. However, the geometry and configuration of the heat pump system is so complex that much validation data is still needed for high accuracy. Also, because complex systems were described in detail, one model cannot be generally applied to other systems.

In order to develop a charge prediction equation applicable to various heat pump systems, the amount of refrigerant must be estimated from general phenomena in all systems. Therefore, in this chapter, the heat pump system is simplified and theoretically analyzed. This chapter presents a generalized charge prediction equation. Experiments with commercial heat pump system were performed to verify the charge prediction equation. Both cooling mode and heating mode experiments were performed with various operating conditions.

Various assumptions have to be made in order to perform

theoretical analysis of the system, which become the constraints of applying the charge prediction equation. Therefore, various extended charge prediction equation may exist to overcome this limitation. In this chapter, a charge prediction method while transient driving, and a charge prediction method with extremely limited number of sensors are presented and verified experimentally.

3.2 Development of charge prediction equation

In The amount of refrigerant charge in the system should be predicted only with sensor information during system operation. However, the amount of refrigerant that does not circulate the system, generally the refrigerant stored in the receiver or accumulator, does not affect the sensor information at all. In other words, the system operation information is completely identical when the receiver is filled with liquid refrigerant or completely empty although the charge amount in the system is significantly different. Therefore, it is impossible to predict the charge amount in the refrigerant charge buffer, such as the receiver or the accumulator, by using operation information. Therefore, in this study, it is assumed that no refrigerant is contained in the charge buffer in order to minimize the influence of the receiver or the accumulator, which is an acceptable assumption if the system has been operating for a while.

Also, some refrigerant is dissolved in compressor lubricant. Nevertheless, the temperature inside the compressor is always higher than other components of the system. Since the solubility of the refrigerant is low as the oil temperature is high, it can be assumed that the amount of refrigerant dissolved in the compressor oil is relatively

small and constant.

Except for the charge buffer and compressor oil, the refrigerant in the system exists in four parts; condenser, evaporator, liquid line and vapor line connecting the indoor unit and the outdoor unit. Here, the refrigerant is in a low-pressure state until it is compressed in the compressor after passing through the expansion valve, and is in a high-pressure state after being compressed in the compressor until passing through the expansion valve. A section where the refrigerant is in a high pressure state is called a high pressure section, and a section where a refrigerant is in a low pressure state is called a low pressure section. In other words, the condenser and the liquid line belong to the high pressure section while the evaporator and the vapor line belong to the low pressure section.

The refrigerant passing through the expansion valve flows into the low pressure section in a two-phase state. The refrigerant receives heat from the evaporator and completely evaporates, and flows into the compressor through the vapor line. That is to say, there is no section in which the refrigerant exists in the liquid state in the low pressure section, and only the two-phase section and the superheated vapor section exist. On the other hand, in the case of the high pressure

section, the superheated refrigerant discharged from the compressor flows into the condenser and becomes liquid state. This liquid refrigerant goes to the expansion valve, the inlet of the low pressure section, through liquid line without heat exchange. Therefore, a considerable amount of liquid refrigerant exists in the liquid line and the condenser. Fig. 3.1 shows the distribution of liquid refrigerant in the heat pump system. As can be seen in the figure, most of the liquid refrigerant is in the liquid line and the condenser, that is, the high pressure section.

Since the density difference between the liquid refrigerant and the vapor refrigerant is very large, in general cases, 100 times or more, most of the refrigerant exists in a liquid state in terms of the mass ratio of total refrigerant. Therefore, it is important to estimate the amount of the liquid refrigerant when predicting the amount of refrigerant charge in the entire system. As described previously, since most of the liquid refrigerant exists in the high pressure section, it is most important to predict the variation in the refrigerant amount in the high pressure section in estimating the total refrigerant amount. As shown in previous chapter, refrigerant charge changes in the condenser and the liquid pipe has a dominant effect on the total refrigerant charge change

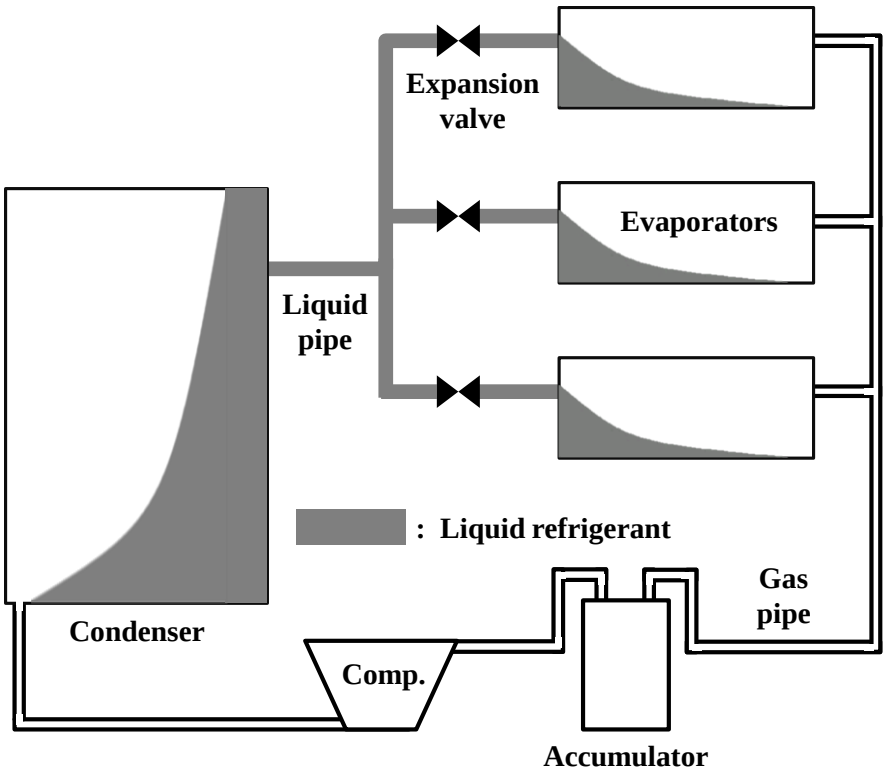

Fig. 3.1 Distribution of liquid refrigerant in the heat pump system (cooling mode operation)

in the system. The low pressure side contains less than 30% of the total charge, and the change is less than 10% of the total charge change. Therefore, if the amount of refrigerant in the high pressure side can be accurately predicted, even if the charge amount in the low pressure side is treated as a constant, the charge amount in the system can be predicted with high accuracy. This can be expressed by the following Eq. (3.1).

$$m_{total} = m_{hps} + m_{lps} \approx m_{hps} + C^* \quad (3.1)$$

In this study, the charge prediction equation should be suitable for all air source heat pump systems, thus a complicated modeling that reflects the characteristics of each system is not appropriate in this case. Therefore, in order to predict the charge amount in the high pressure side, the refrigerant status in the condenser is simply schematized as shown in Fig. 3.2.

If the system is severely undercharged, the refrigerant may not be fully liquefied in the condenser and may exit the condenser in a two-phase state. However, in this case, the undercharged state can be easily diagnosed by measuring DSC. Therefore, excessive undercharge case

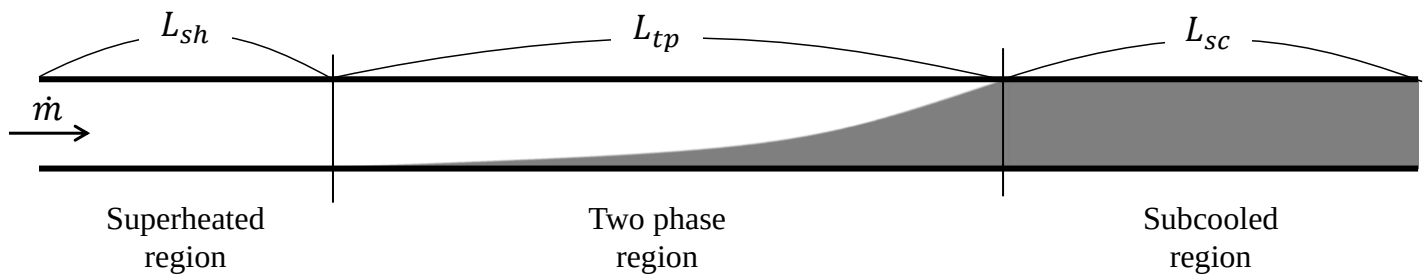

Fig. 3.2 Refrigerant status in the condenser

was not considered in this paper. In general, the liquid pipe is fully filled with the liquid refrigerant because the refrigerant is completely liquefied in the condenser. At this time, the amount of refrigerant in the liquid pipe is a product of the volume of the liquid pipe and the liquid refrigerant density as shown in the Eq. (3.2).

$$m_{ll} = V_{ll}\rho_{ll} \tag{3.2}$$

V_{ll}, the volume of the liquid pipe, is constant since it does not change after installation of the system, and the density of the liquid refrigerant is also constant regardless of the driving status. Therefore, the charge amount in the liquid pipe m_{ll} is constant. The refrigerant amount of high pressure section is the sum of the amount of refrigerant in the condenser and the liquid line. Since the charge amount in the liquid line is constant, the amount of high pressure section refrigerant can be expressed by the following Eq. (3.3).

$$m_{hps} = m_{cond} + m_{ll} = m_{cond} + C^{**} \tag{3.3}$$

Now, it is required to estimate the charge amount in the

condenser to predict the charge amount in the system. Since the density difference between vapor refrigerant and liquid refrigerant is very large, the amount of refrigerant in the condenser increases as the amount of liquid refrigerant increases. Therefore, the longer the section in which the refrigerant exists as a liquid phase in the condenser, the greater the amount of refrigerant in the condenser. As shown in Fig. 3.2, when the length of the subcooled region L_{sc} becomes longer, the amount of refrigerant in the condenser m_{cond} increases. For typical air source heat pump system, the two variables have a linear relationship with each other as Eq. (3.4).

$$m_{cond} = kL_{sc} + C^{***} \tag{3.4}$$

In the condenser, the contribution of the vapor refrigerant is relatively low. Also, many researchers reported that the void fraction is relatively high even if the quality of the refrigerant is very low. (Hughmark, 1962; Zivi, 1964) In other words, there is almost no liquid refrigerant in the two-phase region. Thus, not only the amount of superheated vapor refrigerant and the two-phase refrigerant is small, but also the change does not greatly affect the total charge amount. As

a result, if the length of the subcooled region can be predicted, the amount of refrigerant in the entire condenser can be obtained through Eq. (3.4).

However, the length of the subcooled region is related to various operating parameters such as refrigerant flow rate, refrigerant pressure, and air temperature. Therefore, it is not easy to predict it generally without using the empirical formula.

In this paper, instead of directly calculating the length of the subcooled region, a new variable called the length of the 2-phase region and the superheated region is introduced. As can be seen in Fig. 3.2, the condenser can be divided into three sections; superheated region, two-phase region, and subcooled region. The length of the subcooled region is the remaining length excluding the length of the superheated region L_{sh} and the length of the two-phase L_{tp} region in the length of the whole condenser L_{cond} as shown in Eq. (3.5).

$$L_{sc} = L_{cond} - L_{sh} - L_{tp} \tag{3.5}$$

Here, L_{cond} is constant, since it is a fixed value for each system. Therefore, L_{sh} and L_{tp} should be predicted to estimate the length of the

subcooled region.

In contrast to the difficulty of directly predicting the length of the subcooled region, the length of the two-phase region can be predicted accurately through the analysis of the heat exchange process in the condenser. First of all, to analyze the heat transfer process in the two-phase region, the two-phase region is divided into N small sections as shown in Fig. 3.3.

The quantity of heat transferred to the air from the refrigerant in each section is a value obtained by multiplying the heat flow rate per length Q'_k by the length of the section l. As shown in Eq. (3.6), the enthalpy change of refrigerant in each section should be the quantity of transferred heat divided by the mass flow rate $\dot{m}$ of the refrigerant.

$$\Delta i_k = i_{k+1} - i_k = \frac{Q'_k l}{\dot{m}} \tag{3.6}$$

The sum of the enthalpy change of the refrigerant of each section is the enthalpy change from the inlet to the outlet of the two-phase region. Since the refrigerant at the inlet of this region is a saturated vapor state and the refrigerant at the outlet is a saturated liquid state, the enthalpy change from the inlet to the outlet is equal to the latent

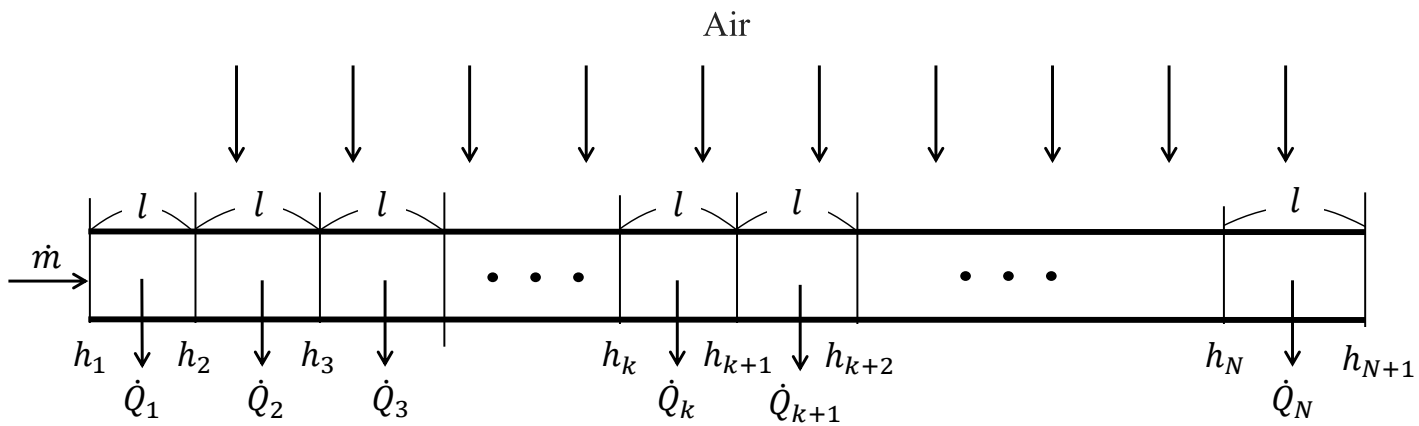

Fig. 3.3 2-phase refrigerant flow in a condenser

heat of the refrigerant. By this reason, the total enthalpy change in the two-phase region can be expressed as Eq. (3.7).

$$h_{fg} = \sum \Delta i_k = \sum \frac{Q'_k l}{\dot{m}} \tag{3.7}$$

The transferred heat quantity Q_k for each section is a value obtained by multiplying the heat flow rate per unit length Q'_k by the length of the section l. Since Q_k can be expressed by Eq. (3.8), which is the basic heat transfer equation, the heat flux per length can be expressed as Eq. (3.9).

$$Q_k = (UA\Delta T)_k \tag{3.8}$$

$$Q'_k l = U_k A_k \Delta T_k \tag{3.9}$$

Since the two-phase region is the phase change region, the temperature of the refrigerant in the tube does not change. In addition, the temperature of the inlet air is assumed uniform throughout the heat exchanger. Therefore, T_k is constant as the difference between the condensation temperature of refrigerant and the air inlet temperature as shown in Eq. (3.10).

$$\Delta T_k = T_{sat} - T_{air\ inlet} = \Delta T_{cond} = constant \tag{3.10}$$

In addition, since the heat transfer coefficient of the refrigerant during phase charge is much larger than the heat transfer coefficient of air. In other words, the heat transfer coefficient of the air has a dominant influence on the overall heat transfer coefficient. Additionally, the variation of heat transfer coefficient of air is very small under normal operating conditions. (Wang et al., 2000) Therefore, $U_{k,air}A_k$ can be expressed by Eq. (3.11), where the heat exchange area A_k is proportional to the length of the section l.

$$U_k A_k \approx U_{k,air} A_{k,air} = k^* l \tag{3.11}$$

As a result, the heat transfer coefficient for each section is a function of T_{cond} only as shown in Eq. (3.12).

$$Q'_k l = U_k A_k \Delta T_k = k^* l \Delta T_{cond} \tag{3.12}$$

From Eqns. (3.7) and (3.12), the following Eq. (3.13) can be derived. In this equation, the total sum of each section, Nl, is equal to

the length of the 2-phase region L_{tp}, and L_{tp} can be expressed as Eq. (3.14).

$$h_{fg} = \sum \Delta i_k = \sum \frac{Q'_k l}{\dot{m}} = \frac{k^* \Delta T_{cond}}{\dot{m}} Nl = \frac{k^* \Delta T_{cond}}{\dot{m}} L_{tp} \tag{3.13}$$

$$L_{tp} = \frac{h_{fg}}{k^*} \frac{\dot{m}}{\Delta T_{cond}} \tag{3.14}$$

Next, the length of the superheated region should be predicted. Unlike the 2-phase section, the heat transfer coefficient of the refrigerant must be considered in the superheated region. However, it is very difficult to accurately obtain the heat transfer coefficient of the refrigerant. In other words, if the superheated region is treated excessively in detail, it requires too much additional sensor information and computation. In addition, the superheated region is generally very short compared to the 2-phase region. Therefore, it is appropriate to predict the length of the superheated region relatively simply. This does not significantly reduce the accuracy of the prediction. The length of superheated region can be predicted by analyzing the temperature distribution in the superheated region. Fig. 3.4 shows the temperature distribution of the superheat region of the condenser. Since the specific heat of the

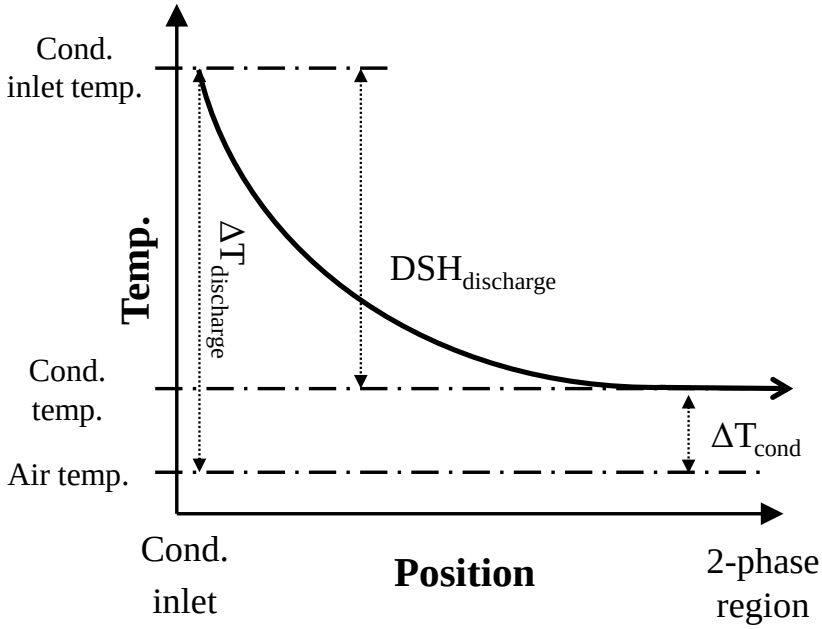

Fig. 3.4 A temperature distribution in superheated region in a condenser

refrigerant is almost constant, the amount of heat transferred in the superheated region is proportional to the DSH at the compressor discharge as shown in Eq. (3.15).

$$L_{sh} \propto \Delta i \propto \mathrm{DSH_{dis}} \tag{3.15}$$

On the other hand, the larger the temperature difference between the air and the refrigerant, the faster the heat exchange occurs, thereby reducing the length of the superheated region. That is, the average temperature difference between the inlet of the superheated region and outdoor air and between the outlet of the superheated region and outdoor air is inversely proportional to the length of the superheated region as shown in Eq. (3.16).

$$L_{sh} \propto \frac{1}{(\Delta T_{dis} + \Delta T_{cond})/2} \tag{3.16}$$

As a result, the length of the superheated region can be expressed as Eq. (3.17). Here, T_{dis} is the temperature difference between the refrigerant at compressor discharge and the condenser air inlet, and DSH_{dis} is the difference between the compressor discharge

temperature and the condensation temperature.

$$L_{sh} = k^{**} \frac{DSH_{dis}}{\Delta T_{dis} + \Delta T_{cond}} \tag{3.17}$$

The final equation for estimating the refrigerant charge is obtained here by summarizing the above equations as shown in Eq. (3.18).

$$m = -K_1 h_{fg} \frac{\dot{m}}{\Delta T_{cond}} - K_2 \frac{DSH_{dis}}{\Delta T_{dis} + \Delta T_{cond}} + C \tag{3.18}$$

In Eq. (3.18), there are two proportional constants K_1 and K_2 and one constant C in the refrigerant charge prediction equation. All of these values are specific values for each system. These can be obtained through a performance experiments. Since there are three unknowns, at least three experimental data are required to assign the value of them. However, in order to guarantee the higher reliability, it is appropriate to derive the coefficients through at least nine experimental data performed under the three different temperature conditions and three different charge amounts.

Once the coefficients K_1 and K_2 and C are obtained through experiments, the charge amount in the system can be predicted regardless of the operating condition and the system control.

The information required to use this equation is the mass flow rate, the condensing pressure (or temperature), the compressor discharge temperature of the refrigerant, and the inlet temperature of the air at the condenser. In general, compressors information such as isentropic or volumetric efficiency is given as a pre-obtained value from the compressor manufacturer. Therefore, the mass flow rate of the refrigerant can be calculated through the inlet condition of the refrigerant. Therefore, to apply the charge prediction equation, at least 4 sensors are required which are condensing and evaporating pressure (or temperature) sensors, compressor suction or discharge temperature sensors, and the condenser inlet air temperature sensor. In addition, condenser outlet temperature sensor is needed to confirm the existence of DSC in order to guarantee whether the assumptions of the charge prediction equation are satisfied. Operating information, including sensor information, required for the charge prediction equation, is summarized in Table 3.1. Typical air source heat pump system is equipped with various sensors including the aforementioned sensors,

for controlling the system. Therefore, the charge prediction equation proposed in this study can be applied to general air source heat pump systems.

Table 3.1 Required driving information and sensors or alternative sensor

Required driving information	Sensors	Alternatives
Mass flow rate of refrigerant	Mass flow meter	Pressure sensor and temperature sensor at compressor inlet
Condensing pressure	Pressure sensor at condenser	Temperature sensor at condenser mid point
Condenser inlet air temperature	Temperature sensor at condenser outside	-
Compressor discharge temperature	Temperature sensor at compressor outlet	-

3.3 Experimental verification of charge prediction equation

3.3.1 Experimental setup and procedure

An experiment was conducted to verify the accuracy of the charge prediction equation. A commercial heat pump system with nominal capacity of 30 kW which is shown in the Fig. 3.5 was used for the experiments. Fig. 3.6 shows a schematic diagram of the experimental facilities. The system is installed in an environmental chamber that can control the air temperature and humidity of the indoor chamber and outdoor chamber separately. The heat pump is composed of two identical indoor units and one outdoor unit. Since the geometry and operating conditions of two indoor units are exactly the same, they can be treated as one large indoor unit.

The compressor is located in the outdoor unit. Using the scroll type inverter compressor, the rotational speed of the compressor is controlled. Electronic expansion valves are installed in both indoor units and outdoor unit. EEVs of indoor units activate during cooling mode operation, and EEV of outdoor unit operates during heating

Fig. 3.5 Commercial heat pump
(left - indoor unit / right - outdoor unit)

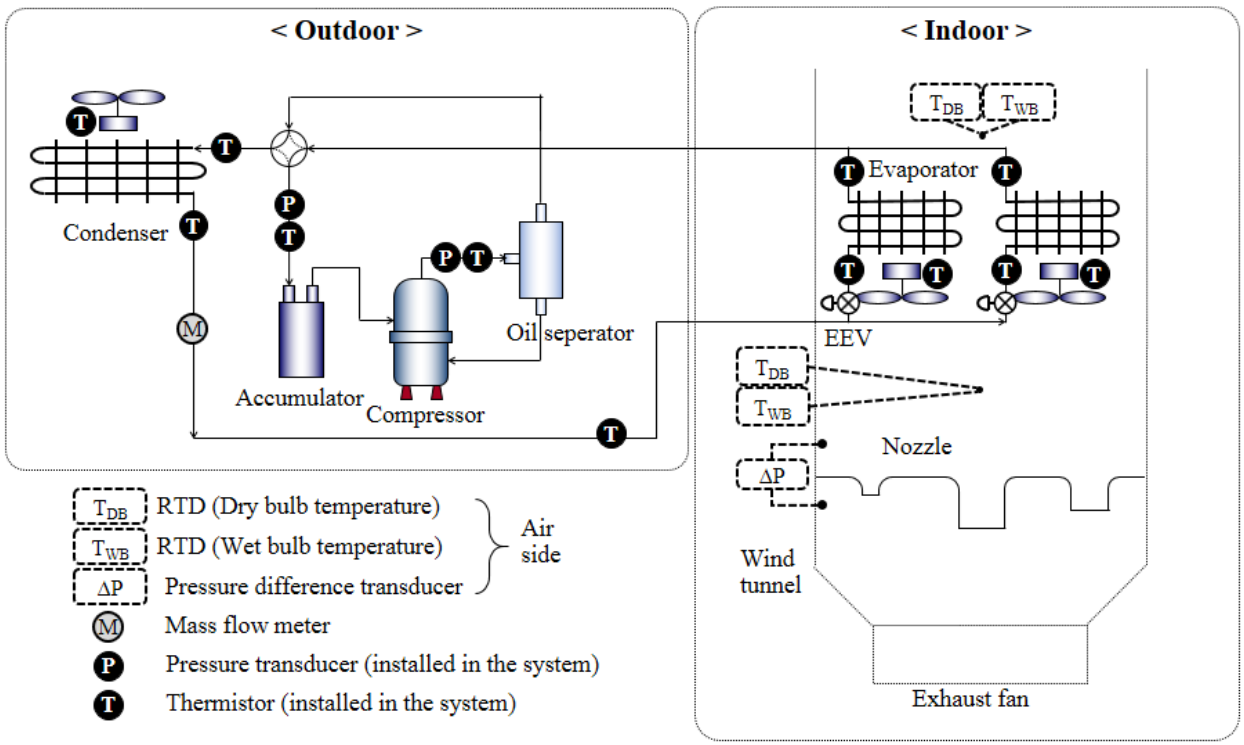

Fig. 3.6 Schematic diagram of experiment setup (commercial heat pump)

mode operation. In each case, unused EEVs were kept fully open. In order to measure the state of refrigerant and air during system operation, a number of temperature, pressure sensors and mass flow meter are installed. In addition, a wind tunnel and nozzles are installed in the indoor chamber to accurately measure the cooling (or heating) capacity of the system. Based on ANSI / AMCA 210 (2007), indoor unit capacity was calculated through air temperature, humidity and flow rate information.

Detailed experimental conditions for cooling operation and heating mode operation are shown in the Table 2.1 and 2.2, respectively. According to ANSI / AHRI Standard 1230 (2010), four temperature conditions for cooling mode and three temperature conditions for heating mode were selected. Prior to the experiment, a reference case experiment was conducted to find the optimum refrigerant charge of the system. The experimental range of refrigerant charge condition was selected approximately from 70% to 120% of the optimum charge amount.

3.3.2 Data reduction and uncertainty analysis

The optimum charge amount of the system was determined through reference case experiment. Here, the optimum charge amount is defined as a point at which the COP reaches its maximum. The cooling (or heating) capacity and the COP are calculated from the following Eqns. (3.19) and (3.20).

$$Q_{air} = \rho_{air}\dot{V}_{air}(i_{air,inlet} - i_{air,outlet}) \quad (3.13)$$

$$\mathrm{COP} = Q_{air}/W \quad (3.14)$$

The uncertainty of measurement data is shown in Table 3.2. The total error of cooling (or heating) capacity is 5.2% and the total error of COP is 5.2% on 95% confidence level.

Table 3.2 Uncertainty analysis at reference condition (commercial heat pump)

Variables	Fixed error	Random error	Total error
Pressure at condenser	0.6%	0.4%	0.8%
Pressure at evaporator	1.7%	0.3%	1.7%
Dry bulb air inlet temperature	0.20 K	0.03 K	0.21 K
Wet bulb air inlet temperature	0.19 K	0.10 K	0.21 K
Dry bulb air outlet temperature	0.18 K	0.04 K	0.19 K
Dry bulb air outlet temperature	0.18 K	0.06 K	0.19 K
Thermistor	0.70 K	0.26 K	0.75 K
Mass flow rate (refrigerant)	0.2%	0.9%	0.9%
Mass flow rate (air)	3.0%	0.5%	3.1%
Power consumption	0.4%	0.3%	0.5%
Cooling capacity	5.2%	1.8%	5.5%
COP	5.2%	1.8%	5.5%

3.3.3 Verification of charge prediction equation

The relation between the DSC and the refrigerant charge amount and the relation between $h_{fg}\dot{m}/\Delta T_{cond}$ and the charge amount are compared using the experimental results. The results are shown in Figs. 3.7 and 3.8. As the figure shows, the DSC has a positive correlation with the charge amount, but the variation of DSC is very large even under the same charge condition. This is because the DSC varies not only with the charge amount but also with the other operating conditions and the control. On the other hand, $h_{fg}\dot{m}/\Delta T_{cond}$ has a very linear relationship with the refrigerant charge amount as expected in Eqns. (3.14) and (3.18). Since this linear relationship is maintained regardless of control or operating conditions, it is appropriate to use this variable for estimating the refrigerant amount in the system.

Figs 3.9 and 3.10 represent the variation of DSC and $h_{fg}\dot{m}/\Delta T_{cond}$ with change in compressor inverter speed at the reference case experiment, respectively. Comparing Figs. 3.7~3.10, the difference between $h_{fg}\dot{m}/\Delta T_{cond}$ and other variables can be found. According to Fig. 3.9, as the compressor inverter speed increases, the mass flow rate of the refrigerant increases, thereby the DSC decreases. Also, as

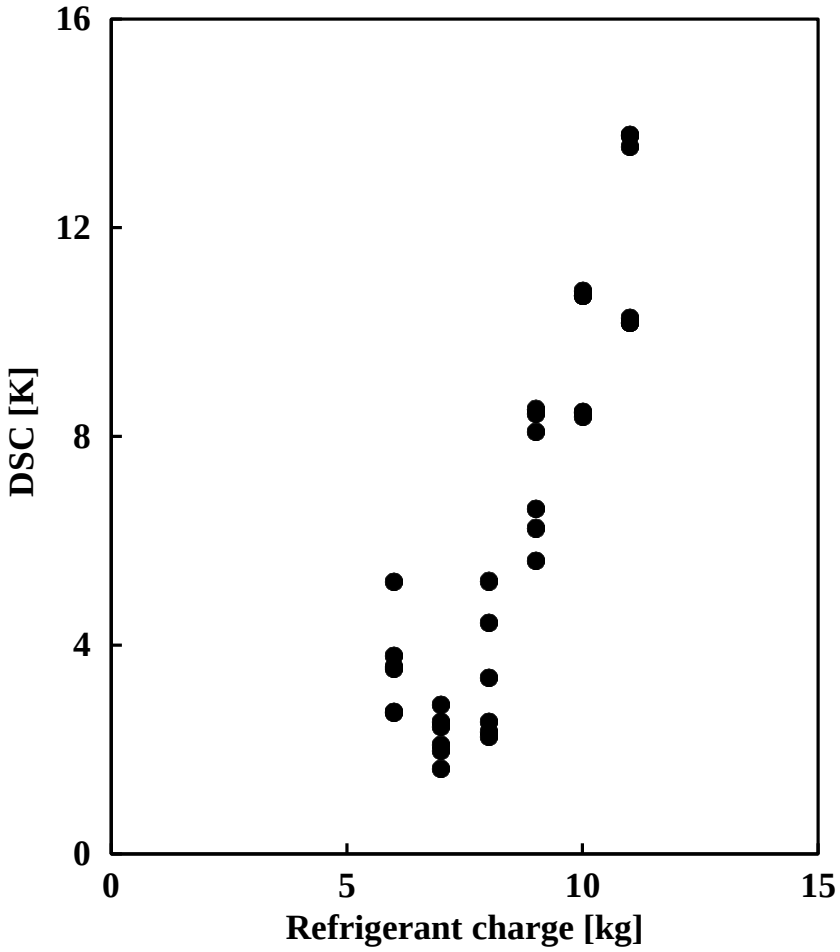

Fig. 3.7 Variation of degree of subcooled (DSC) with respect to charge amount

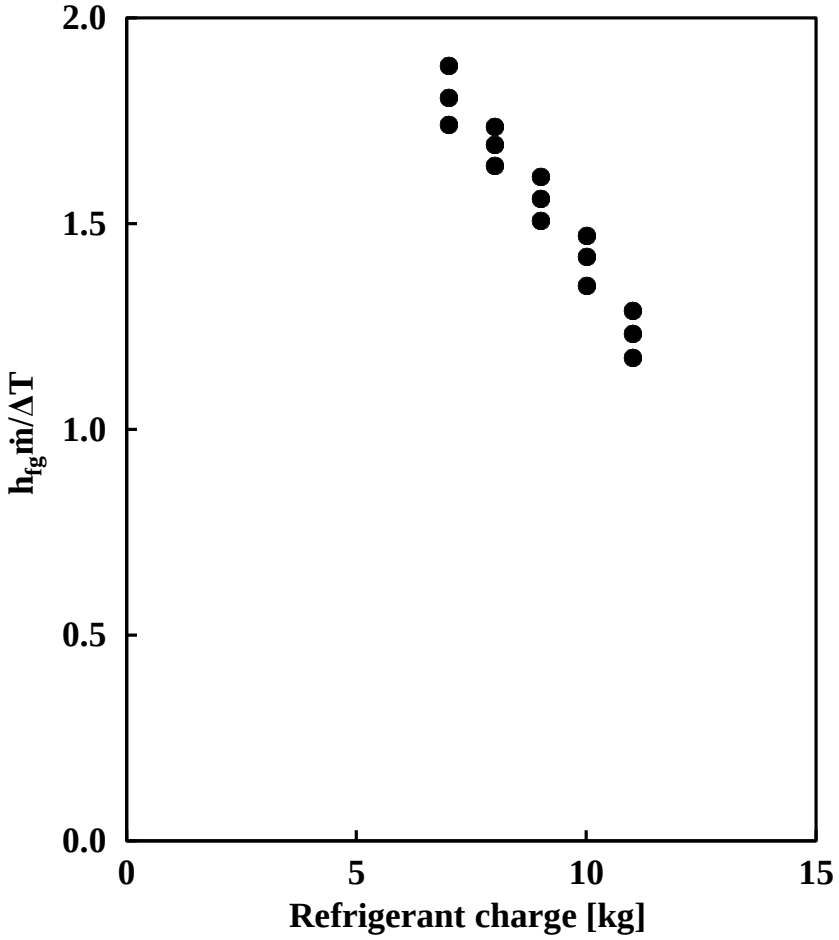

Fig. 3.8 Variation of $h_{fg}\dot{m}/\Delta T$ with respect to charge amount

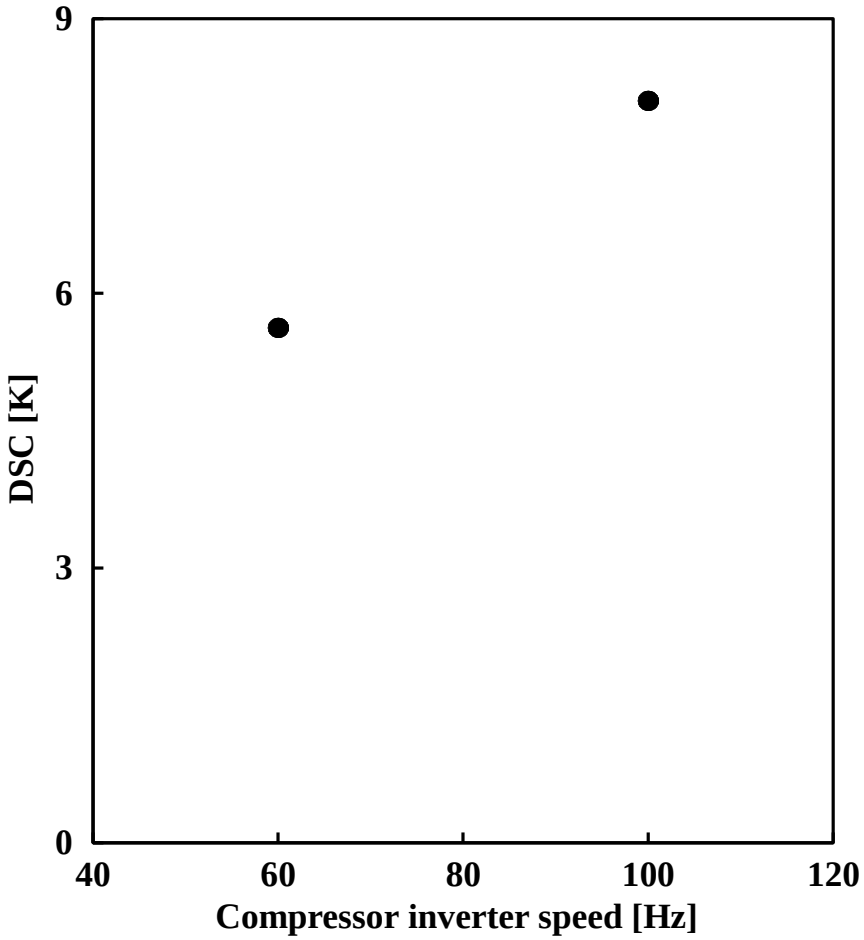

Fig. 3.9 DSC change according to compressor inverter speed

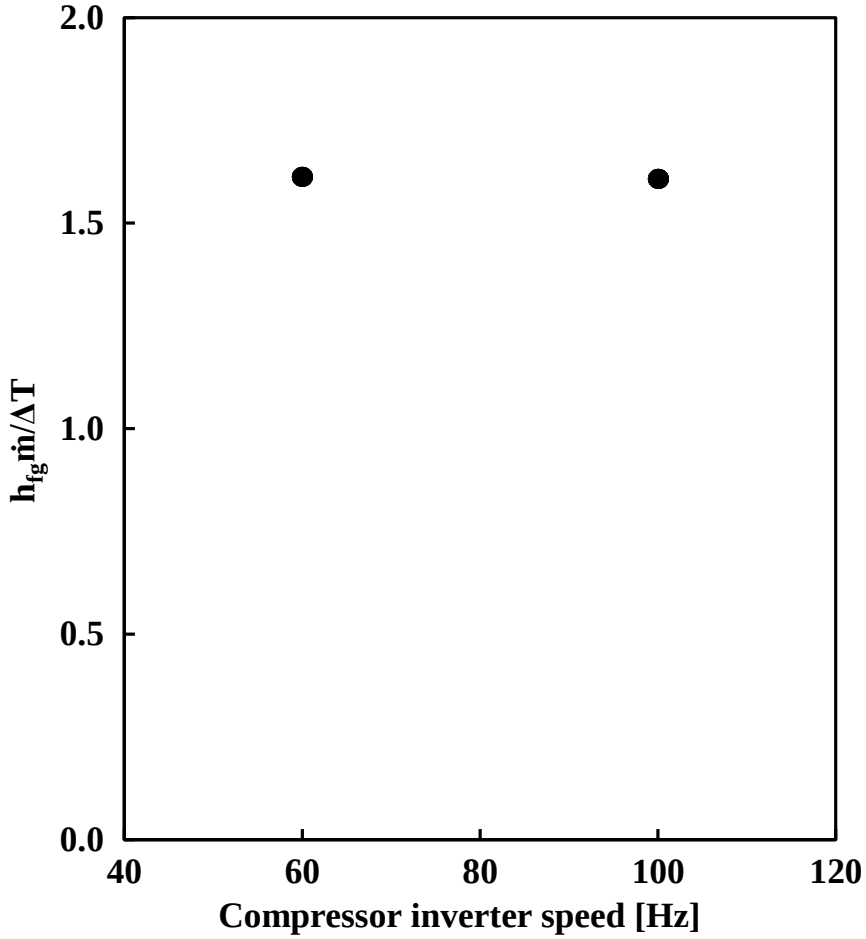

Fig. 3.10 $h_{fg}\dot{m}/\Delta T$ change according to compressor inverter speed

shown in Fig. 3.7, when the charge amount decreases, the DSC decreases as the length of the subcooled region in the condenser shorten. As a result, it is hard to distinguish whether the variation of DSC is due to operating condition transition or refrigerant amount change. On the other hand, as shown in Figs. 3.8 and 3.10, $h_{fg}\dot{m}/\Delta T_{cond}$ is sensitive to refrigerant charge change, but does not respond to operating condition transition. In addition, very similar tendency were observed in the other experimental conditions. Therefore, it can be said that $h_{fg}\dot{m}/\Delta T_{cond}$ can distinguish operating condition transition and charge amount variation. Consequently, for this reason, $h_{fg}\dot{m}/\Delta T_{cond}$ is a more appropriate variable for predicting the charged amount than others.

The accuracy of presented refrigerant charge amount prediction equation was verified by experimental data. First, the coefficients K_1, K_2 and C in the prediction equation should be obtained from the experimental data. During training and validation of the equation, experimental data with zero or very low DSC were excluded from the verification process, since the liquid line was previously assumed to be filled with liquid refrigerant. Randomly extracted 10 or 20 data sets in the cooling mode were used as a training set to obtain the

coefficients of prediction equation. The training of the equation was performed 9 times with different training sets and the results are shown in Fig. 3.11. As can be seen in the figure, even though the number of training data is very small compared to the total data, the training result is similar to the training result using the whole data. This suggests that the proposed charge prediction equation can predict the refrigerant charge even if only a small number of training data are given.

By substituting the coefficients into the charge prediction equation, Eq. (3.18), it is possible to predict the refrigerant amount with driving sensor information under the corresponding operating conditions. The figures comparing charge prediction results with actual charge for cooling and heating mode operation is shown in Figs. 3.12 and 3.13.

Fig. 3.12 displays the verifying result of the charge prediction equation under cooling mode operation. As figure shows, the accuracy is very high, where the maximum error of prediction is 9.1%. The root mean square (RMS) error is 3.7% and the average absolute deviation (AAD) is 3.0%.

Fig. 3.13 demonstrates the result to verify the charge prediction

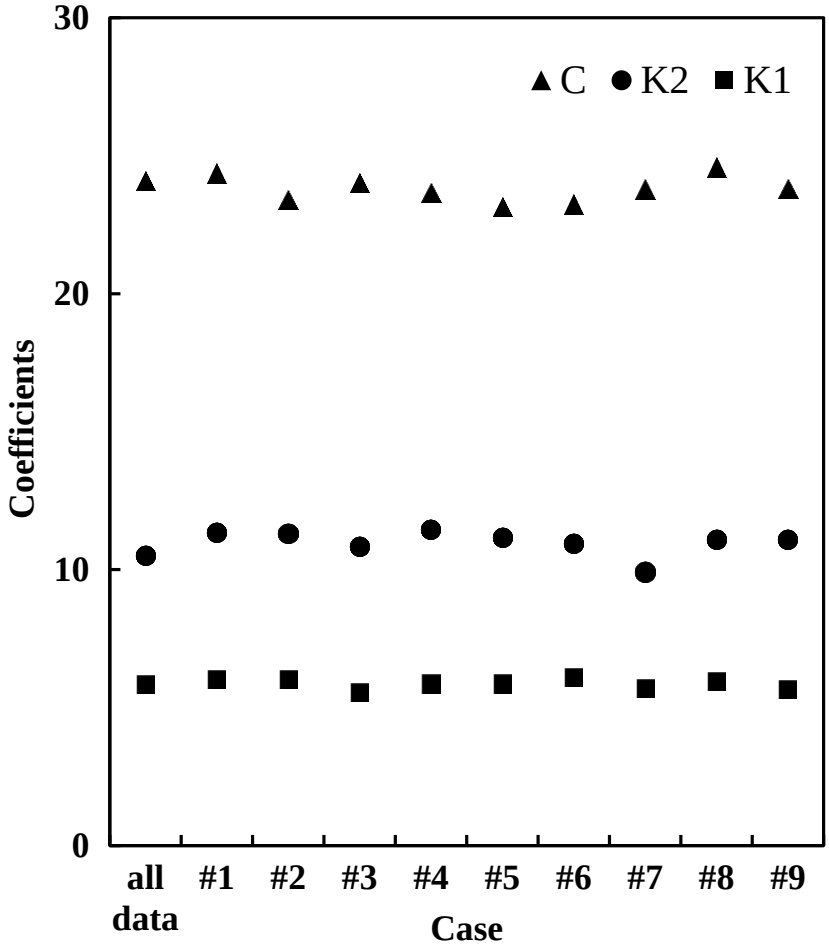

Fig. 3.11 Comparison of training results using all data sets and using limited number of data sets
(#1~#5: 10data sets, #6~#9: 20data sets)

equation under the heating mode operation. Even in the heating mode, the RMS error of the predicted refrigerant amount is 8.2% and the AAD is 6.6%. The maximum error of prediction is 14.3%, which indicates that the overall accuracy of the charge prediction equation is quite acceptable. However, the prediction error was slightly higher than that of the cooling operation, because the outdoor unit of heat pump was relatively large compared to the indoor unit. Therefore, the refrigerant variation of the evaporator of the heating operation has a greater effect than that of the cooling operation.

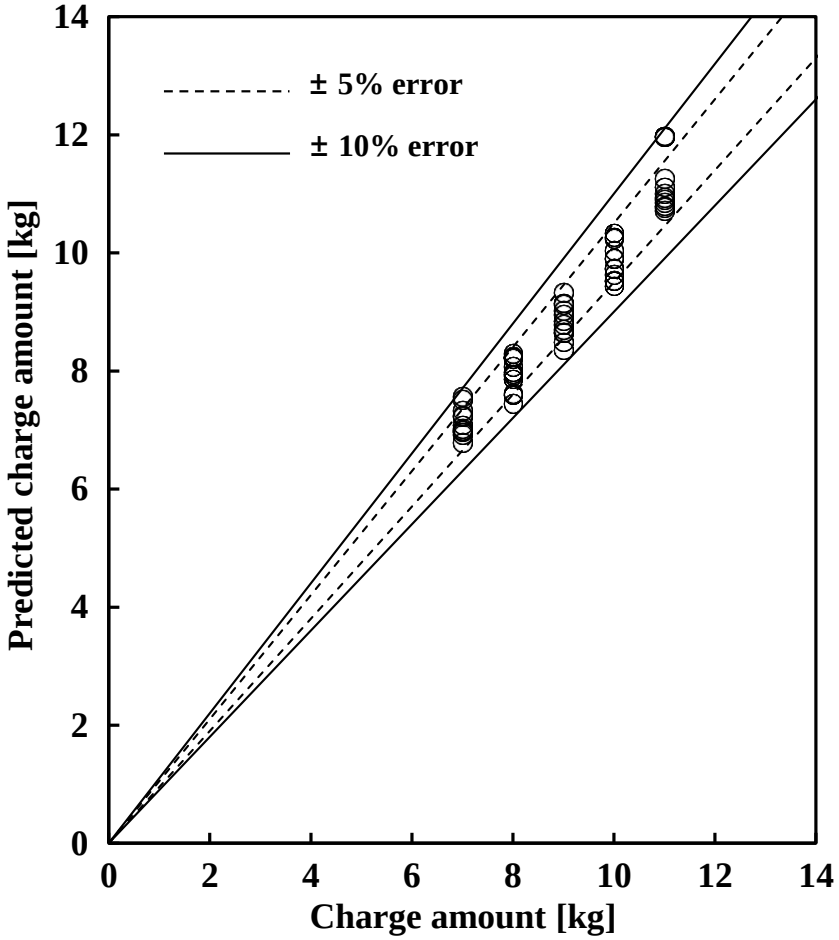

Fig. 3.12 Validation of refrigerant charge prediction equation (cooling mode)

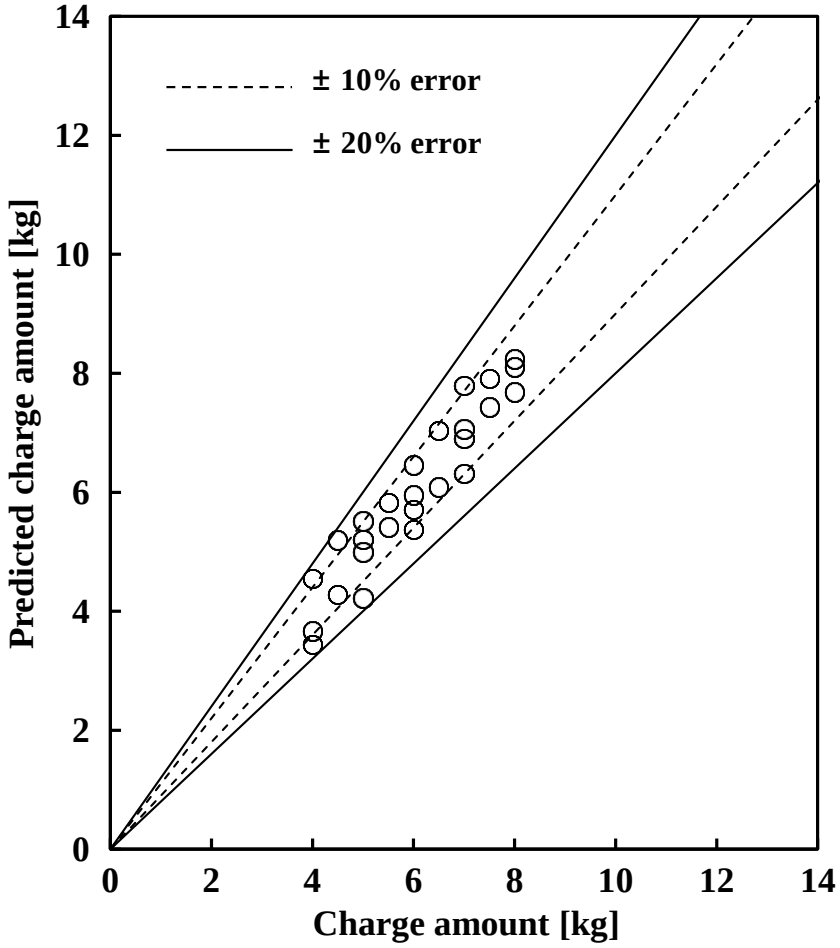

Fig. 3.13 Validation of refrigerant charge prediction equation (heating mode)

3.4 Charge prediction while continuous driving

3.4.1 Charge prediction using field test data

As demonstrated in the previous part, the charge prediction equation can accurately predict the amount of refrigerant charge in an air source heat pump system under various operating conditions. However, because there are various assumptions in the derivation of the prediction equation, there is a limit to the application range of the charge prediction equation. The steady-state of the system was assumed for charge prediction equation. Thus, the charge prediction equation is reliable only for steady-state driving. However, most of the operating conditions are transient state for common commercial and residential heat pump systems. Therefore, the accuracy of the charge prediction equation cannot be guaranteed in most situations.

About 5 month field test results of continuous heating mode driving of commercial heat pump system were given by heat pump manufacturer. (LG electronics) First of all, the charge prediction equation was trained by extracting data that satisfy the assumption of the charge prediction equation. (fixed fan speed, compressor operating,

and steady-state) Fig. 3.14 shows the prediction result of refrigerant charge using the trained equation. As can be seen, the predicted refrigerant charge fluctuates very significantly and the accuracy of charge prediction is poor. Fig. 3.15 shows the fan speed and compressor inverter frequency of the heat pump for the same period. As shown in the figure, the heat pump system responds to changing load by repeating on / off or changing compressor rotational speed and fan speed according to the change of operating conditions. This causes the heat pump to be in a transient state in most cases, thus reducing the accuracy of the charge prediction equation. Fortunately, charge prediction does not have to be done constantly. Since the maintenance or control cycle of the refrigerant charge is long, it is sufficient to be able to estimate the refrigerant amount periodically. Reliable prediction of charge amount is much more important than continuous prediction of charge amount. Therefore, during continuous charge prediction, it is necessary to determine which values are reliable and which values are not reliable.

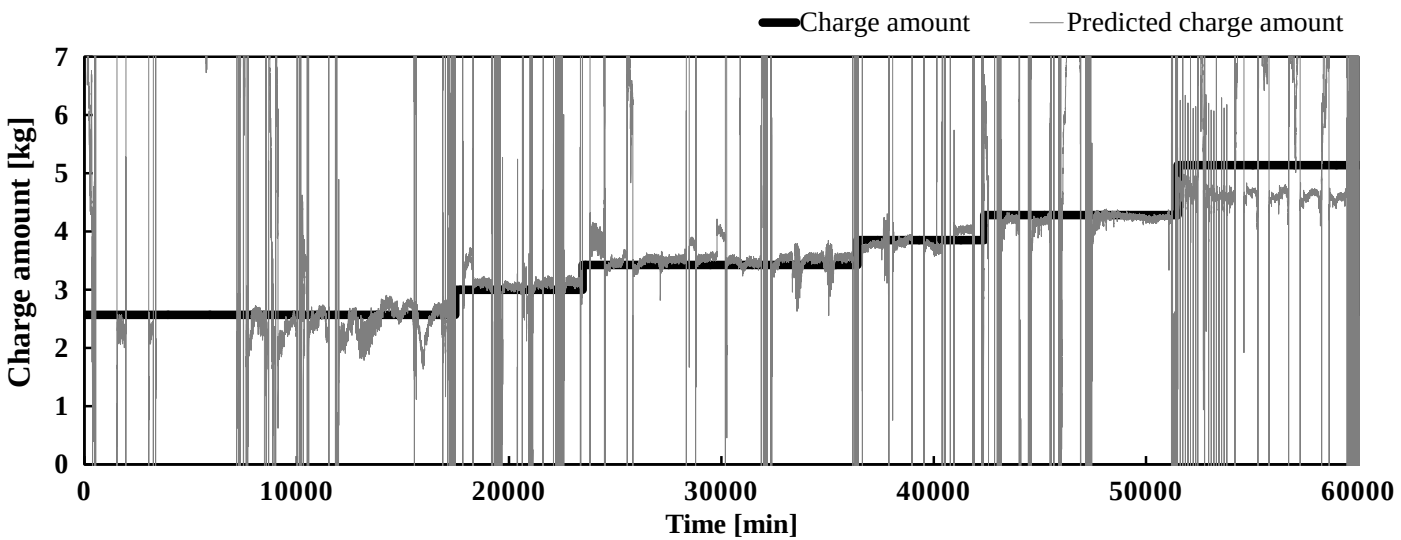

Fig. 3.14 Prediction result of refrigerant charge using continuous driving test data

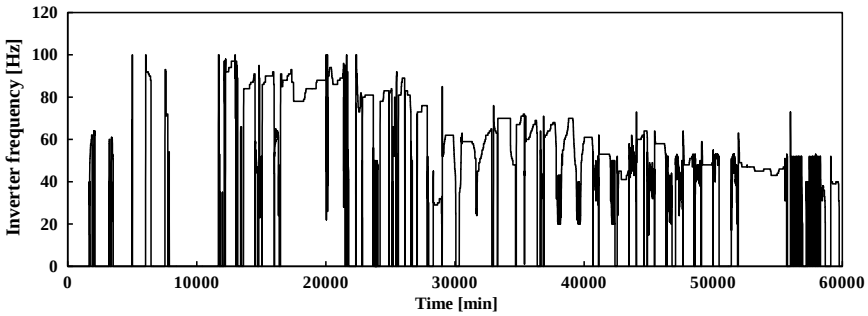

(a) Inverter frequency

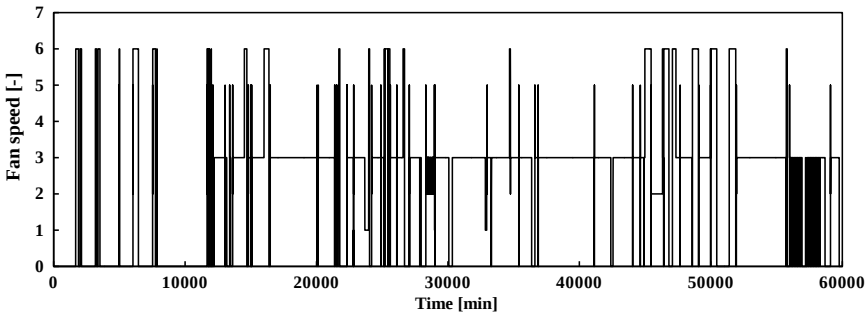

(b) Fan speed

Fig. 3.15 Driving information of heat pump system during continuous driving

3.4.2 Criteria of reliable state

The error in charge prediction arises from an error of assumption. In other words, if all of the above-described assumptions are satisfied, the accuracy of the charge prediction equation can be guaranteed. Therefore, the criteria for charge prediction during continuous operation can be suggested as follows.

1. Compressor operating
2. Fixed fan speed
3. Stable (or quasi steady)

First, the compressor must be operating. If the compressor is turned off, the mass flow rate of refrigerant which is the denominator in the charge prediction equation becomes zero, in which case the amount of charge cannot be predicted.

Second, the fan speed of heat exchangers (evaporator, condenser) must be fixed at a certain value. In most cases, the fan speed of outdoor unit is fixed close to the maximum value, so it is important that the fan speed of the indoor unit is fixed. Here, if a specific fan speed is selected, the charge prediction equation should be trained

using the data having the selected fan speed, and at the same time, the charge amount can be predicted only when the fan speed is selected value. If prediction of charge at different fan speeds is desired, new coefficients of the charge prediction equations should be obtained using the experimental results with the corresponding fan speeds.

Finally, the system should be stable. As mentioned earlier, the outdoor temperature is out of control, so a complete steady-state does not exist in real situation. Nevertheless, the accuracy of the charge prediction equation can be guaranteed for slow changes, i.e., conditions that can be considered quasi-steady. However, it is difficult to expect the accuracy of the charge prediction equation when there is a sudden change in system control such as a change in compressor speed or a change in EEV opening. So, the system is required to be stable for a reliable prediction of charge amount.

In order to verify the accuracy of charge prediction equation with a criterion, three different criteria are presented as shown in Table 3.3. There are many ways to determine the stability of the system, but this study used the stability of the predicted charge amount.

Table 3.3 Criteria for reliable points

Criterion	Compressor	Outdoor fan	Stable time	Stable range
Criterion 1	Operating	Fan speed 3	Stable for 30 min	Maximum error 2.5%
Criterion 2	Operating	Fan speed 3	Stable for 30 min	Maximum error 5.0%
Criterion 3	Operating	Fan speed 3	Stable for 10 min	Maximum error 5.0%

3.4.3 Prediction result with criteria

Fig. 3.16 shows the charge prediction result include accuracy determination. As can be seen from the figure, it can be seen that the presented criteria accurately selects the reliable points. However, the refrigerant charge is no longer continuously predicted, and the charge amount is predicted only in a specific situation. Nevertheless, as shown in Fig. 3.16 (a), there were 6,000 reliable points, about 1/10 of 60,000 points. That is to say, the refrigerant charge can be predicted at least once every 10 minutes on average. In this case, the RMS error and AAD of reliable points were 6.49% and 4.28% respectively. A criterion 2 is a milder condition than criterion 1. The results using criterion 2 are shown in Fig. 3.16 (b). In this case, the number of points satisfying the criterion was 26,000, which is highly increased from case 1, and the RMS error was 6.11% and ADD was 4.37%. In this case, the refrigerant charge is detected about once every two minutes. Finally, Fig. 3.16 (c) shows the case using criterion 3. Criterion 3 is the mildest condition and attempts to predict the amount of refrigerant even if it remains stable for only 10 minutes. In this case, the number of reliable points was 32,000, slightly higher than criterion

2, but the RMS error and ADD increased to 7.00% and 4.99%, respectively.

In conclusion, the accuracy of the charge prediction equation can be guaranteed using criteria to determine the reliable state during continuous driving. In this case, the harsher the criterion, the higher the accuracy of the prediction but the lower the continuity of the prediction.

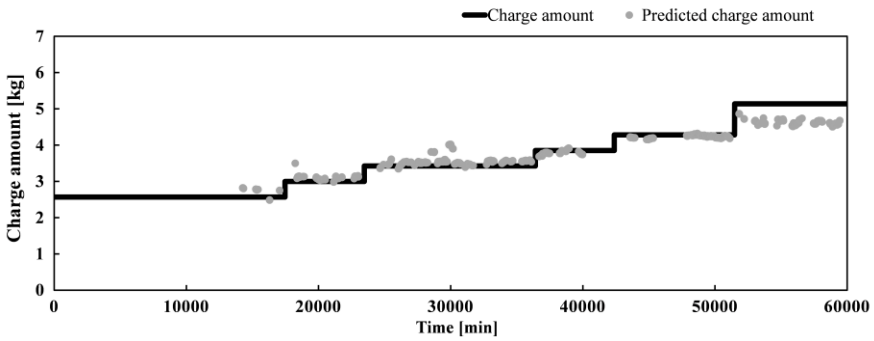

(a) Prediction result using criteria 1

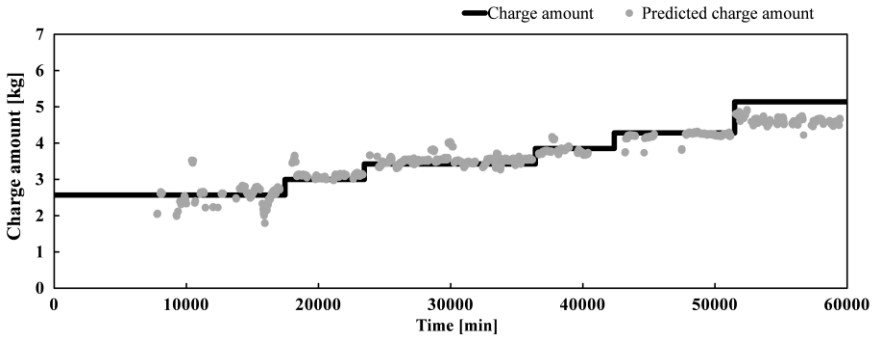

(b) Prediction result using criteria 2

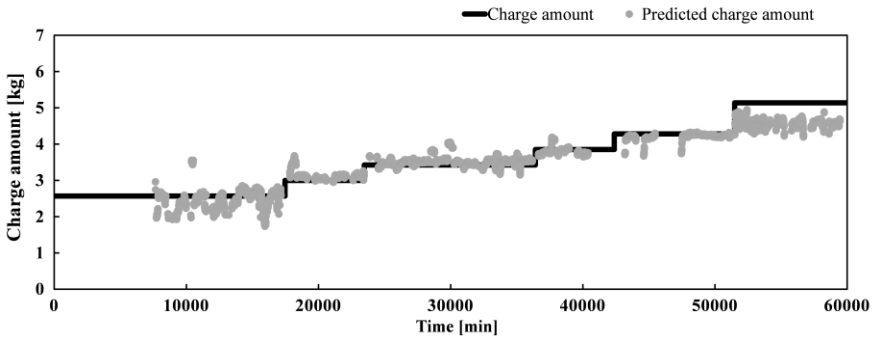

(c) Prediction result using criteria 3

Fig. 3.16 Charge prediction result with reliability criteria

3.5 Charge prediction with extremely limited number of sensors

3.5.1 Charge prediction of residential heat pump system

The charge prediction equation uses various sensors. Large heat pump systems such as commercial heat pumps have most of the sensors used in the prediction equation. However, not all heat pumps have this sensor installed. Extremely limited sensors are installed in residential heat pump system, which is much smaller system compared to commercial system, due to cost reduction. The residential heat pump system targeted in this study is equipped with only five temperature sensors and control sensors as shown in Table 3.4.

As mentioned above, in order to apply the charge prediction equation, condensing and evaporating pressure (or temperature) sensors, compressor suction or discharge temperature sensors, and the condenser inlet air temperature sensor are required. Residential heat pump systems do not have all these sensors, but fortunately there are alternatives. The cost of the pressure sensor is high, so the condensing and evaporating pressure sensors are not installed in a residential heat

Table 3.4 Installed sensors in residential heat pump system

Temperature sensors	**Other information**
Indoor air inlet	Compressor speed
Outdoor air inlet	Fan speed
Evaporator midpoint	Voltage
Condenser midpoint	Current
Compressor discharge	Power consumption

pump system. Instead, a residential heat pump is equipped with a temperature sensor at the mid-point of the condenser and evaporator. In most cases, at the mid-point of the condenser and evaporator, the refrigerant is in a 2-phase state, so the condensing temperature and evaporating temperature can be obtained from the temperature sensor, and the condensing pressure and evaporating pressure can be calculated. In addition, assuming polytropic compression, the compressor suction temperature can be calculated from the compressor discharge temperature. Then, the flow rate of the refrigerant can be calculated using the same method as the commercial heat pump. Through this process, all the operating information required for the charge prediction equation can be obtained. In this way, the charge prediction equation can be applied to the system with extremely limited number of sensors which only has the sensors for control.

Fig. 3.17 shows the result of estimating the amount of refrigerant using only limited number of sensors. As shown, the prediction accuracy is very high in most areas. However, there is an area where the refrigerant amount prediction error is greatly high. This is a severe undercharged case where DSC no longer exists. Since the existence of

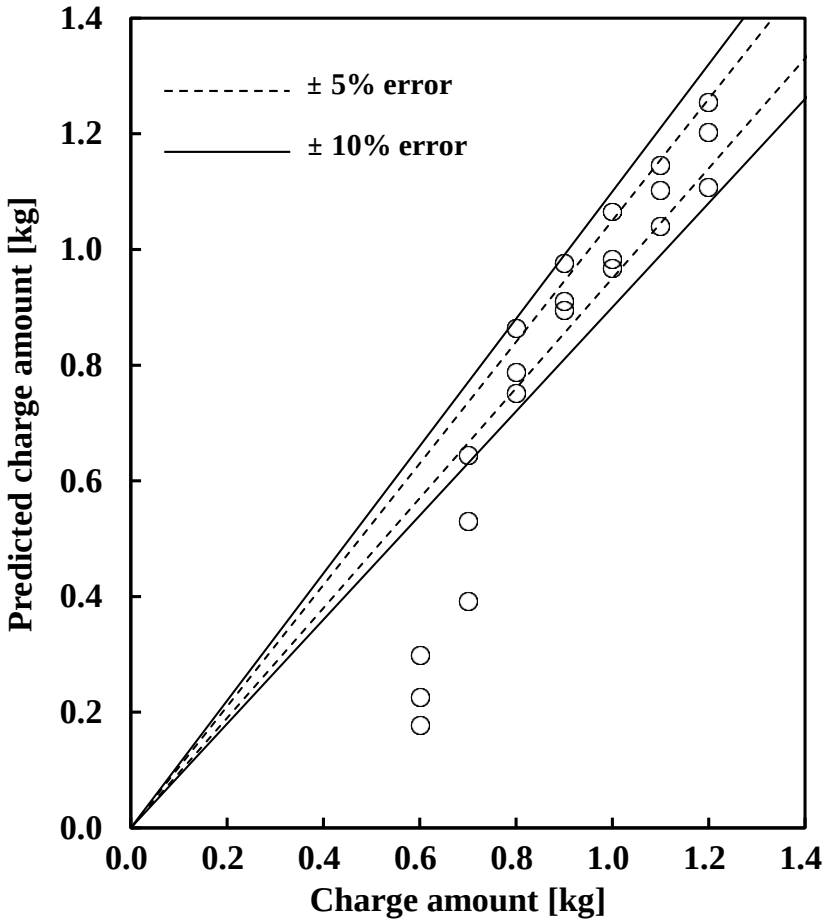

Fig. 3.17 Charge amount prediction result
(residential heat pump system)

DSC is assumed during the derivation of the charge prediction equation, the accuracy of the charge prediction equation can only be guaranteed if these assumptions are satisfied. In a commercial heat pump system, a temperature sensor is installed at the condenser outlet to measure the DSC. However, the residential heat pump system does not measure DSC. Thus, although the charge prediction equation can be applied, it cannot guarantee the accuracy of the charge prediction equation. To ensure the accuracy of the charge prediction equation in residential heat pumps, severe undercharged cases should be distinguished by other method than the presence of DSC. Therefore, the undercharged region has to be distinguished by applying a leakage detection method of a refrigerant in a heat pump system having an extremely limited sensor. Refrigerant leakage detection method detects refrigerant charge level of less than about 60~70%, so if such refrigerant leaks are detected, it is obvious that additional refrigerant must be added. Therefore, if the sensor is extremely limited, it is appropriate to add a refrigerant when a refrigerant leak is detected, and otherwise optimally adjust the charge by predicting the refrigerant charge quantitatively.

3.5.2 Leakage detection method

In order to determine whether the results of the charge prediction equation are reliable, the presence of DSC should be known. However, DSC is not known if the sensor is extremely limited. The absence of DSC and the leaked condition is almost similar case. Therefore, the leakage detection method should be used to determine whether the current charge is within range of 70 to 120% to guarantee the accuracy of charge prediction equation.

As mentioned in the introduction, various refrigerant leakage detection methods exist. Any leakage detection method that can detect 30% leakage is applicable. In this study, the leak detection method suggested by Yoo et al. (2017) was applied. The leakage detection method uses only two temperature sensors (evaporator midpoint and evaporator inlet air), making it easy to apply to residential heat pumps. The principle of the leakage detection method is shown in Fig. 3.18. The figure shows temperature distribution at evaporator. As can be seen, under normal conditions, the refrigerant at the mid-point of the evaporator is in 2-phase. Therefore, in general, the temperature difference between the air and the refrigerant is maintained at 10℃ or more. However, when the refrigerant leaks more than 30%

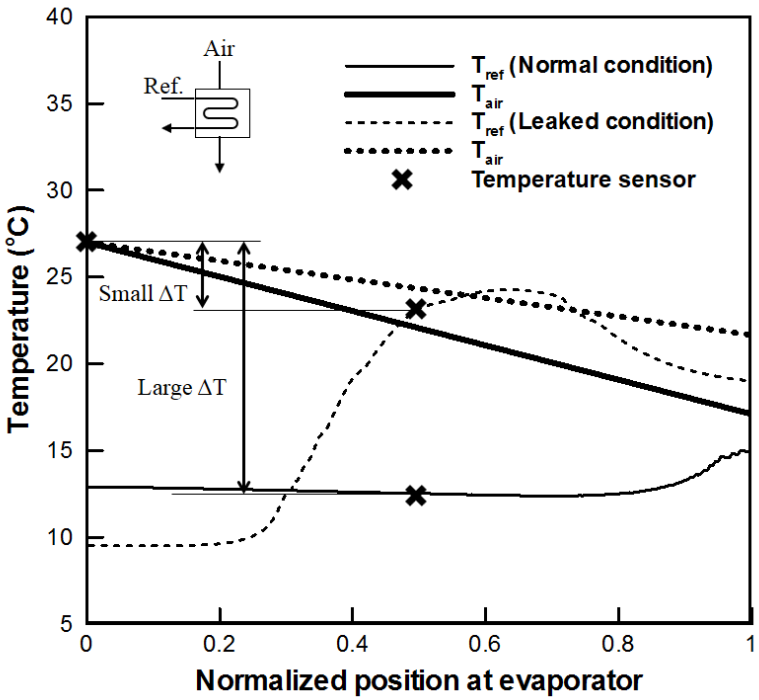

Fig. 3.18 Principles of leakage detection method (Yoo et al., 2017)

(leaked condition), the refrigerant is vaporized too quickly, and the refrigerant is no longer present in the 2-phase state at the evaporator mid-point. In this case, the DSH rises and the refrigerant temperature at the evaporator mid-point quickly approaches the air inlet temperature.

This method detects the leakage when the temperature difference between the refrigerant and air at the evaporator mid-point goes below a certain level. At this time, it is important to determine the criteria temperature for determining the refrigerant leakage. The higher the criteria temperature, the faster the refrigerant leak is detected, but the higher the rate of misdiagnosis of leakage. Therefore, in this study, the criteria temperature was selected as 5K to minimize the error rate.

Finally, for charge prediction with extremely limited number of sensors, first, the refrigerant leakage determined based on the difference between the evaporator mid-point temperature and the evaporator inlet air temperature.

If the charge level is determined to be at the proper level (70% or more), the charge prediction equation is applied to calculate he amount of refrigerant charge in the system.

3.5.3 Experimental setup and procedure

A residential heat pump experiment was conducted to verify the accuracy of the charge amount prediction method with limited number of sensors. Fig. 3.19 shows a targeted residential heat pump with nominal capacity of 3 kW used in the experiments. A schematic diagram of the experimental facilities is shown in Fig. 3.20. As same in the previous experiments, the heat pump system is installed in an environmental chamber. The compressor and EEV located in the outdoor unit. The compressor rotational speed can be controlled by inverter and the EEV controls the evaporating pressure for both cooling and heating mode operation. A number of temperature, pressure sensors and mass flow meter are installed as shown in Fig. 3.20. In addition, a wind tunnel and nozzles are installed in the indoor chamber to accurately measure the cooling (or heating) capacity of the system. Based on ANSI / AMCA 210 (2007), indoor unit capacity was calculated through air temperature, humidity and flow rate information.

Table 3.5 describes detailed experimental conditions. Prior to the experiment, a reference case experiment was conducted to find the optimal refrigerant charge of the system. The experimental range of

refrigerant charge condition was selected approximately from 60% to 120% of the optimal charge amount.

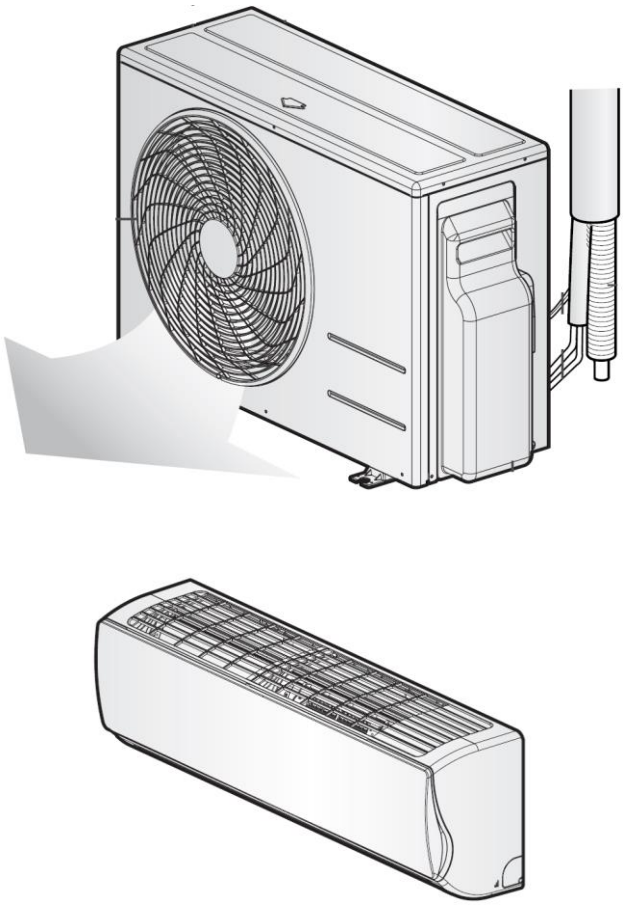

Fig. 3.19 Residential heat pump
(upper - outdoor unit / lower - indoor unit)

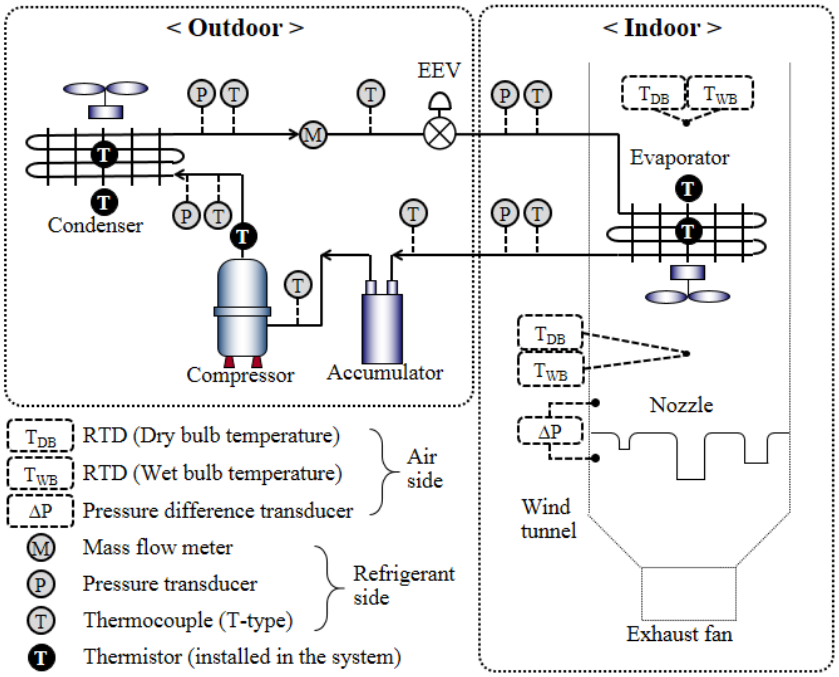

Fig. 3.20 Schematic diagram of experiment setup (residential heat pump)

Table 3.5 Experimental condition for residential heat pump system

Variables	**Values**		
Refrigerant	R410A		
Number of indoor units	2		
Driving mode	Cooling		
Charge amount (g)	400~1200 (Δ=100 g)		
Target DSH (K)	5		
Air temperature condition	Rating	Maximum	Minimum
Indoor dry bulb temp. (^{o}C)	27.0	32.0	21.0
Indoor wet bulb temp. (^{o}C)	19.5	23.0	15.0
Outdoor dry bulb temp. (^{o}C)	35.0	43.0	21.0
Outdoor wet bulb temp. (^{o}C)	24.0	26.0	15.0
Compressor inverter speed (Hz)	50	40	50

3.5.4 Uncertainty analysis

The optimal charge amount of the system was determined through reference case experiment.

The uncertainty of measurement data is shown in Table 3.6. The total error of cooling capacity is 6.4% and the total error of COP is 6.5% on 95% confidence level.

Table 3.6 Uncertainty analysis at reference condition (residential heat pump)

Variables	Fixed error	Random error	Total error
Pressure at condenser	0.6%	0.4%	0.7%
Pressure at evaporator	1.3%	0.3%	1.4%
Dry bulb air inlet temperature	0.20 K	0.02 K	0.20 K
Wet bulb air inlet temperature	0.19 K	0.06 K	0.20 K
Dry bulb air outlet temperature	0.18 K	0.01 K	0.18 K
Dry bulb air outlet temperature	0.18 K	0.03 K	0.18 K
Thermistor	0.70 K	0.32 K	0.76 K
Mass flow rate (refrigerant)	3.1%	0.8%	3.2%
Mass flow rate (air)	4.6%	0.5%	4.6%
Power consumption	0.2%	0.7%	0.7%
Cooling capacity	6.3%	1.2%	6.4%
COP	6.3%	1.6%	6.5%

3.5.4 Experimental verification

As mentioned above, in order to increase the accuracy of the charge prediction equation in the residential heat pump system, it is necessary to exclude the unreliable point through the refrigerant leakage detection method. In this study, when the difference between evaporator mid-point temperature and evaporator inlet air temperature is less than 5K, the amount of refrigerant was determined to be less than 70% of proper charge.

Fig. 3.21 is the result of charge prediction through this process. As can be seen from the figure, the accuracy of charge prediction equation is very high except for the black solid dots. RMS error has been greatly reduced from 18.6% to 5.16%. If leakage of refrigerant is detected, it is not possible to quantitatively predict the current charge amount using charge prediction equation. Nevertheless, it is very clear that the refrigerant must be recharged in those cases. In conclusion, the charge prediction equation is reliable even when applied to the heat pump system with extremely limited number of sensors.

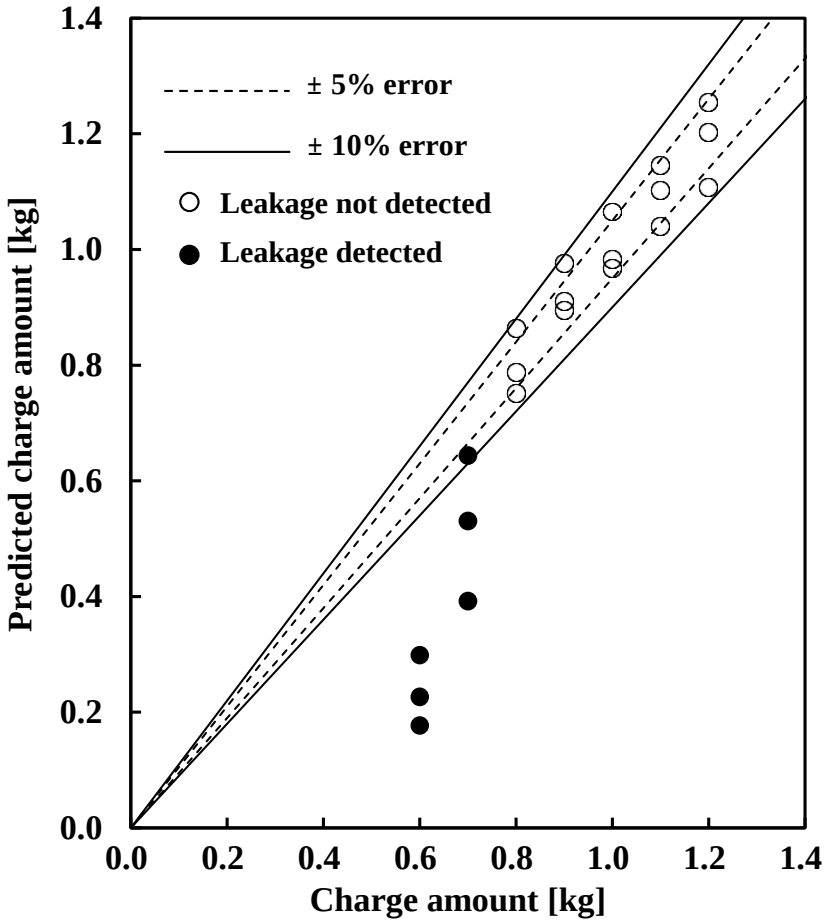

Fig. 3.21 Charge amount prediction result combined with leakage detection method (residential heat pump)

3.6 Summary

The aim of this study is to propose a method of predicting refrigerant charge that can be physically explained. The previous chapter presented the first method, simulation-based charge prediction. As can be seen from the results, the simulation could accurately predict the charge amount in the heat pump. However, the heat pump is very complicated in its configuration and geometry, and there are coefficients that can only be predicted experimentally. Thus, one modeling cannot be applied to another heat pump system. Therefore, charge prediction method is required, which can be used more widely.

In this chapter, a generalized charge prediction equation was developed. First, as shown in chapter 2, it is important to accurately predict the charge amount in the condenser to predict the total refrigerant charge. To predict the amount of refrigerant in the condenser, the geometry of the condenser was simplified. Using the heat transfer equations and assumptions, the charge prediction equation was presented. Since the equation does not reflect the characteristics of each heat pump, this method can be universally applied to an air source heat pump.

Commercial heat pump experiments were performed to verify the

accuracy of the charge prediction equation. In cooling mode, the RMS error was 3.7%, and in heating mode, RMS error 8.2%, which indicate high accuracy of the charge prediction equation.

The charge prediction equation is a very accurate and universal method. However, some assumptions are required to use the charge prediction equation. If these constraints are not satisfied, the accuracy of the charge prediction equation cannot be guaranteed. This chapter presents a method for improving accuracy in continuous driving conditions and limited sensor information cases where the accuracy of the charge prediction equation is low.

If the system is in a transient state, or the compressor is not operating, the accuracy of the charge prediction equation is poor. In order to improve the accuracy of the charge prediction equation even in continuous driving conditions, a criterion was proposed that selects only reliable prediction points. The prediction accuracy of the selected reliable points using criterion was very high, and the RMS error was 6.11%.

Various sensor information is required to apply the charge prediction equation. Since the system such as residential heat pump is small, the number of sensors is extremely limited due to the cost.

Therefore, it may not provide sufficient sensor information for using the charge prediction equation. In this chapter, experiments were conducted to verify the accuracy of the charge prediction equation in residential heat pumps. The charge prediction equation can also be used for residential heat pumps, but the prediction accuracy is poor because the presence of DSC is not certain. Therefore, it is necessary to first verify that the charge level is 70% or more by using the leakage detection method. In case of selecting only the points where the charge level is 70% or more through leakage detection, the accuracy of the charge prediction equation increases dramatically. In the results of this study, RMS error was greatly reduced from 18.6% to 5.16%.

Chapter 4. Optimal charge prediction method for air source heat pump systems

4.1 Introduction

Using the methods of the previous two chapters, it is possible to quantitatively estimate the amount of refrigerant. The reason for predicting the charge amount is to improve the performance of the heat pump by optimal adjusting of the charge amount. Therefore, after accurately predicting the charge in the system, the charge should be optimally adjusted. At this time, refrigerant charge adjustment should be performed annually, seasonally, or in real time. In order to perform charge optimization, it is necessary to know the optimal charge of the heat pump system. Currently, information on the optimal charge amount is provided by the heat pump manufacturer. The heat pump manufacturer determines the appropriate charge amount for each indoor unit and outdoor unit through experiments, and the installer injects the appropriate amount of refrigerant at the actual installation place. However, there is a high possibility that the fixed amount of proper charge provided by the heat pump manufacturer is different

from the actual optimal charge amount.

First, when installing the heat pump system, a liquid line and a vapor line connect the indoor unit and the outdoor unit. The length of the two tubes has a great influence on the refrigerant charge in the heat pump. Heat pump manufacturers have decided the amount of refrigerant to add according to the length of these pipes, but it is often difficult to figure out the exact length of the pipe in actual installation. In addition, heat pump systems are becoming more and more complex, and often multiple outdoor units and multiple indoor units are combined. In this case, the optimal charge of the system is likely to be different from the proper charge provided by the manufacturer.

Secondly, the optimal charge of the heat pump depends on the operating conditions. Fig. 4.1 shows the relationship between COP and charge level at various operating conditions. As can be seen, the optimal charge amount varies with different indoor/outdoor temperature conditions. Fig. 4.2 shows the change of COP when the compressor speed is different. As shown in the figure, the optimal refrigerant charge varies as the control state changes. In other words, even in one heat pump system, the optimal charge amount changes depending on the operating conditions and control. The operating

conditions of the heat pump vary greatly according to the region or season. At the same time, the system configuration is very diverse, so the optimal charge amount of the heat pump system is different from system to system. Therefore, for optimal control of the charge amount, it is necessary to predict the optimal charge amount of each heat pump system. As in the case of predicting the current charge amount, the optimal charge amount must also be predicted using the sensor information. It is very difficult to directly predict the system performance from the charge amount. However, based on the earlier chapters in this study, the relationship between charge and operating conditions can be obtained. Therefore, this chapter aims to predict the performance of the heat pump system from the operating state, and to convert the operating state to charge amount.

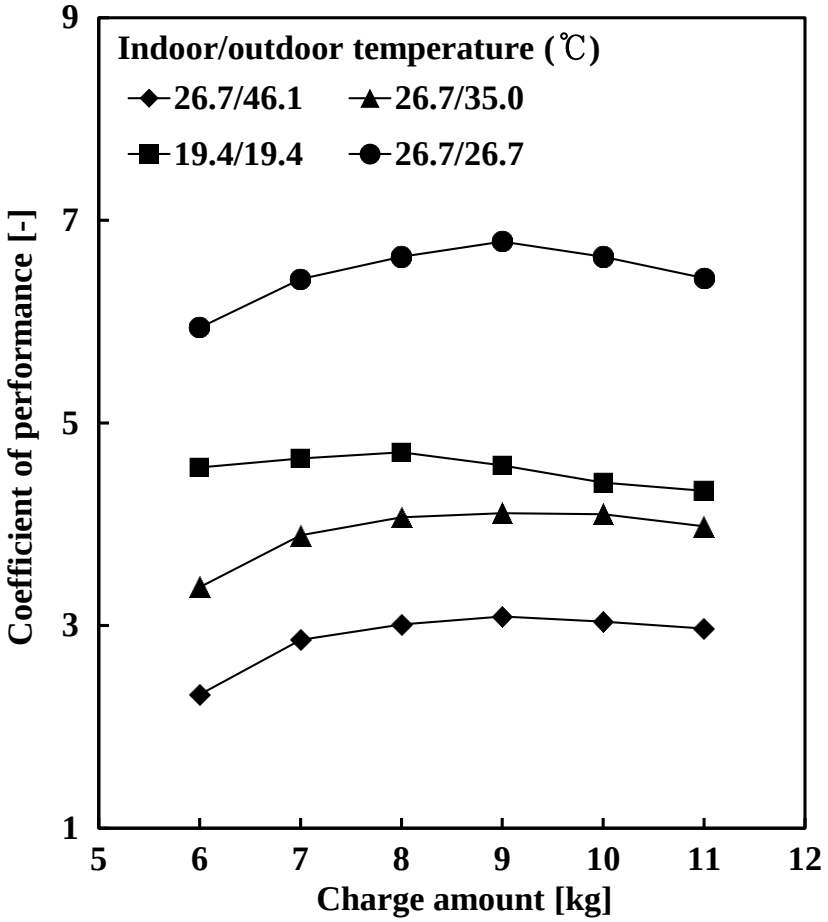

Fig. 4.1 Relation between COP and charge amount under various operating temperature

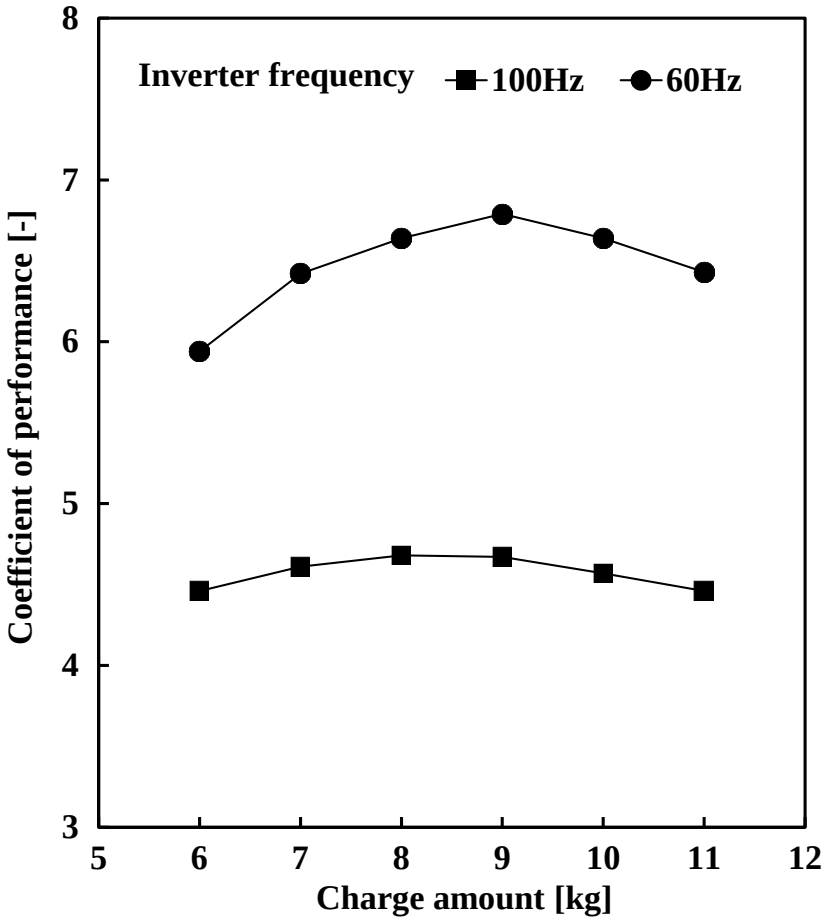

Fig. 4.2 Relation between COP and charge amount under various rotational frequency of compressor

4.2 Development of optimal charge prediction method

To predict the optimal refrigerant charge, the COP should be predicted according to the charge amount. In order to predict the COP, the quantity of heat transferred (Q) and the compressor work (W) should be estimated individually. In this case, the quantity of heat transferred means a useful amount of heat that is, cooling capacity (Q_L) for cooling and heating capacity (Q_H) for heating. In order to calculate the exact quantity of heat transferred, it is necessary to measure the inlet and outlet temperature, humidity, and flow rate of the air at the heat exchangers and calculate the change in enthalpy of the air. However, it is very difficult to measure inlet and outlet temperatures and humidity of air in a real heat pump system. In particular, in the case of the air outlet temperature, since the area of the heat exchanger is large, the temperature of the air varies depending on the place it is measured. Therefore, representative temperature of the air must be measured, which is very inaccurate.

If the heat delivered to air cannot be calculated directly, the heat delivered from the refrigerant must be calculated. In this case, there is a slight error, but since the temperature and pressure sensor are installed at both the inlet and the outlet of the heat exchangers, the

enthalpy change can be calculated. However, the state of the refrigerant at the inlet of the evaporator is 2-phase, so the temperature and pressure sensor do not accurately determine the state of the inlet refrigerant. Therefore, the cooling capacity is difficult to predict only by the sensor information. However, as shown in Eq. (4.1), the heating capacity is theoretically the sum of cooling capacity and the compressor work.

$$Q_H = Q_C + W \tag{4.1}$$

In addition, since COP is defined as *Q/W*, the cooling COP and heating COP has a relation as Eq. (4.2).

$$\mathrm{COP}_{\mathrm{heating}} = \frac{Q_H}{W} = \frac{Q_C + W}{W} = \mathrm{COP}_{\mathrm{cooling}} + 1 \tag{4.2}$$

In other words, the point where the cooling COP maximized is the point where the heating COP also maximized. Therefore, even in the cooling mode, if the optimal point of the heating COP is predicted, the optimal amount of refrigerant can be predicted. Now, to predict the heating COP, estimation of the heating capacity and the compressor

work is required. However, it is very difficult to predict the capacity and work directly from the charge amount. Therefore, first, COP according to the operation information (such as temperature, pressure, etc.) is predicted, and the operation information is converted into the amount of refrigerant through the charge prediction equation. Through this process, it is possible to predict the *Q*, *W*, and COP according to the amount of refrigerant, and finally the optimal charge amount can be predicted.

Fig. 4.3 shows the change of condensing pressure and evaporating pressure depending on refrigerant charge. (Yoo, 2018) As can be seen from the figure, evaporating pressure increases with increasing charge, but is nearly constant at some level. This is because the evaporating pressure is constantly controlled by the EEV at the proper charge level (70~120%). In severe undercharged cases below 70% charge level, refrigerant leaks are easily detected, making it necessary to recharge the refrigerant. Therefore, the region in which the optimal amount of refrigerant needs to be predicted is a 70~120% charge level which is a proper charge level. In this section, the evaporating pressure does not change but the condensing pressure increases monotonously when the charge amount changes.

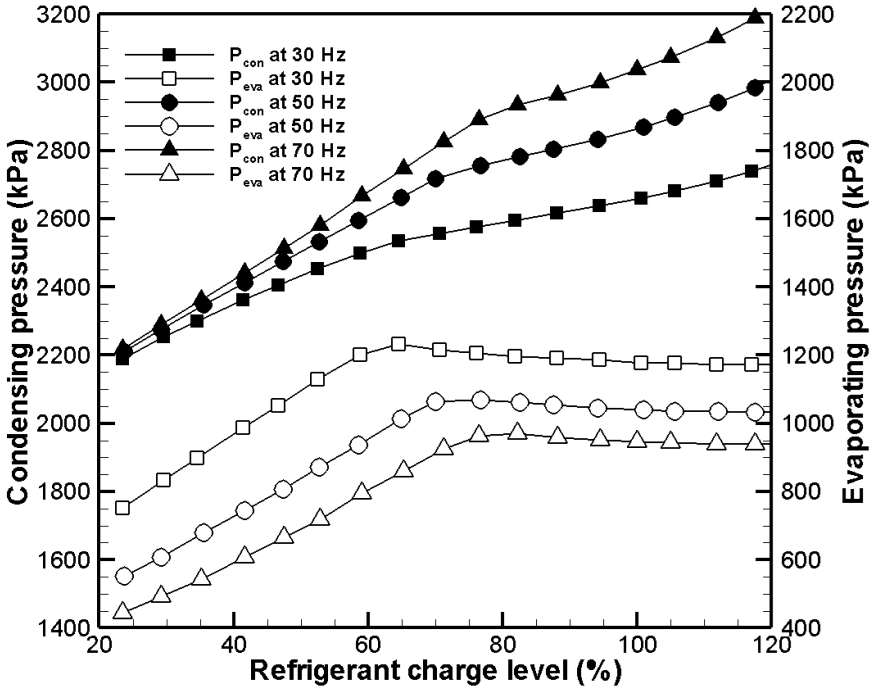

Fig. 4.3 Condensing and evaporating pressure variation according to refrigerant charge level

Therefore, when the heating capacity and the compressor work change according to the condensing pressure (or temperature) are predicted, the relationship between the charge amount and the COP can be predicted.

Since evaporating pressure and DSH are controlled by EEV, the P-h diagram of the heat pump system when the condensing pressure changes by ΔP_{cond} can be described as Fig. 4.4.

First, compressor work can be predicted relatively easily. Compression process can be assumed to be polytropic compression. Then, the polytropic coefficient n can be found as in Eq. (4.3).

$$n = \frac{\ln P_1/P_{2,i}}{\ln v_{2,i}/v_1} \tag{4.3}$$

Specific volume of refrigerant at compressor outlet can be calculated as Eq. (4.4).

$$v_{2,f} = \left(\frac{P_1}{P_{2,f}}\right)^{\frac{1}{n}} v_1 \tag{4.4}$$

Then, the compressor work becomes Eq. (4.5).

$$W_f = \left(i_{2,f} - i_1\right) \dot{m} \tag{4.5}$$

Next, to obtain the quantity of heat transferred at condenser, condenser was divided into three parts as shown in Fig. 4.5; superheated region, 2-phase region, and subcooled region. The heating capacity in the final state is sum of increment of heating capacity and the initial heating capacity. Also, the increment of heating capacity is sum of increment of heating capacity in each region. Therefore, the quantity of heat transferred at condenser of final state can be obtained as Eq. (4.6).

$$Q_f = Q_i + \Delta Q = Q_i + \Delta Q_{sh} + \Delta Q_{tp} + \Delta Q_{sc} \tag{4.6}$$

Since the initial heating capacity is a known value, it is necessary to predict ΔQ_{sh}, ΔQ_{tp}, and ΔQ_{sc}, individually.

First, capacity changes in superheated and 2-phase regions are relatively easy to predict. Assuming that the specific heat of the refrigerant is constant in the superheated region, the superheated region capacity is the product of C_p, DSH at compressor discharge,

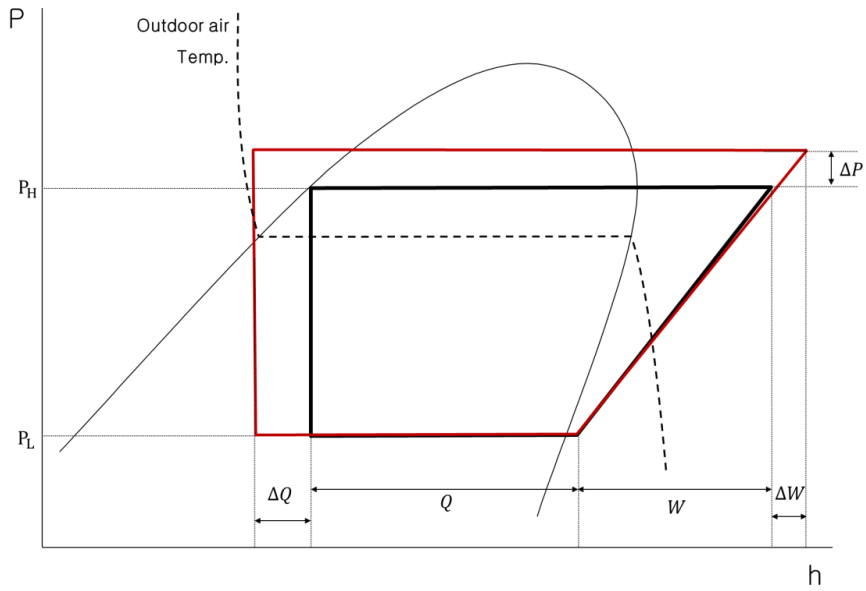

Fig. 4.4 Change of P-h diagram for adding charge

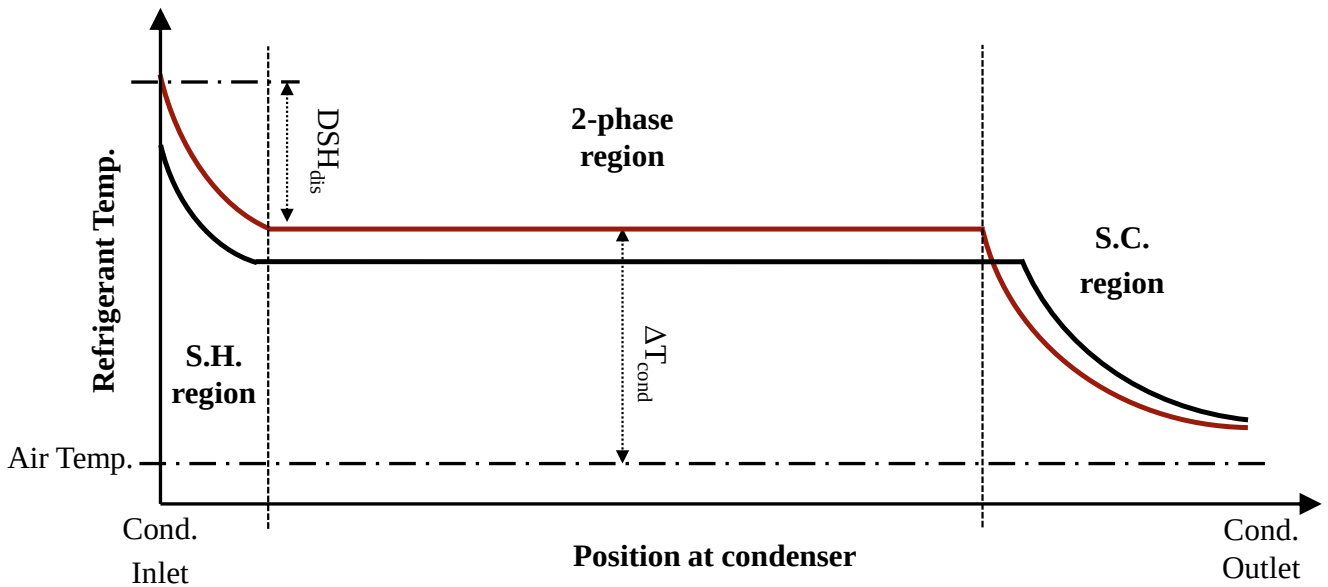

Fig. 4.5 Temperature change in the condenser (proper charged case)

and mass flow rate of refrigerant. In addition, the 2-phase region capacity is the product of latent heat and the mass flow rate of refrigerant. Then, ΔQ_{sh} and ΔQ_{tp} can be expressed as Eq. (4.7) and Eq. (4.8), respectively.

$$Q_{sh} = \dot{m} C_{p,vapor} \Delta DSH_{dis} = \dot{m} C_{p,vapor} (DSH_{dis,f} - DSH_{dis,i}) \quad (4.7)$$

$$\Delta Q_{tp} = \dot{m} \Delta h_{fg} = \dot{m} \, (i_{fg,f} - i_{fg,i}) \quad (4.8)$$

Finally, ΔQ_{sc} is relatively complex to predict. This is because, depending on the condensing temperature, Q_{sc} initially increases steeply and then gradually increases. Q_{sc} is strongly related to difference between condensing temperature and air inlet temperature, which is ΔT_{cond}. Fig. 4.6 shows the Q_{sc} according to ΔT_{cond}. As shown in the figure, Q_{sc} can be described as a curve with two asymptotes. Therefore, when the inclinations of each asymptote are obtained, ΔQ_{sc} can be calculated as Eq. (4.9).

$$\Delta Q_{sc} = \left(s_1 \left(1 - \frac{DSC}{\Delta T_{cond}} \right) + s_2 \frac{DSC}{\Delta T_{cond}} \right) (\Delta T_{cond,f} - \Delta T_{cond,i}) \quad (4.9)$$

First, in order to obtain the steep slope s_1, the case where the refrigerant at condenser outlet is exactly saturated liquid state must be considered. In this case, since the DSC is close to zero, it is an undercharged case. Since difference between condensing temperature and air inlet temperature is very high in this case, Q_{sc} sharply increases as condensing temperature increases. Here, if the change of Q_{sc} according to the change of condensing temperature is predicted, s_1 also can be obtained.

To predict Q_{sc}, the refrigerant temperature change in the condenser is illustrated as shown in Fig. 4.7. As explained in the previous chapter, the overall heat transfer coefficient of the 2-phase region is almost constant since it is dependent on the air side heat transfer coefficient. Therefore, Q_{tp} in the initial state is proportional to the area shown in Fig. 4.7(a). Likewise, in the final state, DSC is nearly zero, so the sum of Q_{tp} and Q_{sc} is proportional to the area shown in Fig. 4.7(b). It can be expressed by Eq. (4.10), and Eq. (4.11).

$$Q_{tp,i} = \dot{m}h_{fg} = UA\Delta T_{cond,i} = kL\Delta T_{cond,i} \quad (4.10)$$

$$Q_{tp,f} + Q_{sc,f} \approx UA\Delta T_{cond,f} = kL\Delta T_{cond,f} \quad (4.11)$$

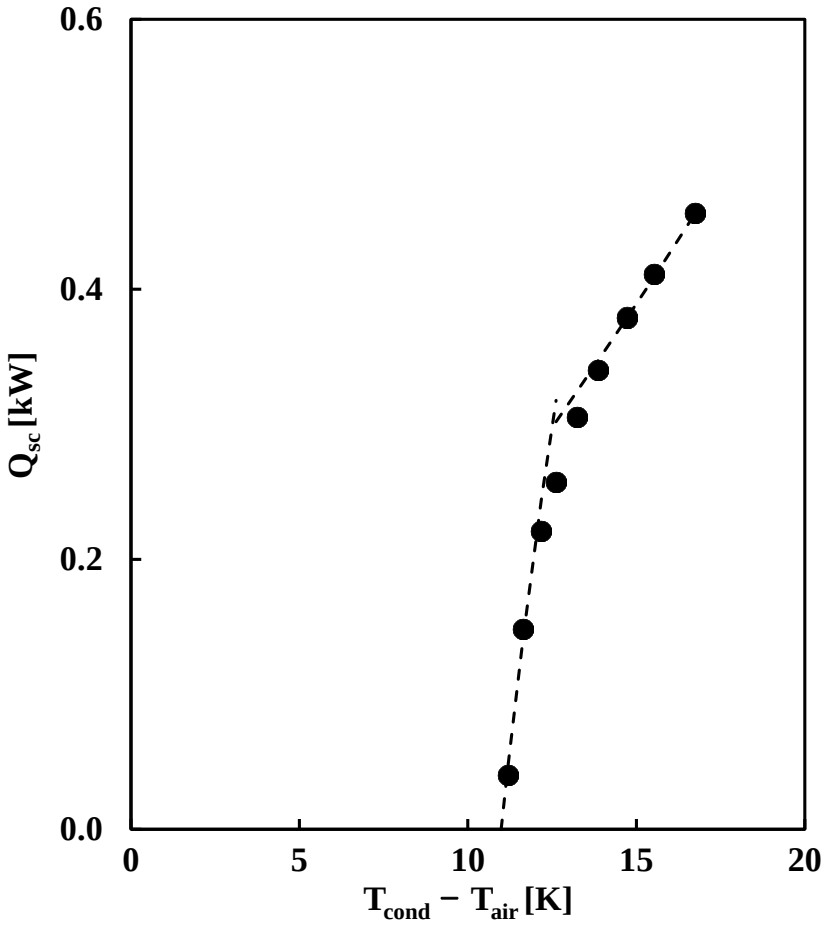

Fig. 4.6 Quantity of heat transferred at subcooled region of the condenser with respect to ΔTcond change

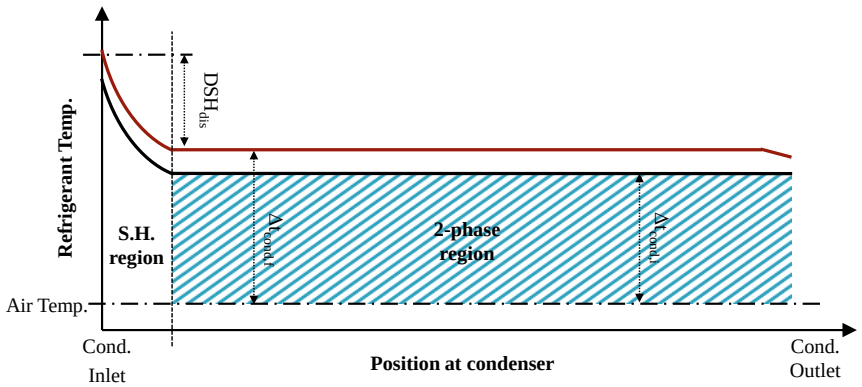

(a) initial state

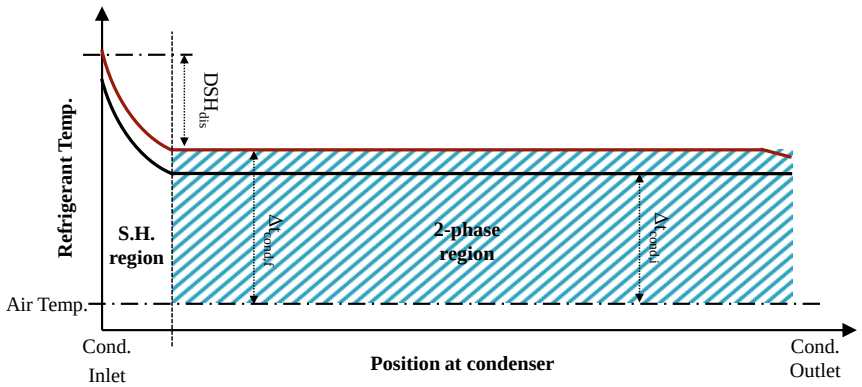

(b) final state

Fig. 4.7 Temperature change in the condenser (undercharged case)

Here, since the initial and final state is the state where the DSC is generated, the latent heat in both cases is the same. That is to say, $Q_{tp,I}$ is equal to $Q_{tp,f}$. Therefore, the previous equation can be substitute as Eq. (4.12).

$$Q_{sc,f} = kL\left(\Delta T_{cond,f} - \Delta T_{cond,i}\right) = \frac{\dot{m}h_{fg}(\Delta T_{cond,f} - \Delta T_{cond,i})}{\Delta T_{cond,i}} \tag{4.12}$$

Since $Q_{sc,i}$ is zero, $Q_{sc,f}$ is equal to ΔQ_{sc}, then from Eq. (4.13), s_1 can be obtained as Eq. (4.14).

$$\Delta Q_{sc} = \frac{h_{fg}\dot{m}}{\Delta T_{cond,i}}(\Delta T_{cond,f} - \Delta T_{cond,i}) \tag{4.13}$$

$$s_1 = \frac{h_{fg}\dot{m}}{\Delta T_{cond,i}} \tag{4.14}$$

To find s_2, the slope of the second asymptote, overcharged case should be considered, when the refrigerant temperature at the outlet of the condenser is very close to the air inlet temperature, as shown in Fig. 4.8. Assuming that the specific heat of the refrigerant is constant in the subcooled region, $Q_{sc,i}$ and $Q_{sc,f}$ can be expressed as Eq. (4.15), and Eq. (4.16).

$$Q_{sc,i} = \dot{m}C_{p,l}\left(T_{condensing,i} - T_{cond,out,i}\right) \quad (4.15)$$

$$Q_{sc,f} = \dot{m}C_{p,l}\left(T_{condensing,f} - T_{cond,out,f}\right) \quad (4.16)$$

In this case, since $T_{cond\_out,i}$ is equal to $T_{cond\_out,f}$, ΔQ_{sc} becomes Eq. (4.17), then, s_2 can be found as Eq. (4.18)

$$\Delta Q_{sc} = Q_{sc,f} - Q_{sc,i} = \dot{m}C_{p,l}\left(\Delta T_{cond,f} - \Delta T_{cond,i}\right) \quad (4.17)$$

$$s_2 = \dot{m}C_{p,l} \quad (4.18)$$

Then, from the Eq. (4.9), Eq. (4.14), and Eq. (4.18), ΔQ_{sc} can be obtained as Eq. (4.19).

$$\Delta Q_{sc} = \left(\frac{\dot{m}h_{fg}}{\Delta T_{cond}}\left(1 - \frac{DSC}{\Delta T_{cond}}\right) + \dot{m}C_{p,l}\frac{DSC}{\Delta T_{cond}}\right)\left(\Delta T_{cond,f} - \Delta T_{cond,i}\right) \quad (4.19)$$

Through the above process, it is possible to predict the compressor work, heating capacity, and COP according to the condensing pressure (or temperature). The charge prediction equation can be used to convert condensing pressure and other operational information into charge amount. Then, it is possible to predict the COP according to the

charge amount, and to predict optimal charge amount. The method proposed in this study is to predict work, capacity and COP from the change of charge amount in heat pump system. Therefore, to apply the method of this study, all driving sensor information of the operating system is required. However, this method does not require any pre-obtained data if only the charge prediction equation is available. Therefore, it is a method that can be universally applied to air source heat pump systems.

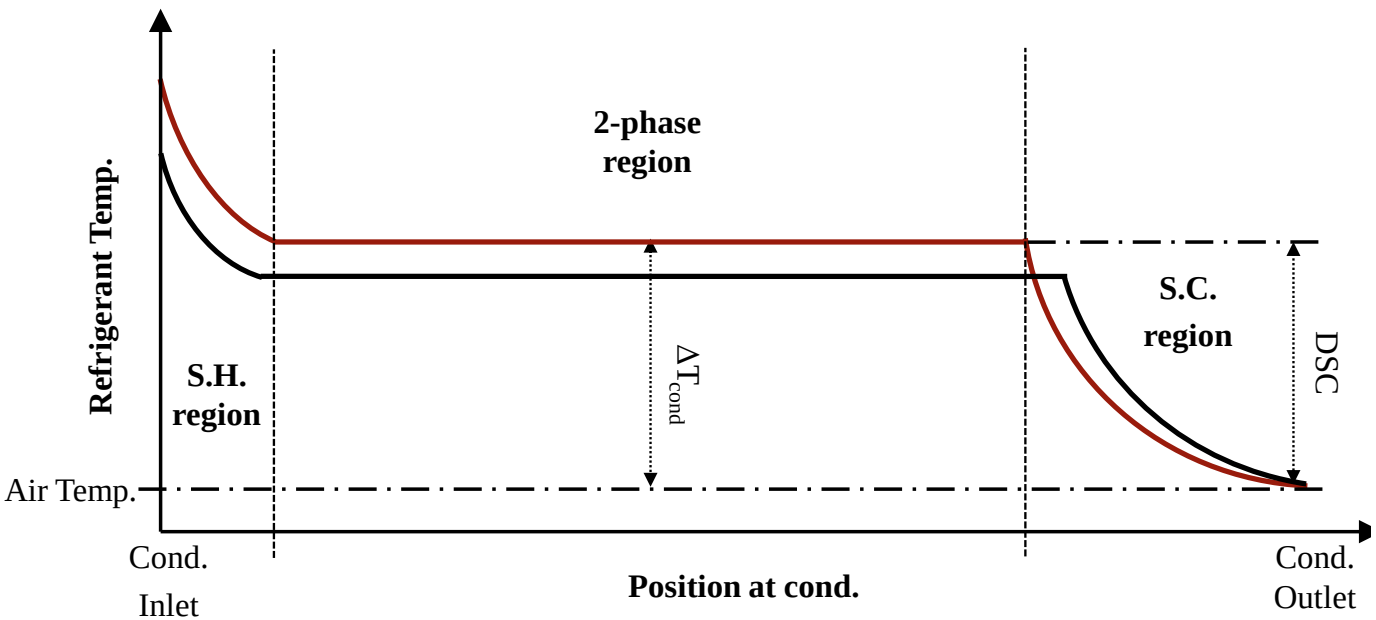

Fig. 4.8 Temperature change in the condenser
(overcharged case)

4.3 Verification of optimum charge prediction

In order to verify the accuracy of the optimal charge prediction method, experimental data from the previous commercial heat pump system experiments was used. The method proposed in this study is to predict the COP according to the charge amount in the current operation state. Therefore, even if the external conditions are the same, the result of the prediction may be changed according to the current charge amount.

Figs. 4.9~4.11 show the results of the compressor work and heating capacity prediction according to the various charged conditions (undercharged (7 kg), proper charge (9 kg), and overcharged (11 kg)) in the rating condition. As shown in the figures, the work and capacity were predicted very accurately with the condensing pressure at all states of charge. Here, the operation information including the condensing pressure can be converted into a charge amount through the charge prediction equation. The graph predicting the COP according to the converted charge amount is shown in Figs. 4.12~4.14. As shown in the figures, the COP according to the charge amount is predicted accurately in all charged condition.

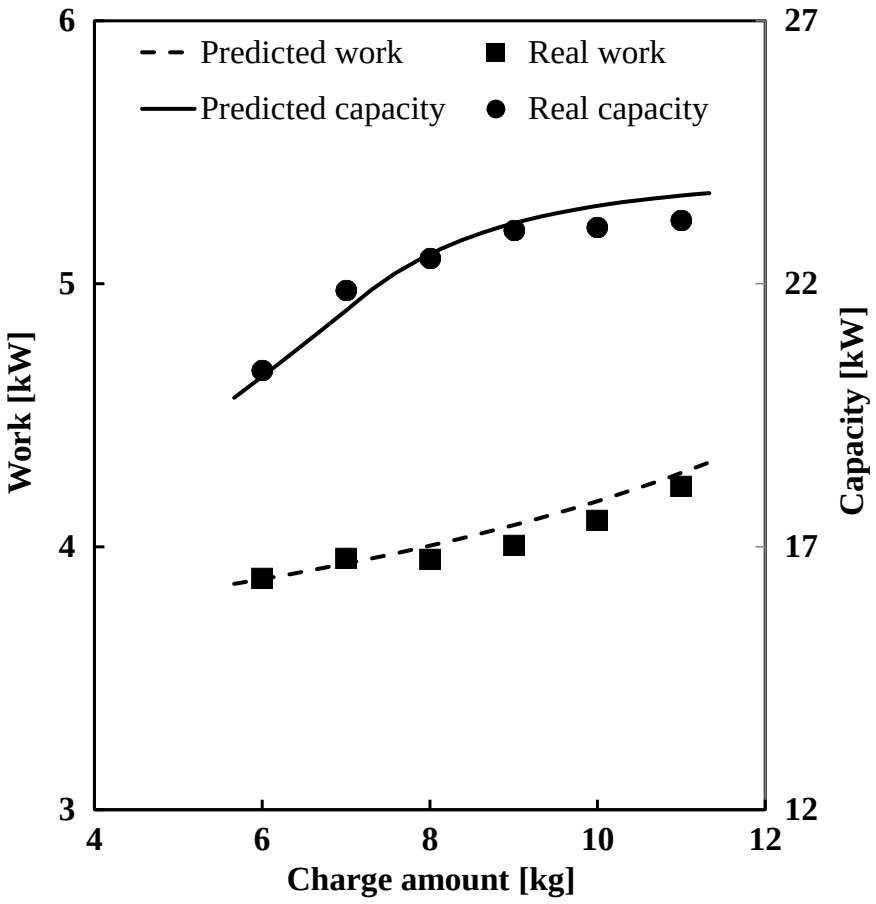

Fig. 4.9 Prediction result of work and capacity (7 kg charged case)

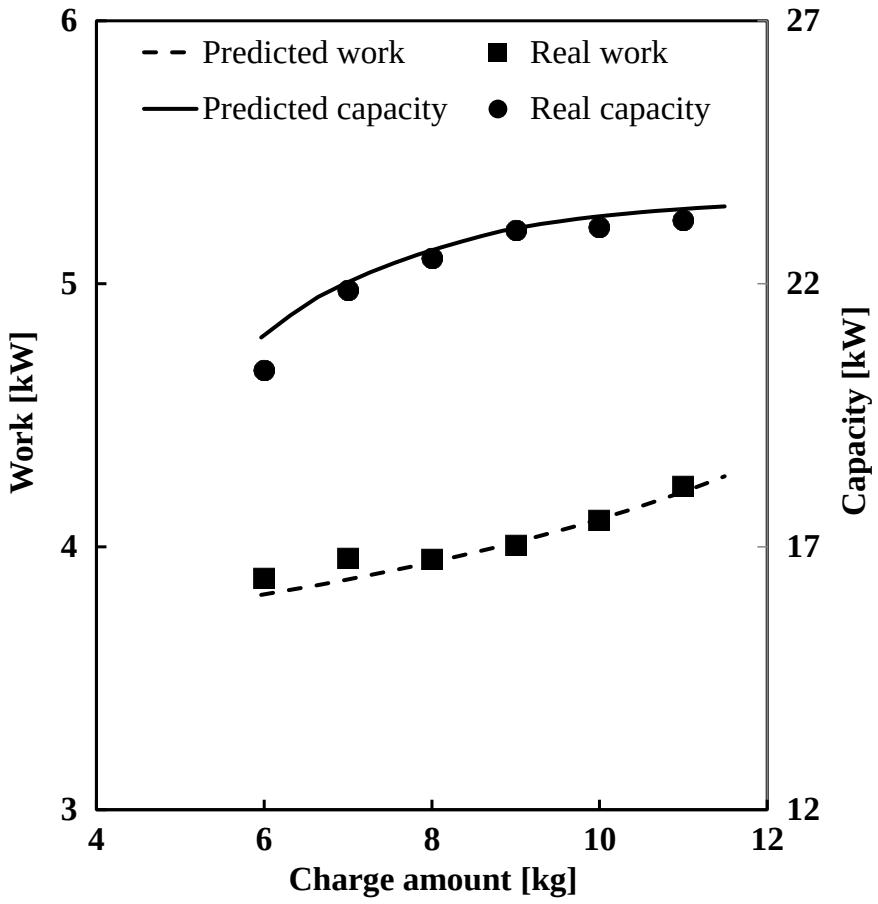

Fig. 4.10 Prediction result of work and capacity (9 kg charged case)

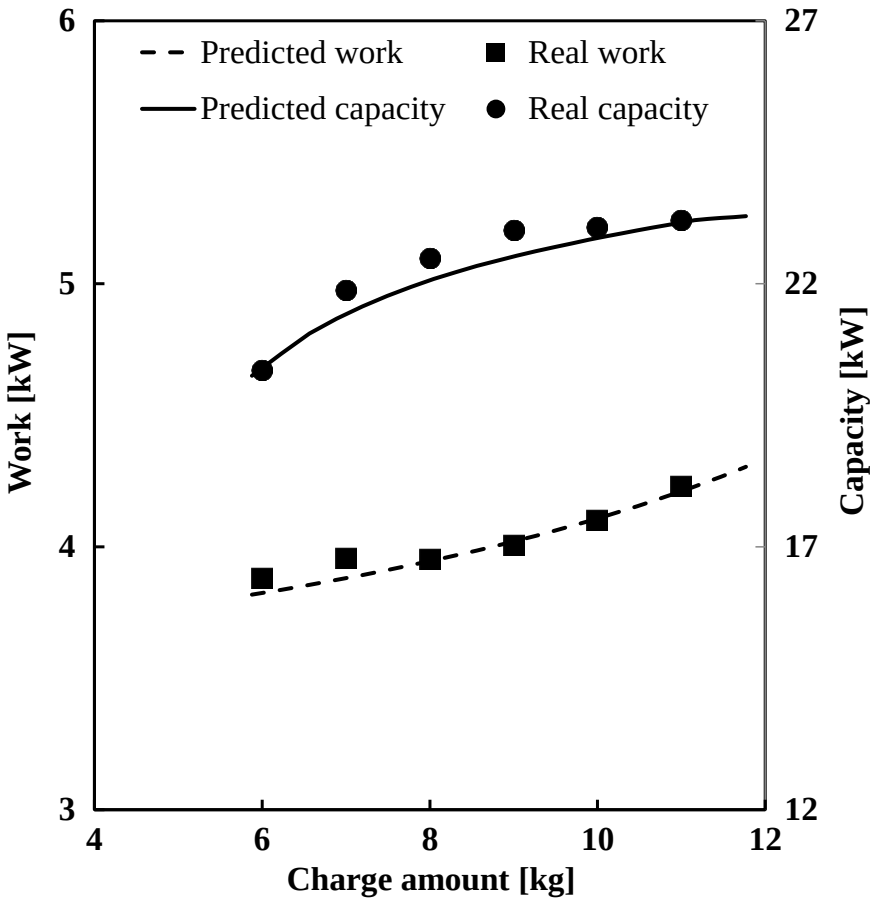

Fig. 4.11 Prediction result of work and capacity (11 kg charged case)

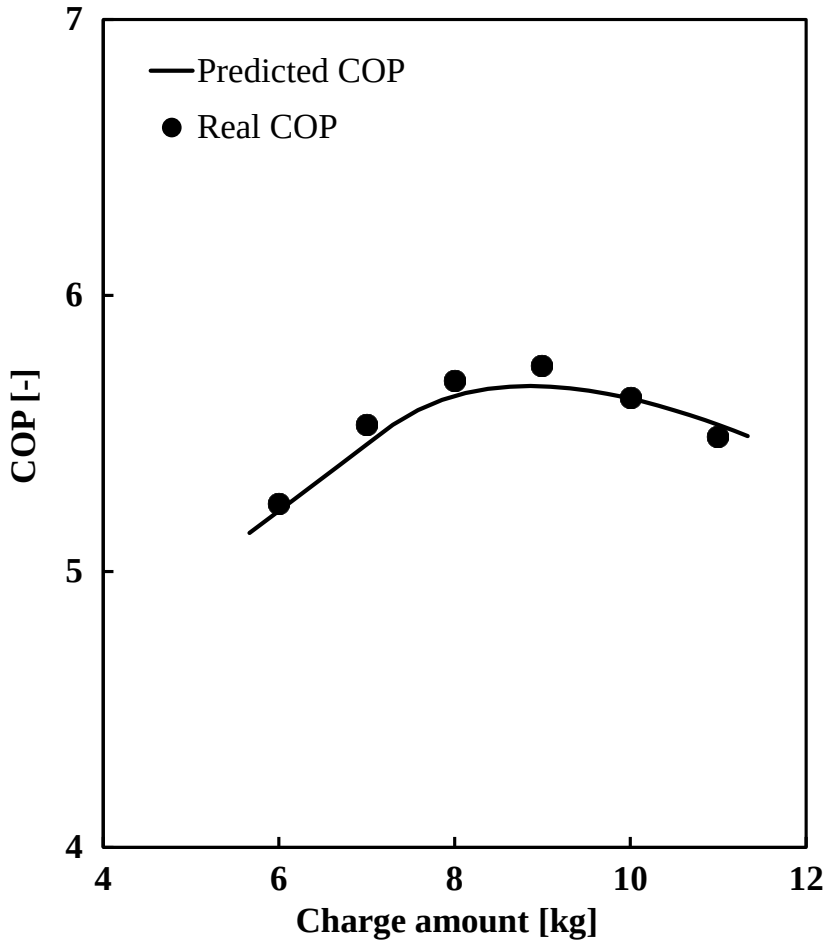

Fig. 4.12 Prediction result of COP (7 kg charged case)

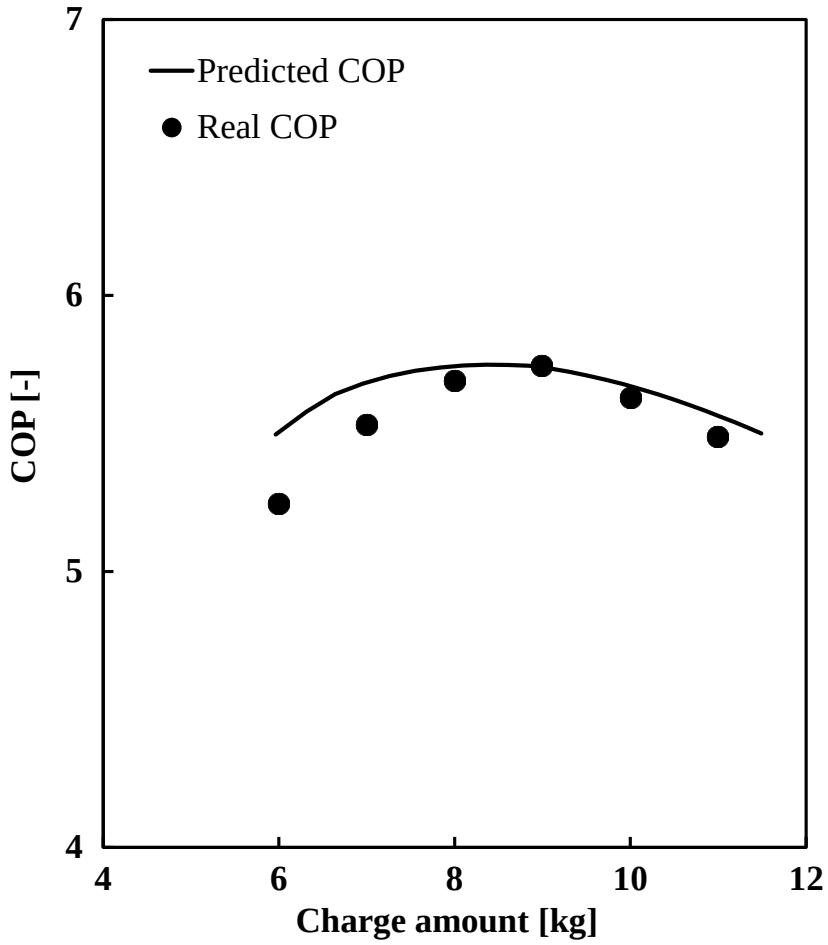

Fig. 4.13 Prediction result of COP (9 kg charged case)

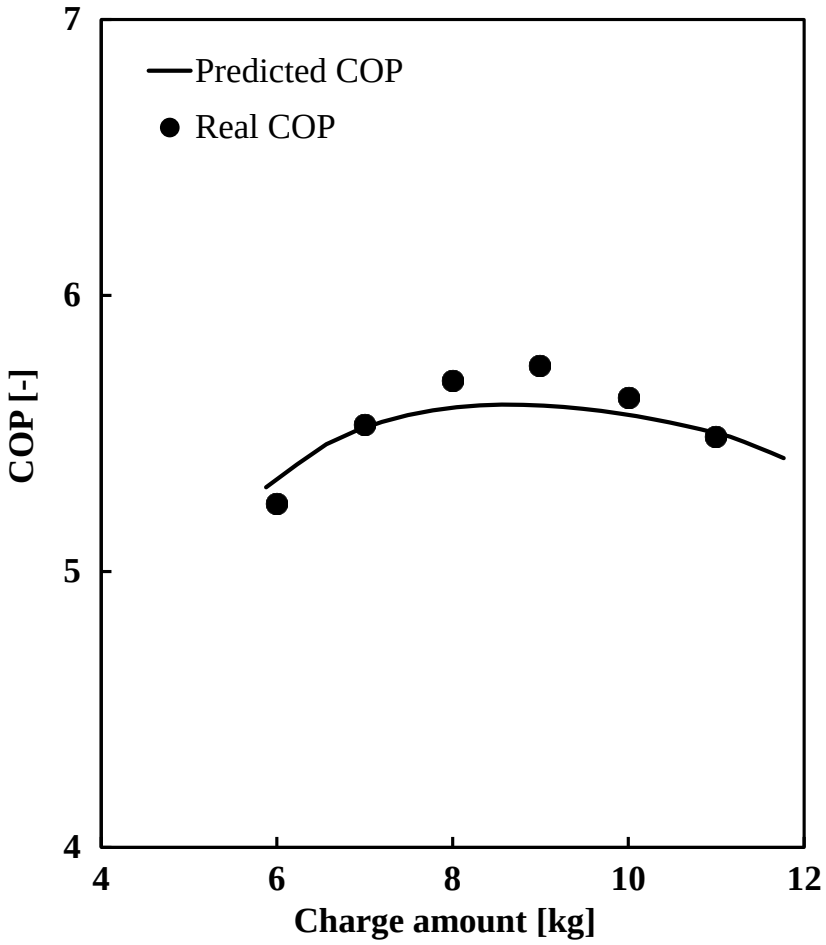

Fig. 4.14 Prediction result of COP (11 kg charged case)

In addition, it was possible to predict the optimal charge amount, which is 8.86 kg at undercharged case (7 kg), 8.85 kg at proper charge case (9 kg), and 8.56 kg at overcharged case (11 kg), which are very close to real optimal charge, 8.8 kg. In fact, in all three cases, all operating conditions are the same except for the current charge, so the COP prediction results should be the same. However, the proposed method predicts the change of the heat pump performance from the change of the charge amount. Therefore, if the initial state (or current charge) is changed, it affects the result of the prediction. Nevertheless, considering that the range of the proper charge level is about 70~120%, if the error of the optimal charge amount prediction is within 10%, significant improvement of the overall performance of the heat pump can be expected.

Finally, Fig. 4.15 and Fig. 4.16 show the results of predicting the optimal charge amount according to various operating conditions and current charge amount in cooling and heating mode, respectively. As can be seen from the figures, the optimal charge amount was accurately predicted under most operating conditions. AAD and RMS error was 6.97% and 8.64%, respectively.

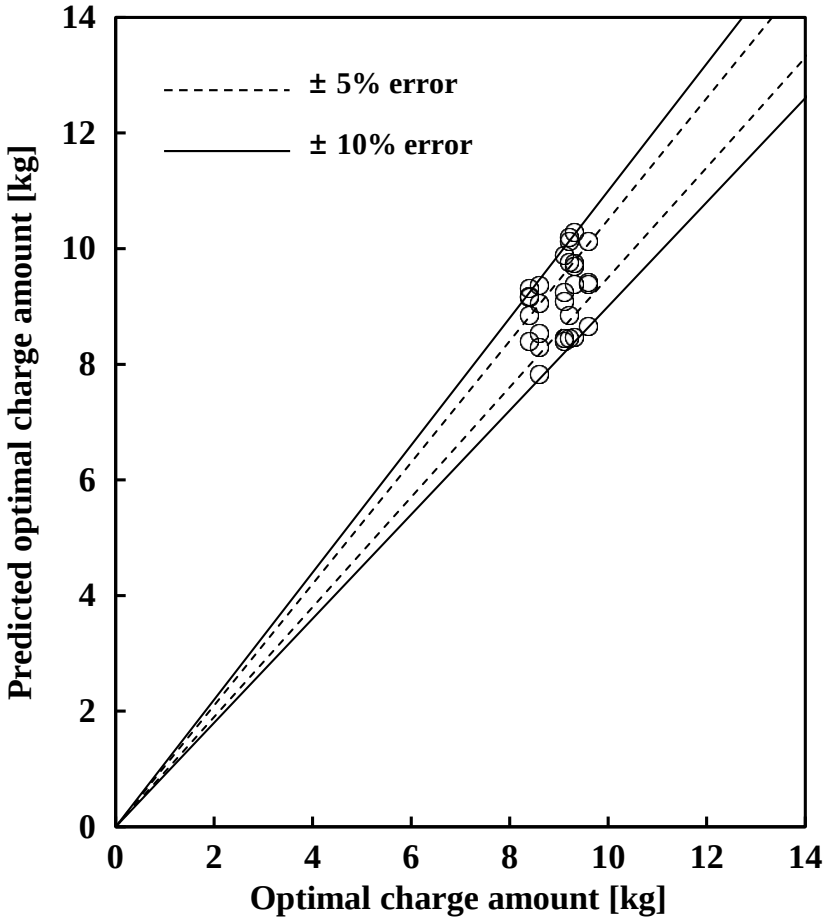

Fig. 4.15 Optimal charge prediction result (cooling mode)

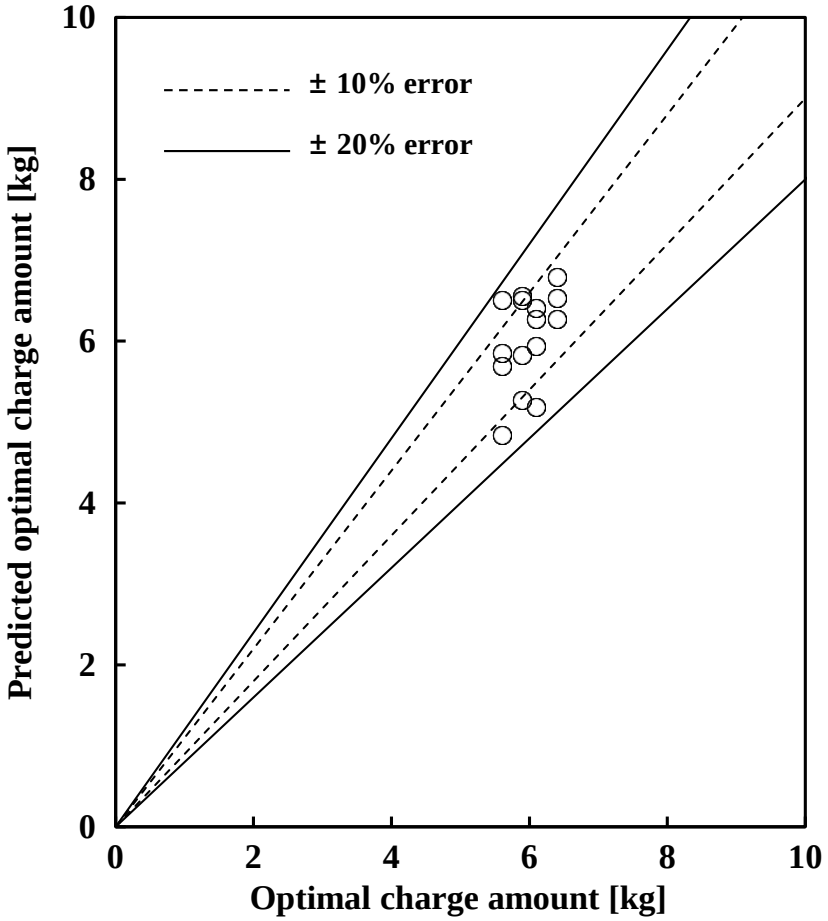

Fig. 4.16 Optimal charge prediction result (heating mode)

4.4 Evaluation of optimum control of refrigerant charge

Using the results of previous parts, an optimal control of the charge amount is possible in the air heat source heat pump system. Fig. 4.17 shows the average performance enhancement that can be expected with optimal control of the charge amount. As can be seen from the figure, a meaningful COP improvement can be expected if the amount of refrigerant is optimally adjusted even the current charge is within 70~120% range which is considered as proper charge level. In particular, the optimal control of charge amount greatly improved the performance in severe undercharged or overcharged cases, in which showed a maximum COP improvement up to 14.3%. Average COP improvement of 6.04% is expected by optimal adjustment of charge amount.

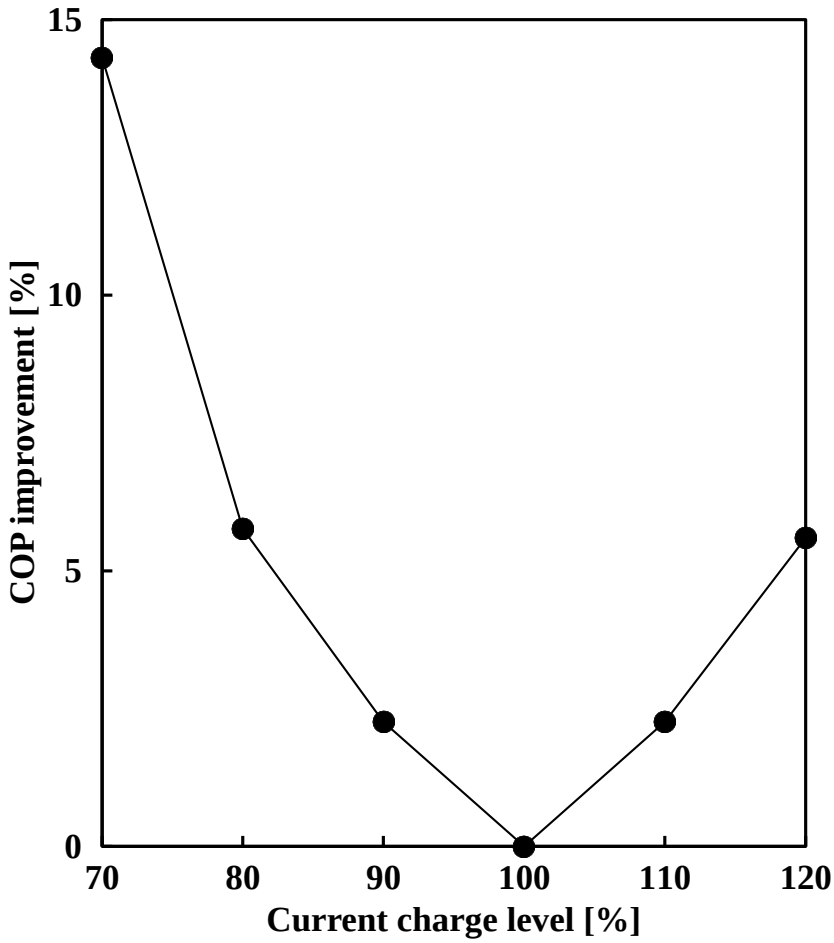

Fig. 4.17 COP improvement by optimal control of charge (cooling mode, rating condition)

4.5 Summary

Using the results in the previous chapter, it is possible to accurately estimate the amount of refrigerant charge in the heat pump system. The reason for predicting the charge amount is to maintain the refrigerant charge in the system at an optimal level. Therefore, it is necessary to know the optimal amount of refrigerant charge as well as the current amount of refrigerant charge of the system. The optimal amount of refrigerant charge, however, depends on the configuration, conditions and operating conditions of the system. Therefore, a real-time prediction method of optimal charge is required rather than the pre-obtained optimal charge.

In order to predict the optimal refrigerant charge amount of the heat pump, it is necessary to predict the performance of the heat pump according to the charge amount. However, it is very difficult to directly predict performance from the charge amount. Therefore, in this chapter, the performance according to the driving information is predicted, and the driving information is converted into the charge amount using the previous charge prediction equation. The accuracy of the optimal charge prediction method was verified using the experimental results. The RMS error of the optimal charge prediction

was 6.97% in cooling mode and 8.64% in heating mode. Finally, the heat pump performance was evaluated when the charge amount was optimally adjusted. Using the optimal charge control, the COP improved by an average of 6.04% and a maximum of 14.3%.

Chapter 5. Concluding remarks

In order to improve the performance of the heat pump system and reduce the energy consumed, the optimal operation of the heat pump system is very important. However, the charge amount which greatly affects the performance of the heat pump is not optimally adjusted in most cases. This is because it is difficult to accurately predict the charge in the heat pump system. While many charge prediction methods exist, there is no method for predicting charge that can be used universally and has high accuracy. In this study, charge prediction method was developed that has high accuracy and applicable universally.

In the chapter 2, modeling of the heat pump system was performed. Since the configuration and geometry of the heat pump system affect the refrigerant charge prediction, detailed modeling was performed considering the complex geometry of all components. In addition, lubricant must be considered for accurate charge prediction. Several empirical coefficients were used to complete the modeling of the heat pump. System simulation was performed using this heat pump model, and the refrigerant charge was predicted. RMS error of charge prediction by simulation was 4.95% in cooling mode and 6.26% in heating mode. In addition, through the simulation, it was possible to predict the distribution of refrigerant in the

heat pump. Simulation results showed that more than 90% of the refrigerant charge change occurs in the condenser.

In the chapter 3, the heat pump was simplified to present a general method of predicting charge amount. Through the analysis of the simplified system, a generalized charge prediction equation was presented. In order to verify the accuracy of the proposed charge prediction equation, a commercial heat pump experiment was performed. RMS error for cooling mode charge prediction was 3.7%, and RMS error for heating mode charge prediction was 8.2% which indicate a high accuracy of charge prediction equation.

The charge prediction equation is a generalized method but requires some assumptions. Two extended charge prediction methods were suggested to increase the accuracy of the charge prediction equation. First, during continuous driving of system, the accuracy of charge prediction equation is not always high. Therefore, a criterion for selecting reliable point was proposed. As a result of selecting reliable points, the RMS error of charge prediction is 6.11%.

Next, the accuracy of the charge prediction equation was verified on the system with limited sensor information such as residential heat pump. Under normal conditions, the accuracy of the charge prediction equation is very

high. However, in severely leaked conditions (less than 70%), the accuracy of the charge prediction equation decreases dramatically. Therefore, in combined with the leakage detection method, the charge prediction equation is applied only to the normal charged region. As a result, the RMS error decreased significantly from 18.6% to 5.2%.

Finally, in the chapter 4, a prediction method for optimal charge of heat pump system was developed. In this chapter, the relationship between operating information and system performance is first predicted, and then the operating information is converted to charge amount using the charge prediction equation. Through this process, it was possible to accurately predict the performance change of the heat pump according to the charge amount. In addition, it was possible to predict the optimal charge to maximize the COP. The RMS error of optimal charge prediction was 6.97% in cooling mode and 8.64% in heating mode. Optimal control of charge is possible using the current charge prediction method and optimal charge prediction method of this study. Finally, the performance of the optimal charge control is evaluated and a maximum COP improvement of up to 14.3% was expected.

In conclusion, in this study, a general prediction method for charge amount and a prediction method for optimal charge were presented. Using

these two methods, an optimal control of charge was possible, which is expected to improve heat pump COP by 6.04%.

References

ANSI/AMCA 210, 2007. Laboratory methods of testing fans for certified aerodynamic performance rating. Air Movement and Control Association International, Inc., Arlington, IL, U.S.A.

ANSI/AHRI Standard 1230, 2010. Performance Rating of Variable Refrigerant Flow (VRF) Multi-Split Air-Conditioning and Heat Pump Equipment. Arlington, VA, U.S.A.

ASHRAE Guideline 2, 2010. Engineering analysis of experimental data. ASHRAE, Atlanta, GA, U.S.A.

Biddle, J., 2008. Explaining the spread of residential air conditioning, 1955–1980. Explor. Econ. Hist. 45, 402-423.

Chato, J.C., 1960, Laminar condensation inside horizontal and inclined tubes. Ph.D thesis, Massachuseits Institute of Technology, U.S.A.

Colburn, A.P., 1964.A method of correlating forced convection heat transfer data and a comparison with fluid friction. Int. J. Heat Mass Transfer. 7, 1359-1384.

Corberán, J.M., Martínez, I.O., Gonzálvez, J., 2008. Charge optimisation study of a reversible water-to-water propane heat pump. Int. J. Refrig. 31, 716-726.

Corberán, J.M., Martínez-Galván, I., Martínez-Ballester, S., Gonzálvez-

Maciá, J., Royo-Pastor, R., 2011. Influence of the source and sink temperatures on the optimal refrigerant charge of a water-to-water heat pump. Int. J. Refrig. 34, 881-892.

Ekren, O., Sahin, S., Isler, Y., 2010. Comparison of different controllers for variable speed compressor and electronic expansion valve. Int. J. Refrig., 33 (6), pp. 1161-1168

Eom, Y.H., Yoo, J.W., Hong, S.B., Kim, M.S., 2019. Refrigerant charge fault detection method of air source heat pump system using convolutional neural network for energy saving. Energy. 187, 115877.

Finn, D.P. , Doyle, C.J., 2000. Control and optimization issues associated with algorithm-controlled refrigerant throttling devices. ASHRAE Trans., 106, p. 524

Garcia, C.E., Prett, D.M., Morari, M., 1989. Model predictive control: theory and practice—a survey. Automatica, 25 (3), pp. 335-348

Geller, V.Z., Lapardin, N.I., 2016. Solubility and miscibility of refrigerants R407C and R410A with synthetic compressor oils. Refrigeration and technology. 52 (3), 36-41.

Goyal, A., Staedter, M.A., Garimella, S., 2019. A review of control methodologies for vapor compression and absorption heat pumps. Int. J. Refrig. 97, 1-20.

Grace, I.N., Datta, D., Tassou, S.A., 2005. Sensitivity of refrigeration system performance to charge levels and parameters for on-line leak detection. Appl. Therm. Eng. 25, 557–566.

Guo, Y., Li, G., Chen, H., Wang, J., Guo, M., Sun, S., Hu, W., 2017. Optimized neural network-based fault diagnosis strategy for VRF system in heating mode using data mining. Appl. Therm. Eng. 125, 1402–1413.

Gungor, K., Winterton, R., 1987. A gernaral correlation for flow boiling in tubes and annuli. Int. J. Heat and Mass transfer. 65 (3), 351-358.

He, X.D., Liu, S., Asada, H.H., 1997. Modeling of vapor compression cycles for multivariable feedback control of Hvac systems, J. Dyn. Syst. Measurem. Control, 119 (2), pp. 183-191.

Heo, J., Jeong, M. W., Jeon, J., Kim, Y., 2008. Effects of Gas Injection on the Heating Performance of a Two-Stage Heat Pump Using a Twin Rotary Compressor with Refrigerant Charge Amount. Int. J. Air-Conditioning and Refrigeration 16(3), 77-82.

Hewitt, N. J., Lemmon, E.W., Huber, M.L., McLinden, M.O., 2013. NIST Standard Reference Database 23: Reference Fluid Thermodynamic and Transport Properties-REFPROP, Version 9.1. National Institute of Standards and Technology, Standard Reference Data Program: Gaithersburg, MD

Hughmark, G.A., 1962. Holdup in gas-liquid flow. Chemical Engineering Progress. 58(4), 62-65.

ISO 5151, 2010. Non-ducted air conditioners and heat pumps - testing and rating for performance. Geneva, Switzerland

Kim, D.H., Park, H.S., Kim, M.S., 2014. The effect of the refrigerant charge amount on single and cascade cycle heat pump systems. Int. J. Refrig. 40, 254-268.

Kim, H.S., 2015. Studies on the Oil Retention and Performance of Oil Separator in Multi Heat Pump System. Ph.D thesis, Seoul National University, Republic of Korea

Kim, H.S., Yoon, P.Y., Sa, Y.C., Chung, B.Y., Kim, M.S., 2014. A study on the flow characteristics of refrigerant and oil mixture in compressor suction line. Int. J. Refrig. 48, 48-59.

Kim, H.S., Kim, M.S., 2015. A Review on Flow Characteristics of Refrigerant and Oil Mixture in a Heat Pump System. International Journal of Air-Conditioning and Refrigeration 23(3), 1530002.

Kim, H.S., Kim, M.S., 2016. A numerical study on the oil retention of R410A and PVE oil mixture in multi heat pump system, Journal of Mechanical Science and Technology 30 (4), 1891~1901.

Kim, J.H., Cho, J.M, Lee, I.H., Lee, J.S., Kim, M.S., 2007. Circulation

concentration of CO2/propane mixtures and the effect of their charge on the cooling performance in an air-conditioning system. Int. J. Refrig. 30, 43-49.

Kim, M., Kim, M.S., 2005. Performance investigation of a variable speed vapor compression system for fault detection and diagnosis. Int. J. Refrig. 28, 481–488.

Kim, M. S., Lee, J. S., Kim, M. S., 2009. An Experimental Study on the Performance of CO_2 Air-conditioning Cycle Equipped with an Ejector. Int. J. Air-Conditioning and Refrigeration 17(3), 100-106.

Kim, W., Braun, J.E., 2013. Performance evaluation of a virtual refrigerant charge sensor. Int. J. Refrig. 36, 1130-1141.

Kim, W., Braun, J.E., 2015. Extension of a virtual refrigerant charge sensor. Int. J. Refrig. 55, 224-235.

Kocyigit, N.,Bulgurcu, H., Lin, C., 2014. Fault diagnosis of a vapor compression refrigeration system with hermetic reciprocating compressor based on p-h diagram. Int. J. Refrig. 45, 44–54.

Larsen, L.F.S., 2006. Model Based Control of Refrigeration Systems. Department of Control Engineering, Denmark, Aalborg University

Li, G., Hu, Y., Chen, H., Shen, L., Li, H., Li, Jiong., Hu, W., 2016. Extending the virtual refrigerant charge sensor (VRC) for variable

refrigerant flow (VRF) air conditioning system using data-based analysis methods. Applied Thermal Engineering 93, 908-919.

Li, H., Braun, J.E., 2009. Development, Evaluation, and Demonstration of a Virtual Refrigerant Charge Sensor, HVAC&R Research 15(1), 117-136.

Madani, H., Roccatello, E., 2014. A comprehensive study on the important faults in heat pump system during the warranty period. Int. J. Refrig. 48, 19-25.

Marcinichen, J.B., Holanda, T.N. d., Melo, C., 2008. A dual SISO controller for a vapor compression refrigeration system. Proceedings of the International Refrigeration and Air-conditioning Conference, West Lafayette, IN

Muller-steinhagen, H., Heck, K., 1986. A simple friction pressure drop correlation for two-phase flow in pipes., Chem. Eng. Process. 20, 297-308.

Nanayakkara, V.K., Ikegami, Y., Uehara H., 2002. Evolutionary design of dynamic neural networks for evaporator control. Int. J. Refrig., 25 (6), pp. 813-826

Navarro, E., Corberan, J.M., Martinez-Galvan, I.O., Gonzalvez, J., 2012. Oil sump temperature in hermetic compressors for heat pump applications. Int. J. Refrig. 35, 397-406.

Nowak, T., Jaganjacova, S., Westring, P., 2014. European Heat Pump Market

and Statistics Report, Brussels.

Outtagarts, A., Haberschill, P., Lallemand, M., 1997. The transient response of an evaporator fed through an electronic expansion valve. Int. J. Energy Res., 21 (9), pp. 793-807

Petukhov, B.S., 1970., Heat transfer and friction in turbulent pipe flow with variable physical properties. Adv. In Heat Trans. 6, 503-564.

Rossi, T.M., Braun, J.E., 1997. A Statistical, Rule-Based Fault Detection and Diagnostic Method for Vapor Compression Air Conditioners. HVAC&R Research 3(1), 19-37.

Rossi, T.M., 2004. Unitary air conditioner field performance. International Refrigeration and Air Conditioning Conference.

Rouhani, Z., 1969. Modified correlations for void and two-phase pressure drop. AE-RTV-8841

Shah, R., Rasmussen, B.P., Alleyne, A.G., 2004. Application of a multivariable adaptive control strategy to automotive air conditioning systems. Int. J. Adap. Control Signal Process., 18 (2), pp. 199-221

Shi, S., Li, G., Chen, H., Liu, J., Hu, Y., Xing, L., Hu, W., 2017. Refrigerant charge fault diagnosis in the VRF system using Bayesian artificial neural network combined with ReliefF filter. Appl. Therm. Eng. 112, 698–706.

Tassou, S.A., Grace, I.N., 2005. Fault diagnosis and refrigerant leak

detection in vapour compression refrigeration systems. Int. J. Refrig. 28, 680-688.

Tassou, S.A., Qureshi, T.Q., 1996. Variable-speed capacity control in refrigeration systems. Appl. Thermal Eng., 16 (2), pp. 103-113.

U.S Energy Information Administration, 2019. Annual Energy Outlook 2019 with projections to 2050.

Wang, C., Chi, K., 2000. Heat transfer and friction characteristics of plain fin-and-tube heat exchangers, part I: new experimental data. Int. J. Heat and Mass transfer. 43, 2681-2691.

Yoo J.W., Hong S.B., Kim M.S., 2017. Refrigerant leakage detection in an EEV installed residential air conditioner with limited sensor installations. Int. J. Refrig. 78, 157-165.

Yoo, J.W., 2018. Study on the detection method of refrigerant leakage amount in air heat pump system. Ph.D thesis, Seoul National University, Republic of Korea

Vargas, J.V.C., Parise, J.A.R., 1995. Simulation in transient regime of a heat pump with closed-loop and on-off control. Int. J. Refrig., 18 (4), pp. 235-243.

Zivi, S., 1964. Estimation of Steady-state Steam Void-fraction by Means of the Principle of Minimum Entropy Production. J. Heat Transfer. 86, 247-251.

국 문 초 록

모든 히트펌프 시스템에는 최적 냉매 충전량이 존재한다. 히트펌프의 성능을 향상하고, 탈설계점 운전을 방지하기 위해서 히트펌프 시스템의 충전량은 항상 최적으로 유지되는 것이 바람직하다. 충전량을 최적으로 유지하기 위해서는 시스템 내의 현재 충전량을 정확하게 예측할 수 있어야 한다. 냉매 충전량을 예측하는 다양한 방법이 존재하지만, 대부분의 연구가 데이터 기반 방식으로, 다양한 시스템에는 적용하기 힘들다는 단점이 있다. 본 연구에서는 냉매 충전량 예측의 비용을 줄이고 정확도를 높이기 위해, 물리 기반의 냉매량 예측 방법을 제시하였다.

먼저, 시뮬레이션 기반의 냉매량 예측 방법을 제시하였다. 히트펌프 시스템의 구성과 형상은 매우 복잡한데, 이러한 시스템 특성은 냉매 충전량에 영향을 준다. 따라서, 모델링에는 히트펌프 시스템의 형상과 특성이 자세하게 고려되었다. 또한, 압축기 내에 충전된 윤활유는 냉매와 매우 잘 섞이는 특성을 가지고 있으므로, 냉매 충전량에 상당한 영향을 준다. 따라서, 본 연구의 모델링에는 압축기 내 윤활유의 영향을 고려하였다. 히트펌프 시스템의 시뮬레이션을 통해 냉매 충전량을 예측할 수 있었고, 예측의 오차는 6.3% 미만으로 시뮬레이션 기반 냉매량 예측 방법이 매우 정확함을 알 수 있었다. 그러나, 모델링 과정에서 히트펌프 시스템이 매우 자세하게 모사되었으므로, 시뮬레이션 기반 냉매량 예측 방법은 범용적으로 적용할 수는 없다는 단점이 있다.

범용적으로 적용할 수 있는 냉매량 예측 방법의 개발을 위해 히트펌프 시스템을 간단하게 모사하였다. 몇 가지 가정과 기본 열전달 해석을 통해, 범용적인 냉매 충전량 예측식을 제시하였다. 제시한 냉매 충전량 예측식의 정확도를 검증하기 위해 상업용 히트펌프의 실험이 수행되었다. 제시한 냉매 충전량 예측식의 예측 오차는 냉방 운전시 3.7%, 난방 운전시 8.2%로 매우 낮았다. 냉매

충전량 예측식은 전반적인 공기 열원 히트펌프에서 생기는 현상을 기반으로 제시되었기 때문에, 범용적으로 사용 가능하다. 그럼에도 불구하고, 사용에 몇 가지 제한 조건이 존재한다. 본 연구에서는 이러한 제한 조건을 극복하기 위해 두 가지 경우에 대한 냉매량 예측식의 범위 확장을 제안하였다.

먼저, 연속 운전시에는 냉매량 예측식에서 설정한 가정이 타당하지 않은 점들이 필연적으로 발생한다. 예를 들어, 비정상상태 운전이나 압축기 비가동시에는 냉매 충전량 예측의 정확도가 급감한다. 따라서, 연속 운전시의 냉매 충전량 예측의 정확도를 높이기 위해, 설정한 가정이 타당한 점만 선별하는 선별식을 제시하였다. 선별식을 이용하여, 냉매 충전량 예측의 정확도가 높은 점만을 선별할 수 있었고, 이를 통해 연속운전시에도 냉매 충전량 예측의 오차는 6.11%로 감소하였다.

다음으로, 가정용 히트펌프 시스템과 같은 소형 시스템에서 냉매 충전량 예측의 정확도를 검증하였다. 소형 히트펌프 시스템에서는 센서의 수가 제한되어있고, 따라서 과냉도의 존재여부를 확신할 수 없다. 과냉도가 존재하지 않는 과누설 상태의 경우 냉매량 예측식의 정확도는 크게 떨어지므로, 이러한 과누설점을 냉매 누설 탐지 방법을 이용하여 확인하였다. 냉매 누설 탐지 방법을 이용하여 냉매의 저충전이 탐지될 경우에는 냉매 충전이 필요한 것이 자명하므로, 냉매 누설이 탐지되지 않은 경우에만 냉매량 예측을 시도하였다. 이 경우, 냉매량 예측의 오차는 기존 18.6%에서 5.16%로 크게 감소하였다.

냉매 충전량의 최적 조절을 위해서는 시스템내의 현재 충전량뿐만 아니라 시스템의 최적 충전량을 알아야 한다. 이때, 시스템의 최적 충전량은 시스템의 구성, 조건, 그리고 운전 상태 등에 따라 변화한다. 따라서, 본 연구에서는 센서 정보를 이용한 실시간 최적 충전량 예측 방법을 제시하였다. 최적 충전량을 예측하기 위해서는 충전량에 따른 시스템의 성능 변화를 예측해야 한다. 이때, 시스템의 성능을 충전량으로부터 직접 예측하는 것은

매우 어렵다. 따라서, 본 연구에서는 운전 상태에 따른 시스템 성능을 먼저 예측하고, 냉매 충전량 예측식을 이용하여 운전 정보를 충전량으로 변환하였다. 이러한 과정을 통해 냉매 충전량에 따른 시스템 성능과 최적 냉매 충전량을 예측할 수 있었으며, 최적 냉매 충전량 예측의 오차는 약 6.97%로 나타났다.

결론적으로, 현재 냉매 충전량 예측방법과 최적 냉매 충전량 예측방법을 결합하여 냉매량의 최적 제어가 가능하다. 본 연구에서는 냉매 충전량 최적 제어의 효과를 평가하였으며, 약 6.04%의 COP 향상이 기대된다. 본 연구에서 제시한 방법은 공기 열원 히트펌프에 범용적으로 적용할 수 있는 것이므로, 연구의 결과가 보급된다면 상당한 수준의 에너지 수요 감축을 기대할 수 있을 것이다.

주요어: 공기 열원 히트펌프, 냉매 충전량, 최적 충전량, 최적 제어, 히트펌프 모델링

학 번: 2014-21573